AD _____

PATHOPHYSIOLOGY AND TOXICOKINETIC STUDIES OF BLUE-GREEN ALGAE INTOXICATION IN THE SWINE MODEL

ANNUAL REPORT

Val R. Beasley
Wanda M. Haschek-Hock
Wayne W. Carmichael
William O. Cook
Andrew M. Dahlem
Stephen B. Hooser
Randall A. Lovell
Nik A. Mahmood
William M. Valentine

September 26, 1989

Supported by

U.S. ARMY MEDICAL RESEARCH AND DEVELOPMENT COMMAND
Fort Detrick, Frederick, Maryland 21701-5012

Contract No. DAMD 17-85-C-5241

University of Illinois
2001 South Lincoln Avenue
Urbana, IL 61801

SECURITY CLASSIFICATION OF THIS PAGE

REPORT DOCUMENTATION PAGE

Form Approved OMB No. 0704-0188

1a. REPORT SECURITY CLASSIFICATION UNCLASSIFIED	1b. RESTRICTIVE MARKINGS
2a. SECURITY CLASSIFICATION AUTHORITY	3. DISTRIBUTION/AVAILABILITY OF REPORT Approved for public release; distribution unlimited.
2b. DECLASSIFICATION/DOWNGRADING SCHEDULE	
4. PERFORMING ORGANIZATION REPORT NUMBER(S)	5. MONITORING ORGANIZATION REPORT NUMBER(S)
6a. NAME OF PERFORMING ORGANIZATION University of Illinois 6b. OFFICE SYMBOL (If applicable)	7a. NAME OF MONITORING ORGANIZATION
6c. ADDRESS (City, State, and ZIP Code) 2001 South Lincoln Avenue Urbana, Illinois 61801	7b. ADDRESS (City, State, and ZIP Code)
8a. NAME OF FUNDING/SPONSORING ORGANIZATION U.S. Army Medical Research & Development Comman 8b. OFFICE SYMBOL (If applicable)	9. PROCUREMENT INSTRUMENT IDENTIFICATION NUMBER DAMD17-85-C-5241
8c. ADDRESS (City, State, and ZIP Code) Fort Detrick Frederick, Maryland 21701-5012	10. SOURCE OF FUNDING NUMBERS PROGRAM ELEMENT NO. 61102A; PROJECT NO. 3M1 61102BS12; TASK NO. AA; WORK UNIT ACCESSION NO. 006

11. TITLE (Include Security Classification)
(U) Pathophysiology and Toxicokinetic Studies of Blue-Green Algae Intoxication in the Swine Model

12. PERSONAL AUTHOR(S) V.R. Beasley, W.M. Haschek-Hock, W.W. Carmichael, W.O. Cook, A.M. Dahlem, S.B. Hooser, R.A. Lovell, N.A. Mahmood, and W.M. Valentine

13a. TYPE OF REPORT	13b. TIME COVERED	14. DATE OF REPORT (Year, Month, Day)	15. PAGE COUNT
Annual	FROM 9/1/87 TO 8/31/88	September 26, 1989	157

16. SUPPLEMENTARY NOTATION

17. COSATI CODES			18. SUBJECT TERMS (~~Continue on reverse if necessary and identify by block number~~)
FIELD	GROUP	SUB-GROUP	
06	16		Blue-green algae, phycotoxin, microcystin, cyanoginosin
06	20		anatoxin-a(s), pathophysiology, radiolabelled toxin, analysis, RAIA, anatoxin-a. (DLS)

19. ABSTRACT (Continue on reverse if necessary and identify by block number)

An attempt by New England Nuclear to produce radiolabelled MCLR involved synthetic labelling using tritiated water and Rh/Al_2O_3. Chromatography and mass spectrometry revealed radiolabel incorporation into both the toxin and contaminants. The nonspecifically tritiated toxin had a specific activity of 0.5 uCi/mg. Subsequently, a method recommended by our laboratory utilizing tritiated water with pyridine was performed by New England Nuclear; however, decomposition of the toxin occurred under the conditions used.

MCLR was highly bound when added to "super-activated" charcoal at 1:100. When given to rats via an ileal loop shortly after toxin administration, "superchar" settled out, but was partially effective in limiting MCLR absorption (as indicated by increases in liver weight). In vitro and in vivo, superchar was less effectively than was cholestyramine in a prior study.

20. DISTRIBUTION/AVAILABILITY OF ABSTRACT	21. ABSTRACT SECURITY CLASSIFICATION
☐ UNCLASSIFIED/UNLIMITED ☑ SAME AS RPT ☐ OTIC USERS	Unclassified
22a. NAME OF RESPONSIBLE INDIVIDUAL Mary Frances Bostian	22b. TELEPHONE (Include Area Code) 301-663-7325 22c. OFFICE SYMBOL SGRD-RMI-S

DD Form 1473, JUN 86 *Previous editions are obsolete.* SECURITY CLASSIFICATION OF THIS PAGE

Toxin-dosed mice were pretreated by feeding (glutathione replete), fasting (mild GSH depletion), fasting and n-acetylcysteine (depletes GSH), or fasting and buthionine sulfoxamine (inhibits GSH synthesis) and diethylmaleate (depletes GSH). To estimate hepatic GSH predosing, livers were obtained from mice similarly treated but not given MCLR. The GSH conjugate (at the N-methyl dehydroalanine) of MCLR was synthesized and tested for toxicity by dosing mice IP. Glutathione depletion did not predispose the animals to MCLR toxicosis; and the GSH-adduct was only slightly less toxic than the parent toxin. The GSH depleted mice lived longer than the fed controls.

The hydrophobic portion of the ADDA group of MCLR was cleaved by ozonolysis, then reduced with sodium borohydride to yield a cyclic peptide saturated at the double bond of the N-methyl dehydroalanine. The product was apparently nontoxic in mice dosed IP at 16,000 nM/kg; compared to minimum LD_{100}s for MCLR and dihydroMCLR of 90 nM and 201 nM/kg, respectively.

In vitro, rat hepatocytes, but not Kupffer or sinusoidal endothelial cells, were highly sensitive to MCLR. Hepatocytes were exposed to MCLR, cytochalasin, or phalloidin, fixed and stained rhodamine-labelled phalloidin, and examined on fluorescence microscopy. Unlike hepatocytes exposed to the other toxins, in the MCLR-treated cells, dose-dependent blebbing of the plasma membrane was observed with rays of actin extended to the tips of the blebs. With sufficient toxin and time, actin filaments lost attachment to the plasma membrane, forming a mass near the center of the cell. MCLR also alterred actin filaments in vivo, especially in centriolobular hepatocytes.

In pigs given lethal doses of MCLR IV, central venous pressures markedly declined, and portal venous pressures increased, particularly in the pigs that died earliest after dosing. Sensitive indicators of toxicosis included reduced platelet counts, and increased bile acids and lactate. Increases in serum enzymes indicative of liver damage were slightly delayed in onset but severe. Serum potassium, total bilirubin, and urea nitrogen, as well as blood pO_2 were increased, whereas pCO_2 and base excess were decreased. Hyperkalemia and hypoglycemia were present, and sometimes severe at the time of death.

Holding anatoxin-a(s) under N_2 at low freezer temperatures stabilizes the molecule for at least 6 months. When rats were dosed IP with anatoxin-a(s), and regions of brain analyzed for cholinesterase activity, none were inhibited, suggesting that the major effects occur in the periphery.

LD_{50}s for (+)anatoxin-a hydrochloride and racemic anatoxin-a HCl were 386 and 913 ug/kg, respectively. No mice died at up to 73 mg of (-)anatoxin-a HCl per kg. In IP-dosed, anesthetized rats, the amplitude of the evoked compound action potential (ECAP) of the sciatic nerve/lumbrical or interosseus muscles decreased rapidly in response to the toxin. There was a subsequent partial recovery over time. The ED_{50} for depression of the ECAP was 47 ug/kg; the mean maximal depression was 85 percent; and the mean time to reach the maximum depression was 8.5 min. The time to onset, duration of action, and severity of effects of anatoxin-a were dose-dependent, and compatible with anatoxin-a associated effects at the postsynaptic membrane. The decrease in the amplitude of the ECAP following repetitive stimulation is compatible with a presynaptic site of action. Exposures to anatoxin-a which produced severe blockade of neuromuscular transmission were reversible with artificial respiration, however, higher exposures were lethal apparently due to an additional site of action

FOREWORD

In conducting research using animals, the investigator(s) adhered to the "Guide to the Care and Use of Laboratory Animals," prepared by the Committee on Care and Use of Laboratory Animals of the Institute of Laboratory Animal Resources Commission on Life Sciences, National Research Council (DHHS, PHS, NIH Publications No. 86-23, Revised 1985).

Citations of commercial organizations and trade names in this report do not constitute an official Department of the Army endorsement or approval of the products or services of these organizations.

TABLE OF CONTENTS

SUMMARY

Radiolabelling of microcystin-LR (MCLR; formerly referred to as microcystin-A) was pursued further. An initial attempt to produce radiolabelled MCLR, initiated by New Eng and Nuclear (a method not approved or recommended by our laboratory), involved synthetic labelling using tritiated water and Rh/Al_2O_3. After evaporation to remove dimethylformamide solvent adducts to MCLR and purification, chromatography and mass spectrometry revealed that radiolabel was incorporated into both the toxin and contaminants. The nonspecifically tritiated toxin had a specific activity of approximately 0.5 μCi/mg. Subsequently, the recommended method utilizing tritiated water with pyridine was performed in the laboratories of New England Nuclear. Unfortunately, decomposition of the toxin appeared to have occurred under the conditions used.

When MCLR was mixed with "superactivated" charcoal at a ratio of 1:100 (toxin:charcoal), the toxin was highly bound. When given to rats via an ileal loop at 30 seconds after MCLR administration, however, the "superchar" was only partially effective in limiting the toxin-induced increase in liver weight (as a fraction of body weight). The limited benefit afforded by the charcoal may have been a result of the material settling out in the intestinal lumen in the gut loop preparation. Both *in vitro* and *in vivo*, the superchar performed less effectively than had been [illegible] in a previous study.

To assess the importance of glutathione (GSH) conjugation in MCLR toxicosis, toxin-dosed mice were pretreated by feeding (glutathione replete), fasting (modest GSH depletion), fasting and administration of n-acetylcysteine (depletes GSH), or fasting and administration of both buthionine sulfoximine (inhibits GSH synthesis) and diethylmaleate (depletes GSH pools). Livers were

obtained from mice of the above groups, except the animals were not dosed with MCLR, in order to determine equivalent hepatic GSH predosing. Also, the GSH conjugate (at the N-methyl dehydroalanine) of MCLR was synthesized and tested for toxicity by administration to mice intraperitoneally. The results indicated that glutathione depletion did not predispose the animals to MCLR toxicosis; and the GSH-adduct of the toxin was only slightly reduced in toxicity. In fact the GSH depleted mice lived somewhat longer than the GSH replete fed controls.

In structure toxicity studies, MCLR was subjected to ozonolysis to cleave the hydrophobic portion of the ADDA group, then reduced with an excess of sodium borohydride to yield a cyclic peptide with saturation of the double bonds in the N-methyl dehydroalanine. Saturation only at the latter site was previously shown to cause only a modest reduction of toxicity. However, when ADDA was cleaved the toxin caused no observed toxic effects on the test mice when given intraperitoneally at up to 16,000 nM/kg, which may be compared to an approximate minimum LD_{100} of 90 nM of MCLR/kg.

In studies <u>in vitro</u>, rat hepatocytes but not Kupffer or sinusoidal endothelial cells were highly sensitive to MCLR. When cultured hepatocytes were exposed to MCLR, cytochalasin, or phalloidin and then fixed and stained rhodamine-labelled phalloidin and examined on fluorescence microscopy, it was found that the effects of the algal toxin were unique from those of the other toxins. In the MCLR-treated cells, not only was dose-dependent blebbing of the plasma membrane apparent, but also there were one or more rays of actin extending to the tips of the blebs. With sufficient toxin and time, the actin filaments appeared to have lost any attachment to the plasma membrane, forming a dense mass in the interior of the hepatocytes. <u>In vivo</u>, MCLR also caused

alterations of the actin filaments, especially in centrilobularly located hepatocytes.

In pigs given MCLR intravenously at lethal doses, central venous pressures declined markedly, indicating a pronounced reduction in return of venous blood to the heart, a manifestation of shock. In addition, there were increases in portal venous pressure suggesting obstruction of blood flow through the damaged liver. Early and sensitive clinical pathologic indicators of MCLR toxicosis included reductions in platelet counts and increases in lactate and bile acids. Slightly delayed but markedly altered were serum enzymes indicative of liver damage, especially arginase. In addition, potassium, total bilirubin, urea nitrogen, and blood pO_2 were increased, while pCO_2 and base excess were decreased. The enzyme indicating muscle damage were slightly increased. Hyperkalemia and hypoglycemia were consistently present, especially terminally.

Storage of anatoxin-a(s) under nitrogen at low freezer temperatures causes marked stabilization of toxin integrity. Using the degree of inhibition of human plasma cholinesterase, anatoxin-a(s) was found to be stable for at least 6 months. When rats were dosed intraperitoneally with anatoxin-a(s) and multiple regions of brain analyzed for cholinesterase activity, none were found to be inhibited, suggesting that all the major effects of the toxin occur in the periphery.

The LD_{99}s for (+)anatoxin-a hydrochloride and racemic anatoxin-a hydrochloride were 386 and 313 µg/kg, respectively. No mice died, however, at up to 73 mg of (-)anatoxin-a hydrochloride/kg. Using ip-dosed, anesthetized rats, the evoked compound action potential (ECAP) of the sciatic nerve/lumbrical or interosseus muscles on the plantar surface of the hind foot was

used to assess the responses to (+)anatoxin-a. The amplitude of the response of the ECAP rapidly decreased in response to the toxin, although there was a subsequent gradual increase toward normal over time. The ED_{50} for depression of the ECAP was 47 µg/kg. The mean maximal depression in the ECAP was 85 percent and the mean time to reach the maximum depression was only 8.5 minutes. The time to onset, duration of action, and severity of effects of anatoxin-a were dose-dependent. These effects are consistent with anatoxin-a associated effects at the postsynaptic membrane. The decrease in the amplitude of the ECAP following repetitive stimulation of the sciatic nerve tends to confirm that there is also a presynaptic site of action of anatoxin-a. No effects on nerve conduction velocity were noted. Exposures to anatoxin-a producing a blockade of up to 95% of neuromuscular transmission were reversible with artificial respiration, however, sufficiently high exposures appeared to be lethal due to a mechanism in addition to neuromuscular blockade.

PEPTIDE HEPATOTOXINS

I RADIOLABELING OF MICROCYSTIN-LR

Andrew M. Carmichael and Ken-Ichi Harada

INTRODUCTION

The high toxicity of peptide toxins from cyanobacteria and the resultant small amount of compound which needs to be given to produce toxic effects make isotopic labeling essential for experiments to characterize the biological fates of the toxins. Radiolabeled algae peptide hepatotoxins have been produced both biosynthetically (Brooks and Codd, 1987a,b) and synthetically (Runnegar et al., 1986; Falconer et al., 1986). The biosynthetic method utilized ^{14}C-labeled bicarbonate to produce toxin of extremely low specific activity. Toxin labeled by this method was subsequently injected intraperitoneally (ip) in mice. Seventy percent of the radioactivity was localized in the liver after 1 minute and 90% of the administered dose was localized in the liver 3 hours after dosing. Radioactive residues were also found in the liver, kidneys, urine, and lungs of toxin-treated animals.

The synthetic method involved incorporation of ^{125}I into microcystin-YR. This method utilized the mild lactoperoxidase method of iodination to produce toxin of rather high specific activity. The purified toxin was then administered either ip to mice or intravenously (iv) to rats. This experiment also showed rapid localization of most of the toxin in the liver of the exposed animals. The major drawback of iodination is that iodine is a nonisotopic label which is known occasionally to change the observed biological activity of xenobiotics. In the case of microcystin-YR (MCYR), the

label is incorporated into one of the variable L-amino acids, and this method will not work for microcystin-LR (MCLR) and other closely related compounds in this same group which do not contain tyrosine or methionine. Nodularin, which similarly does not contain these residues also would not be labeled by this method. For these reasons, the possibility of using alternate methods for synthetic labeling of cyanobacterial peptide toxins was investigated.

MATERIALS AND METHODS

Procedure 1. General Tritium Exchange:

Synthetic Labeling with Rh/Al_2O_3 and Tritiated Water. In this method by New England Nuclear Company, 10 mg of MCLR was dissolved in 0.3 ml of anhydrous dimethylformamide. To this solution, 10 mg of 5% Rh/Al_2O_3 and 25 Ci of tritiated water were added and the mixture was stirred overnight at 50°C. Labile tritium was then removed with ethanol and the sample was shipped to us in ethanol. Mass spectral investigation showed the presence of dimethylformamide solvent adducts to MCLR. The compound was subjected to rotary evaporation under a high vacuum with intermittent washing using 1.0 ml volumes of water for 18 hours. After these evaporation steps, the toxin was transferred with methanol from the evaporation flask to a tared vial and 5 µg of the product was submitted for mass spectroscopy. Figure 1 shows the mass spectrum obtained after the high vacuum evaporation process and in this case the major ion obtained was 995 (M+H). Other ions present are attributable to sodium and/or FAB matrix adducts.

After evaporation, a portion of the toxin was applied to Whatman 60A-K6F silica thin layer chromatography (TLC) plates and separated using a mobile phase consisting of the organic layer of a mixture of 65:35:10 chloroform-methanol-water. Bands of silica were scraped from the plate at the

relative retention (rf: 0.23) of MCLR and subjected to liquid scintillation counting (LSC) to determine if any radioactivity remained with the toxin following removal of the solvent adduct. The toxin was found to contain substantial radioactivity after removal of the dimethylformamide so the purification process was continued.

After TLC and LSC confirmation of the toxin identity and radioactivity, respectively, the compound was subjected to gel filtration using TSK Toyopearl HW-40f gel (Supelco Inc., Bellefonte, PA). The column size was 90 cm x 2.0 cm ID and the solvent system was 100% methanol at a flow rate of 2.0 ml/minute. The toxin was detected by UV absorbance at 238 nm. Under these conditions, the toxin was eluted in approximately 120 minutes and was well separated from identifiable impurities (Figure 2). Fractions (10.0 ml) were collected and those corresponding to MCLR were combined and evaporated on a rotary evaporator. The residue was transferred with methanol to a tared vial and again evaporated to dryness. The mass of the toxin was determined and a fraction of the material again subjected to LSC.

Procedure 2. Specific Tritium Exchange:

Synthetic Labeling with Pyridine and Tritiated Water. In this case, New England Nuclear Company Inc. followed the procedure designated by our laboratory and discussed at our trip to USAMRIID in November of 1986. MCLR (10 mg) was placed in a reaction vessel with 25 curies of tritiated water and pyridine (5 µl). A clear solution was observed. Acetic anhydride (15 µl) was added at 0°C and stirred for 5 minutes followed by an additional stirring for 20 minutes at room temperature. Thirty µl of pyridine was again added and then 30 µl of acetic anhydride at 0°C, the mixture was again stirred for 5 minutes at 0°C, then stirred for an additional 1 hour at room temperature.

Labiles were removed by repeated evaporation with 10% acetic acid, and the compound was shipped to us in water.

In this case, 10 mg of greater than 95% pure MCLR produced 450 µCi of activity following removal of labile tritium. The first shipment of compound consisted of 25 µCi of this material. It was initially examined on TLC using Whatman silica gel 60A-K6F plates and the organic layer of a mixture of 65:35:10 chloroform-methanol-water as a solvent system. Bands of silica (0.5 cm) were scraped from the TLC plate and the silica rinsed with 100 µl of methanol. Aliquots were than counted on LSC and the resultant radioactivity plotted (Figure 3). Twenty percent of the applied radioactivity was found to reside in the band of silica corresponding to the same rf as MCLR. Mass spectral analysis of the toxin showed a molecular ion of 995 corresponding with authentic MCLR (MH^+) standard.

The remaining compound was subjected to purification using Bond Elut C-18 cartridges. The cartridge was first rinsed with 2 x 2.0 ml of methanol followed by 2 x 2.0 ml of water. The toxin was applied to the cartridge in water and then the cartridge was rinsed with 3 x 2.0 ml of water. The toxin was eluted from the cartridge in 100% methanol. The toxin in methanol was evaporated to dryness on a rotary evaporator and then transferred to a silica column (22 x 1.0 cm). The silica column chromatography step was performed using Whatman flash silica and the solvent system already described for TLC. Fractions (0.5 ml) were collected and an aliquot was applied to TLC as already described. Bands of silica were again scraped and counted on LSC. The results of this analysis are shown in Figure 4.

An additional shipment of this reaction product (50 µCi) was obtained from NEN and investigated in our laboratories. TLC was performed as described for

the initial check of the first shipment described above. Instead of silica column purification we used TSK Toyopearl HW-40F as described in part A of this report for toxin purification.

RESULTS AND DISCUSSION

Method 1

Prior to adduct removal, we were not certain if the toxin was labeled due to the presence of the adduct on the majority of toxin molecules. Removal of the dimethylformamide adduct and subsequent LSC has showed that radioactivity resided both in the toxin and in the adduct.

This exchange reaction is normally used in the case of very complex molecules which otherwise could not be tritium labeled. This exchange results in a "generally" labeled compound in which the tritium atom(s) are di tributed in a random fashion throughout the molecule. Under these conditions, the specific activity of the material obtained was calculated to be approximately 0.5 μCi/mg. Labeling by this method is seldom uniform and the recovered toxin is believed to be heterogenous in tritium composition.

Another problem with preparation of labeled MCLR by this method was that catalytic tritium replacement can result in saturation of double bonds which we believe are important for toxin bioactivity. Compounds reduced at the N-methyldehydroalanine moiety have HPLC retention times which are very similar to unreduced compounds and care is needed to resolve these closely related compounds.

Reaction 2

Initial TLC results of the original shipment of compound were so promising that a large amount of labeled material was quickly subjected to the silica purification method we have previously established for MCLR. However, in the

case of the labeled molecule, decomposition appeared to have occurred. Following silica column clean-up, the toxin could no longer be identified.

To avoid the confusion which resulted following the silica column step, we have now begun to purify the reaction product by nonsilica based gel filtration. Using the latter method, the chromatograph obtained is identical to that obtained with the labeled material described in part A.

The concerns expressed in the case of the material described in part A also pertain to this compound with the exceptions of: 1) in this case the label is not random and we can predict the precise location of incorporation, and 2) saturation of double bonds is not anticipated. This material has the obvious advantages of fewer unknowns to deal with in biological fate studies, but as with the other material, it is not possible to predict the stability of the material under biological conditions. The initial examination of reaction product by silica TLC showed much promise with approximately 20% of the applied radioactivity present in a narrow band at the same relative retention (Rf: 0.23) as the authentic standard of MCLR. Toyopearl gel filtration also gave a peak at approximately the same retention time as standard. Silica column chromatography, however, showed very different results and we hypothesized that perhaps silica had acted to degrade the labeled material.

We have established that the peak observed on Toyopearl chromatography, along with the concentration of radioactivity found on TLC at the rf of microcystin, were not attributable to labeled toxin. The peak observed under Toyopearl chromatography was not reproducible and did not show the same UV spectrum as authentic toxin. When the reaction product was subjected to C-18 reverse phase chromatography, the only peaks in the chromatogram observed occurred before microcystin. Apparently the toxin was degraded in the hands

of NEN as a result of this synthetic labeling technique. Examination of the reaction product showed no compounds present which structurally resembled the parent compound. This confirmed our results observed in earlier experiments involving purification of this reaction product by silica column chromatography.

One hypothesis to explain the degradation observed under the experimental conditions is that the extremely high specific activity of tritiated water used by NEN did not behave in the same fashion as previous material used with much lower specific activity. The higher molecular energy associated with the higher specific activity of the tritiated water may have resulted in the breakage of peptide bonds resulting in hydrolysis of the parent peptide toxin. Amersham Company did, however, subsequently utilize this method to synthetically label MCLR and is now providing this service commercially. It is not known why NEN was not successful in this method, and yet toxin was produced successfully by Amersham.

Figure 1. Mass spectrum of tritium labelled microcystin after removal of dimethylformamide adduct.

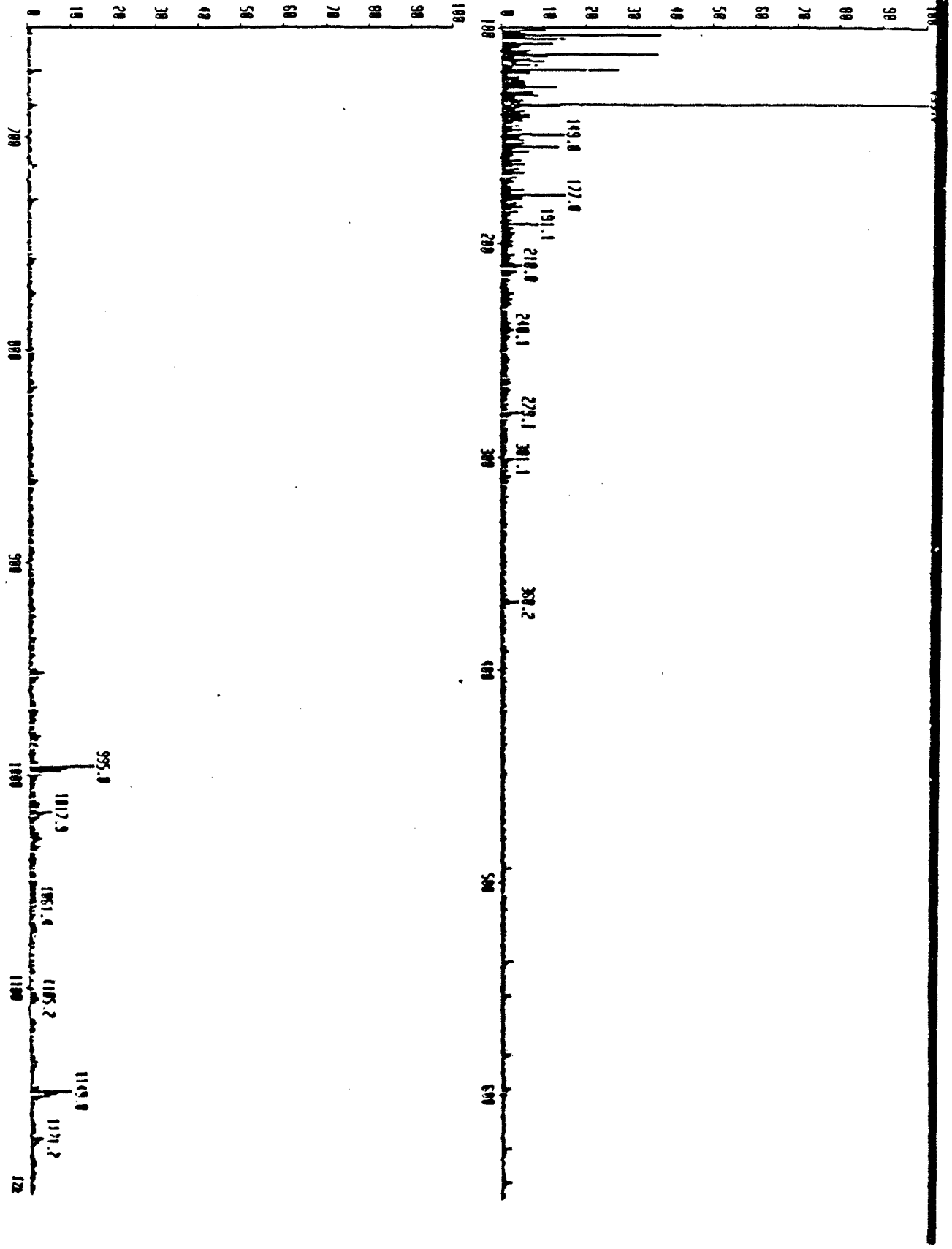

Figure 2. Chromatogram of Toyopearl purification of tritium labelled microcystin.

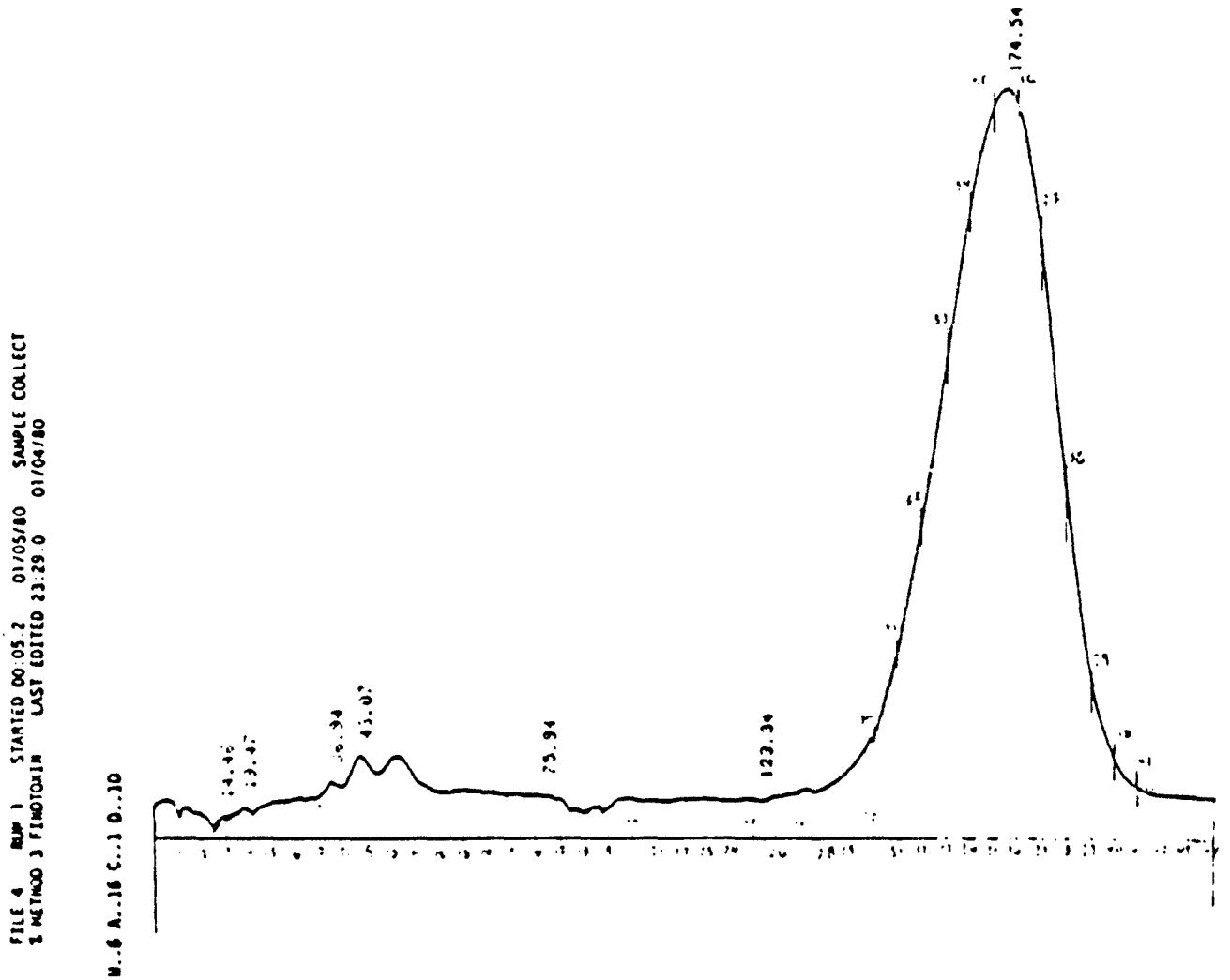

FILE 4 RUN 1 STARTED 00 05 2 01/05/80 SAMPLE COLLECT
% METHOD 3 FINOTOXIN LAST EDITED 23:29.0 01/04/80

RT	AREA	HEIGHT	BC	AREA PERCENT	HEIGHT PERCENT
14.46	192024		T	0.1004	
19.47	491004		V	0.2567	
36.94	109709		V	0.0578	
43.07	338545		V	0.1770	
75.94	759129		V	0.3968	
123.84	61460		V	0.0321	
174.54	189355920	155.7579		98.9797	100.0000

* PEAKS > AREA REJECT 191307776 TOTAL AREA
1 PEAK > HEIGHT REJECT 115.7579 TOTAL HEIGHT

KEYBOARD DIRECTED EVENTS

TIME	EVENT	VALUE
220.619	Stop Data	

Figure 3. TLC radiochromatogram of crude reaction product.

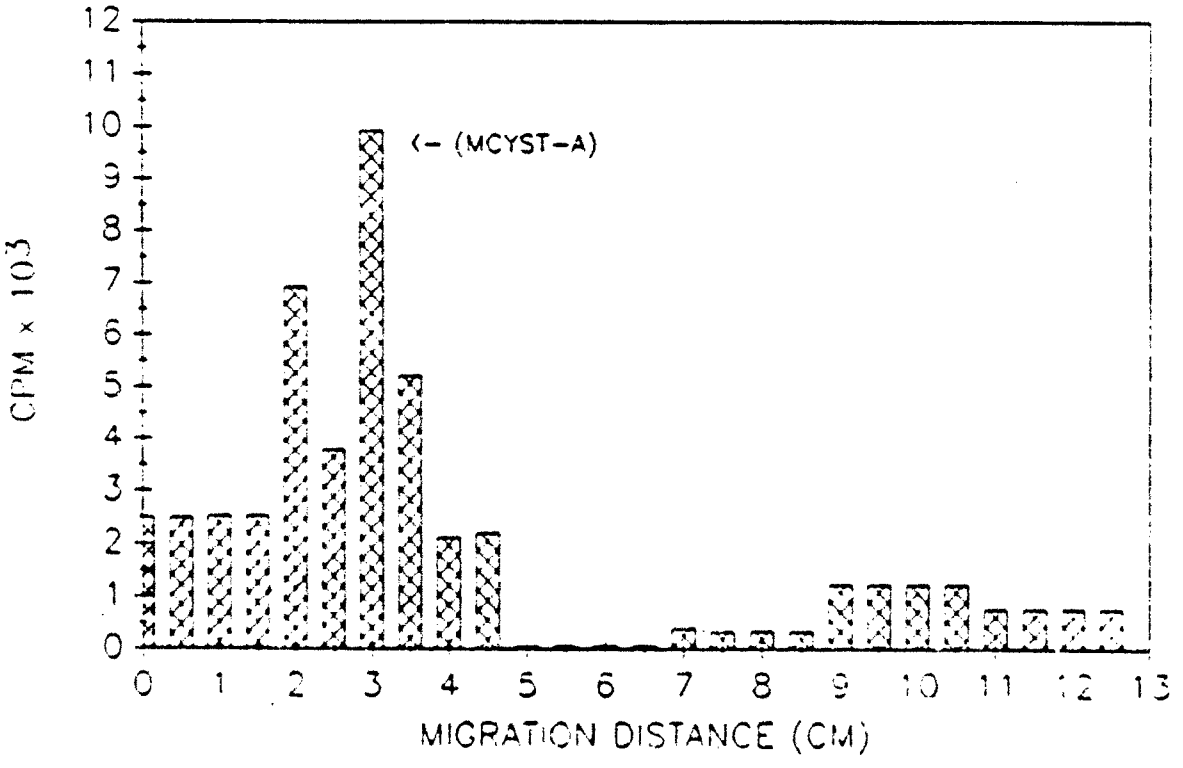

Figure 4. Radiochromatogram of fractions from silica column.

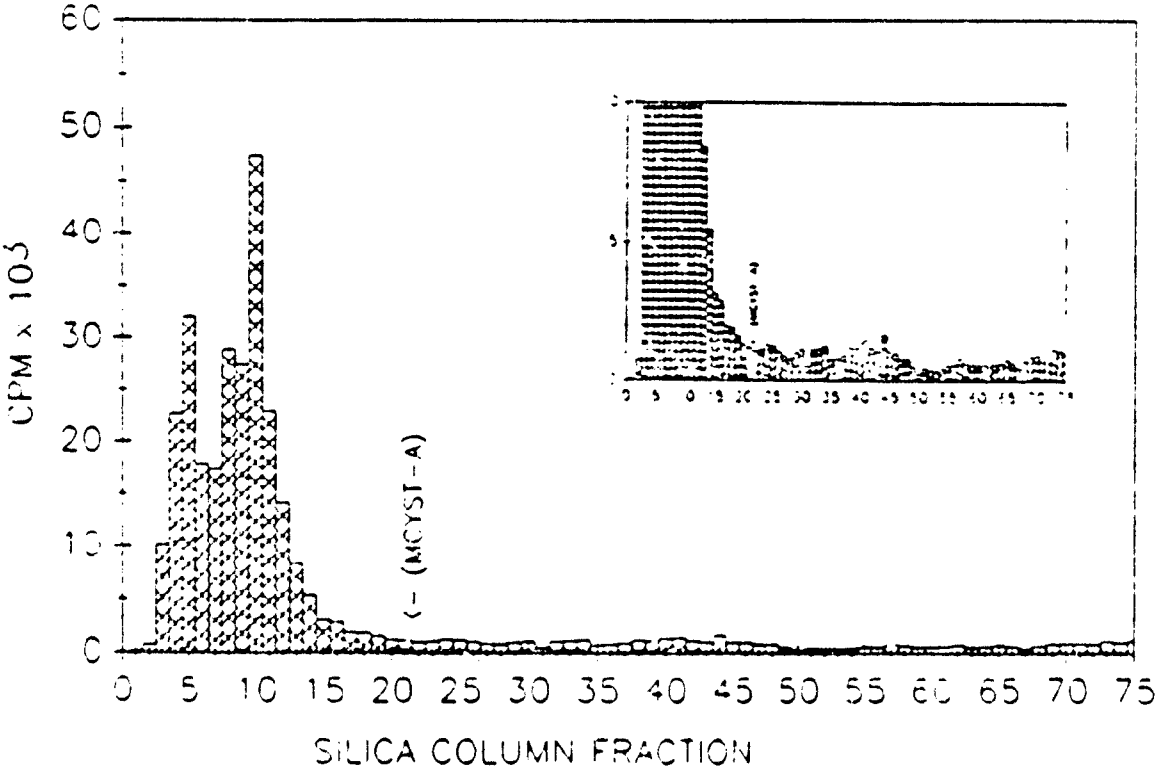

II. COMPARISON OF THE IN VIVO AND IN VITRO BINDING CAPACITIES OF SUPERACTIVATED CHARCOAL TO MICROCYSTIN-LR

Andrew M. Dahlem, Aslam S. Hassan, and Leslie L. Waite

INTRODUCTION

Dense blooms of toxic genera of cyanobacteria sometimes occur when proper conditions of light intensity, nutrients, temperature and pH (neutral or alkaline) are found. The increasing eutrophication of water from urban and industrial sources have apparently increased the occurrence and intensity of algal blooms in recent years (Carmichael, 1988). Blooms of these species are not homogeneous in composition and toxic strains as well as nontoxic strains can be cultured from the same blooms (Carmichael, 1981). The conditions which lead to toxin formation by algae are not known, but environmental conditions which promote bloom formation include; moderate to high levels of nutrients (especially phosphorus, ammonia, and nitrate), water temperatures between 15 and 30°C, and a pH higher than 6 (Skulberg et al., 1984).

Activated charcoal has been suggested to be effective for use as a treatment for animals which have ingested toxic cyanobacteria (Stowe et al., 1981; Galey et al., 1986). In order to test the possible efficacy of activated charcoal for adsorption of cyclic peptide toxins from cyanobacteria a study was performed to compare the adsorptive power of charcoal with cholestyramine resin, a compound already shown to have possible therapeutic potential in cases of microcystin toxicosis (Dahlem et al., 1988).

In Vitro

Superactivated charcoal (superchar) from a commercially available sample (Gulf Biosystems) was used in this experiment. Fifty milligrams of superchar

was weighed into individual tubes to which 5.0 ml of normal saline was added. The tubes were capped and then placed on a rocker mixer for 2 hours prior to analytical experiments. Repeated aliquots of superchar in suspension were removed and the amount of superchar present was calculated on a weight per volume basis.

Microcystin-LR was dissolved in deionized water and the appropriate volumes of toxin were added to the superchar suspension (Table 1). The final volumes of each tube were adjusted to 1.0 ml with deionized water. The experimental samples were then placed on a rocker mixer for 15 minutes followed by centrifugation at 5,000 g for 5 minutes. The supernatant was removed from each tube and passed through individual 0.2 μ filters (Gelman Scientific) to remove remaining charcoal. Samples were analyzed by HPLC with UV detection and quantification was accomplished with linear regression against a toxin standard curve

In Vivo

In situ isolated rat ileal segments were prepared according to the methods of Dahlem et al. (1989). Male, Harlin Sprague-Dawley rats (approximately 100 g body weight) were randomly assigned to 1 of 2 groups and given, via the intestinal loop, either water (0.5 ml) followed 30 seconds later by superchar (50 mg) in a saline vehicle (0.5 ml) or toxin at 5 mg/kg in water (0.5 ml) followed 30 seconds later with superchar (50 mg) in a saline vehicle (0.5 ml). The animals were allowed to recover from surgery, then were killed 6 hours after treatment by an overdose of ether anesthesia. The toxic effects were assessed as a change in liver weight as a percentage of animal whole body weight and the groups compared by Student's t-test.

RESULTS AND DISCUSSION

When mixed with superchar at a ratio of 1:100 (toxin:charcoal), the free toxin concentration was found to be below the limit of detection (20 ppb). In the *in vivo* experiments, a ratio of approximately 1:100 was used. Despite the superactivated charcoal, there was a statistically significant ($p < 0.01$) increase in liver weights as a percent of whole body weights of the treated animals with the toxin as shown in Table 2, indicating that this *in vivo* dose of superchar did not sufficiently reduce toxin bioavailability.

These results are in contrast to our earlier results obtained with cholestyramine resin (CTR). In that study a ratio of 1:100 of toxin to CTR infused into similar *in situ* rat gut loop preparations ameliorated the toxicoses and the liver weights as a percentage of animal whole body weights were indistinguishable from those of control animals which did not receive toxin.

One probable reason for the differences in adsorption of toxin *in vivo* as compared to *in vitro* is that the superactivated charcoal apparently does not stay in suspension and quickly settles out within the gut loop. At necropsy we found the superchar clumped together on the dependent aspect of the mucosa of the isolated gut loop. With constant mixing as occurs on the rocker mixer, the charcoal is not able to settle out so that it presumably can better adsorb the algal toxin. CTR seems more prone to stay in suspension and settles out much slower. Perhaps in an unaltered intestine *in vivo*, the peristaltic movement of ingesta would facilitate mixing of toxin with either the activated charcoal or the ion-exchange resin. Another factor may be the weight of water present in the superchar which offsets the amount of adsorbent available for binding of the toxin.

In conclusion, it appears that the concentrations of toxin and adsorbents used in these experiments that CTR is more efficacious than superchar in reducing the bioavailability and associated toxic effects of microcystin-LR.

Table 1. *In vitro* binding of microcystin-LR to superactivated charcoal.

Charcoal Conc. (µg/ml)	% Absorbed
25	< .01
50	< .01
100	4.0
200	7.2
500	20.0
1,000	45.2
2,500	98.4
5,000	> 99.0
10,000	> 99.0

Table 2. Comparison of relative liver weights of rats dosed with superactivated charcoal and either microcystin-LR (Tox) or the saline (Sal) vehicle.

Tox/Charcoal	Sal/Charcoal
7.35%	4.61%
6.11%	3.97%
6.08%	4.12%
6.90%	3.71%
6.70%	4.13%
----	4.06%
----	----
Mean = 6.63	Mean = 4.1
SEM = .242	SEM = .120

III. THE ROLE OF GLUTATHIONE IN THE TOXICITY OF MICROCYSTIN-LR

Andrew M. Dahlem, Aslam S. Hassan, Val R. Beasley, Stephen B. Hooser, Ken-Ichi Harada, Kenji Matsunaga, Makota Suzuki, Wayne W. Carmichael

INTRODUCTION

Glutathione is a tripeptide consisting of the amino acids; glycine, cysteine, and glutamic acid. The tripeptide can bind spontaneously with electrophiles but more commonly serves as a cofactor and binds via enzymatic conjugation (Igwe, 1986). In the latter reactions, glutathione-S-transferases enzymes catalyze the reaction of the nucleophilic sulfhydryl of glutathione with electrophilic carbon atoms resulting in the formation of a thioether bond. Glutathione-S-transferases are ubiquitous in animals and are located in the highest concentrations in the cytosol of liver, kidney, gut, and other tissues. Compounds that are substrates for the glutathione-S-transferases share three common characteristics: they must be hydrophobic to some degree, they must contain an electrophilic carbon atom, and they must react nonenzymatically with GSH at some measurable rate. These enzymes catalyze the initial step in the formation of N-acetylcysteine (mercapturic acid) derivatives of a diverse group of potentially toxic compounds (Sipes and Gandolfi, 1986).

The GSH conjugates are cleaved to cysteine derivatives, primarily by enzymes located in the kidney. These derivatives can then be acetylated to give N-acetylcysteine (mercapturic acid conjugates). Mercapturic acid conjugates are readily excreted via the urine. The loss of glutamic acid from the GSH conjugate is catalyzed by the enzyme gamma-glutamylpeptidase, a membrane associated enzyme found in high concentrations in cells that exhibit

absorptive or excretory functions. Cysteinyl glycinase catalyses the loss of glycine from the conjugate to yield the cysteine conjugate. Finally, N-acetyl transferase enzymes acetylate the amino group of cysteine to form the mercapturic acid derivative. Acetyl-CoA is needed for the acetylation reaction. Conjugated compounds are then excreted directly in urine, or more usually bile (Sipes and Gandolfi, 1986).

There exists a balance within cells between the rate of intake of reactive compounds and their inactivation by GSH. Factors which affect this balance can markedly alter the toxicity of certain xenobiotics. Cellular stores of GSH may be depleted in 2 ways: 1) directly by binding GSH and thus promoting excretion, or 2) by inhibition of synthesis of the glutathione S-transferase enzymes. Since GSH is also a cofactor for glutathione peroxidase, its depletion can promote lipid peroxidation which can lead to deleterious effects.

Glutathione Biosynthesis

A source of cysteine is important for the biosynthesis of GSH. A dietary source of cysteine is usually required, which tends to make the biosynthesis of GSH follow a cyclic pattern associated with animal photoperiods and associated times of ingestion of meals. Cysteine can also be supplied to animals through direct injection, however, this method is often impractical due to the toxicity of cysteine. Cysteine can also be supplied in the form of pro-drugs which contain cysteine in a bound state such as N-acetyl-L-cysteine (NAC) which has a much lower toxicity than free cysteine.

The dose of NAC given in acetaminophen overdose situations, a compound often used as a model for hepatotoxicity, is 140 mg orally (Savides et al., 1985) or 5.0 mmol/kg orally (Hazelton et al., 198-). Acetaminophen is a common antipyretic agent which is often used as a model for hepatotoxic injury

when administered at toxic concentrations. Acetaminophen-induced (750 mg/kg po) hepatotoxicity in mice is characterized by massive centrilobular congestion which precedes the appearance of necrosis. Liver weights increase when toxic doses of acetaminophen are administered to animals due to pooling of blood in the hepatic sinusoids. Congestion and hypovolemia are reversible and can be largely prevented by administration of the protective compound NAC (1,200 mg/kg po) 3 hours after acetaminophen (Corcoran and Wong, 1986; Corcoran et al., 1985; Walker et al., 1985). The role of NAC is then most often thought of as one of detoxification by direct binding with toxic agents and by increasing the biological pool size of GSH by serving as a precursor. In the acute situation, however, NAC is also known to decrease hepatic GSH content in rats (Estrela et al., 1983; Vina et al., 1980).

L-buthionine sulphoximine (BSO) is an inhibitor of gamma-glutamylcysteine synthetase, an enzyme essential for GSH synthesis. Consequently it lowers tissue GSH concentrations (Drew and Miners, 1984). Administration of BSO has permitted experimental studies on GSH where depleted pools are not replenished due to specific inhibition of GSH-transferases (Sun et al., 1985).

Diethylmaleate (DEM) depletes GSH pools by conjugating with GSH and promoting excretion of bound GSH into bile and urine. Toxic effects of GSH reactive compounds may be enhanced when GSH pools are depleted because excretion of bioactive toxic agents are delayed. The major drawback of the use of DEM in studies of the role of GSH in detoxification are the untoward effects displayed by this compound which are independent of GSH depletion.

Conjugation reactions involving GSH are not always reactions of detoxification. Recently, compounds have been described which have enhanced toxicity following conjugation (Green and Lock, 1984; Igwe, 1986). In these

cases, GSH conjugation reactions activate xenobiotics despite the structural alterations brought about by binding of the toxicant. At least one compound, dichloroethane, is known to ennance toxic manifestations in rat liver when given with disulfiram due to activation as a result of direct GSH binding (Igwe, 1986).

Microcystin-LR (MCLR, microcystin-A, cyanoginosin-LR, toxin BE-2, fast death factor) is a cyclic peptide hepatotoxin produced by the blue-green alga Microcystis aeruginosa. This genus has been associated with numerous toxicoses involving domestic animal and wildlife following ingestion of contaminated water (Carmichael, 1981; Galey et al., 1987). Human toxicosis has been implicated following contamination of municipal water supplies (Hawkins et al., 1985; Falconer et al., 1983). The predominant toxic effects of this compound are markedly liver-specific and consist of hepatocyte necrosis with destruction of sinusoidal endothelium followed by extensive hemorrhage into the liver (Falconer et al., 1981; Runnegar et al., 1981). The observed toxicosis from a lethal dose proceeds rapidly, and death typically occurs within 2 hours of intravenous (iv) or intraperitoneal (ip) administration of a lethal dose.

Little is known about metabolism of MCLR in mammals. Recent reports have presented conflicting data on the effect of phenobarbital induction of membrane bound cytochrome P_{450} metabolism systems in mice (Cote et al., 1986; Brooks and Codd, 1987a). Since the toxin contains both glutamic and ß-methylaspartic acids within its primary structure, it is ionized at biological pH and is an unlikely candidate for membrane bound metabolism. The structure of MCLR contains, N-methyldehydroalanine, an α,ß-unsaturated amino acid of the same type which has been shown to be of toxicologic importance in

structurally related compounds (Dahlem et al., 1987). This dehydroamino acid is also believed to be susceptible to glutathione (GSH) conjugation. Since GSH binding reactions occur principally within the cytosol where the MCLR molecule likely resides; we investigated the role of GSH on the toxicity of this algal hepatotoxin.

MATERIALS AND METHODS

MCLR was isolated from a semi-continuous unialgal laboratory culture of Microcystis aeruginosa (strain PCC-7820) in the laboratories of W. Carmichael by the method of Krishnamurthy et al. (1986). Toxin integrity was assessed by the methods of Harada et al. (1988), and all materials were found to be greater than 95% pure prior to dosing of animals. MCLR was dissolved in deionized water and warmed to 37°C prior to animal dosing.

The L-isomer of buthionine sulphoximine (BSO) was obtained from Chemical Dynamics Co., Plainfield, NJ, USA, dissolved in saline (40 mg/mL) and used at a dose of 1 g/kg body weight. Diethylmaleate (DEM) and N-acetylcysteine (NAC) were purchased from Sigma Chemical Company, St. Louis, MO, USA. DEM was mixed with corn oil (1:19, DEM-corn oil, V/V) and used at a dose of 1 g/kg body weight. All other chemicals were reagent grade, and all solvents were distilled in glass.

Treatments to adjust hepatic GSH levels in male Swiss Webster mice (20 to 25 g, Harlin Sprague Dawley, Indianapolis, IN) were randomly assigned to 1 of 4 groups and treated as follows:

Group	Feeding Status	Treatment
I	Fed	Saline
II	Fasted	Saline
III	Fasted	NAC
IV	Fasted	DEM+BSO

Ninety minutes following the treatments, 5 to 7 animals from each group were killed by decapitation for the estimation of hepatic GSH content as described below. The remaining animals were injected with MCLR (55 µg/kg body weight) and monitored for time of death. Animals which survived 4 hours following toxin administration were killed by cervical dislocation. The livers were removed from all animals blotted dry and weighed. Liver weight was expressed as a percentage of animal body weight in order to normalize the data. Hepatic GSH content in toxin-treated mice was not measured directly following toxin administration since the liver was engorged with blood. Measurement of hepatic GSH content under blood swollen conditions would only have yielded anomalous values which would have been difficult to interpret. Hence, we chose to measure hepatic GSH content in mice immediately prior to dosing with the toxin. Toxin-treated mice were given MCLR dissolved in deionized water by ip administration. Negative control animals were given the appropriate vehicles.

For measurement of hepatic GSH content, the liver was removed and homogenized with 5 mL of 4% sulfosalicylic acid. The homogenate was centrifuged at 20,000 x g* for 20 minutes, and then an aliquot of the protein-free supernatant fraction was used for GSH determination using glutathione-S-transferase method described by Asaoka and Takahashi (1981).

Glutathione conjugation at the N-methyldehydroamino Acid--Microcystin-LR and -RR. The microcystins (3.12 mole) were dissolved in 5% K_2CO_3 (aq, 0.8 ml, pH 10) in individual tubes. Glutathione (31.2 mole) was added slowly to the toxin solution and stirred continuously for 2 hours. After the reaction period, the solution was neutralized with 0.2 N HCl a placed on preconditioned Baker C-18 cartridges. The cartridge was rinsed with 2.0 ml of

water and the reaction product was eluted with 2.0 ml of methanol and evaporated to dryness under a stream of nitrogen. The final isolation of the glutathione adduct of the microcystins (Figure 1) was accomplished by reverse phase HPLC using a C-18 column and a mobile phase ratio of 58:42 of methanol to 0.05 M phosphate buffer (pH 3). The identity of the glutathione adducts were confirmed by fast atom bombardment mass spectroscopy with characteristic masses of parent compound plus adduct (Figure 2).

The location of the adduct at the dehydroamino acid was confirmed by the disappearance of the two olefinic protons at 5.85 and 5.35 ppm in the parent toxins by 1H-NMR spectroscopy (Figure 3). Mice were given the GSH adduct product ip.

Histopathology

Sections of liver, lung, kidney, heart, spleen, and intestine were fixed by immersion in 10% neutral, buffered formalin for histological examination. After fixation, the sections were routinely processed, embedded in paraffin, cut at 4 to 6 μm, and stained with hematoxylin and eosin.

RESULTS AND DISCUSSION

The effect of GSH depletion on the apparent survival times of animals dosed with MCLR following fasting and treatment are shown in Figure 4. The absolute survivability was similar for the test groups but there were slight differences in the mean survival times of groups of nonsurvivors. There were no significant differences in liver weights as a percentage of whole body weights among animals that died, indicating a similar lethal action in the animals given toxin alone and the GSH-depleted, toxin-treated mice. Even though NAC is most often thought of as a precursor for GSH synthesis, in the acute situation the effect is often one of depletion rather than augmentation

(Estrela et al., 1983). As shown in Table 1, NAC-treatment caused less of a GSH depletion than that induced by DEM+BSO. The intermediate degree of GSH depletion by NAC was accompanied by an intermediate increase in mean survival time, as compared to the more pronounced effects in the BSO+DEM treated animals. These trends (Figure 4) are consistent with a hypothesis that a decrease in GSH content would prolong survival in MCLR exposed animals.

Runnegar et al. (1987) have recently reported that hepatocyte GSH concentrations decrease following administration of MCLR. In that study, morphologic changes in cells were observed before large depletions of GSH were observed, thus the authors concluded that a small pool of GSH within the cell is critical for maintenance of cytoskeletal structure or that activation of phosphorylase A cannot be a consequence of thiol depletion. The present study supports their conclusion and gives further evidence that GSH is important for the observed hepatotoxic effects.

The results of the toxicity testing of the GSH-adduct of MCLR are reported in Table 1. The binding of GSH to MCLR results in a product which has slightly reduced bioactivity but which remains potent and highly hepatotoxic. The survival times of treated animals were slightly longer than those of MCLR-treated positive controls; but this was expected because of the increased hydrophilic nature of the GSH adduct product. Animals which died acutely following administration of the GSH adduct product had liver weights which were similar to animals which died acutely following MCLR administration. Animals which survived for 24 hours following GSH adduct administration had organ weights which were similar to survivors of MCLR administration and vehicle treated controls.

Mice dosed ip with the GSH adduct product at 0 to 400 µg/kg had no treatment associated lesions in any of the tissues examined. In the animals dosed with 600 to 1,000 µg/kg, treatment associated lesions were similar and were present in the livers of all mice that died and in the lungs of 2 of the 4 at 600 µg/kg and in all of the lungs at 800 and 1,000 µg/kg. The hepatic lesion was characterized by severe, widespread centrilobular and midzonal hepatocyte disassociation and rounding which frequently extended into periportal regions. This was accompanied by breakdown of the sinusoidal endothelium resulting in severe hemorrhage in these areas. These lesions appeared identical to those seen in mice that died following microcystin-LR administration (Hooser et al., 1989). The liver of the mouse which survived the administration of 600 µg/kg had numerous, large centrilobular to midzonal areas of hemorrhage and hepatocyte disassociation and necrosis; however, cells and their nuclei were extremely pale staining. Small numbers of neutrophils intermixed with the cellular debris were present. Lung lesions were limited to the presence of variably sized clumps of eosinophilic material within the pulmonary capillaries. This material occasionally contained pyknotic nuclei and/or a few, small, clear intracytoplasmic vacuoles and presumably was hepatocyte debris.

The results of this experiment clearly show that the GSH adduct of MCLR is a potent hepatotoxic compound. The toxicity is reduced when administered intraperitoneally to mice but the compound remains highly toxic and hepatospecific. We found that reduction in hepatic GSH concentrations seemed to result in a brief prolongation of survival times in toxin-treated mice. In addition, we found that the GSH adduct of MCLR retains potent hepatotoxicity.

Altered delivery of MCLR to the target cell in the liver may be the reason for the reduction in toxicity of the adduct compound as compared with parent MCLR. Conjugation with GSH occurs in the cytosol or mitochondria of the cell and conjugation before uptake into the cell probably results in a reduced membrane solubility. However, effects on receptor affinity could be either diminished or enhanced. Further investigation will be necessary to answer this question.

These results show that conjugation of MCLR with GSH does not result in significant detoxification of the MCLR molecule. The extent of conjugation in vivo has yet to be determined in independent studies but toxicity evaluation of the GSH adduct predicts that GSH conjugation may not greatly aid detoxification of MCLR.

Table 1. Toxicity of microcystin-glutathione adduct in mice dosed intraperitoneally.

Dose (µg/kg)	Survival Time (min)	Liver Weight % BW	$\bar{x}$	SD	Kidney Weight % BW	$\bar{x}$	SD
0	1,440	5.60			1.72		
0	1,440	6.72			1.82		
0	1,440	5.70			1.87		
0	1,440	6.97			1.76		
0	1,440	5.37	6.07	± 0.65	1.69	1.77	± 0.07
200	1,440	5.36			1.54		
200	1,440	6.09			1.85		
200	1,440	5.13			1.53		
200	1,440	6.21			1.80		
200	1,440	6.47	5.85	± 0.52	1.74	1.69	± 0.13
400	1,440	7.06			1.73		
400	1,440	6.60			2.06		
400	1,440	6.82			1.84		
400	1,440	6.00			1.69		
400	1,440	5.15	5.73	± 1.52	1.52	1.77	± 0.18
600	326	9.37			1.90		
600	431	9.07			1.97		
600	346	9.82			2.06		
600	311	9.85			1.74		
600	1,440	6.56	8.93	± 1.22	1.61	1.86	± 0.16
800	329	9.77			2.17		
800	226	9.72			2.09		
800	312	9.59			2.15		
800	233	9.83			2.06		
800	257	9.41	9.66	± 0.15	2.07	2.11	± 0.04
1,000	252	9.57			2.20		
1,000	223	10.20			2.07		
1,000	395	9.82			2.06		
1,000	253	9.40			1.85		
1,000	222	9.69	9.74	± 0.27	2.15	2.07	± 0.12

Table 2. Hepatic glutathione concentrations in mice prior to microcystin-LR treatment.

Treatment Group	GSH Concentration (umole g liver)[1]	Number of Animals
Fasted	5.58 ± 0.68	5
Fed	6.80 ± 0.30	7
NAC	3.21 ± 0.38	7
BSO+DEM	0.24 ± 0.10	6

[1] Mean ± Standard error of the mean

Figure 1. Glutathione adduct of microcystin-LR.

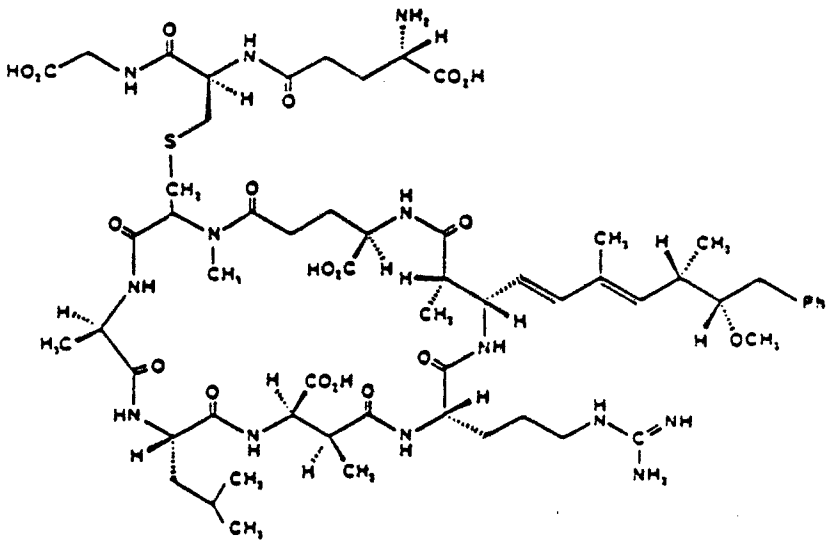

Figure 2. Mass spectrum of glutathione-bound microcystin-LR.

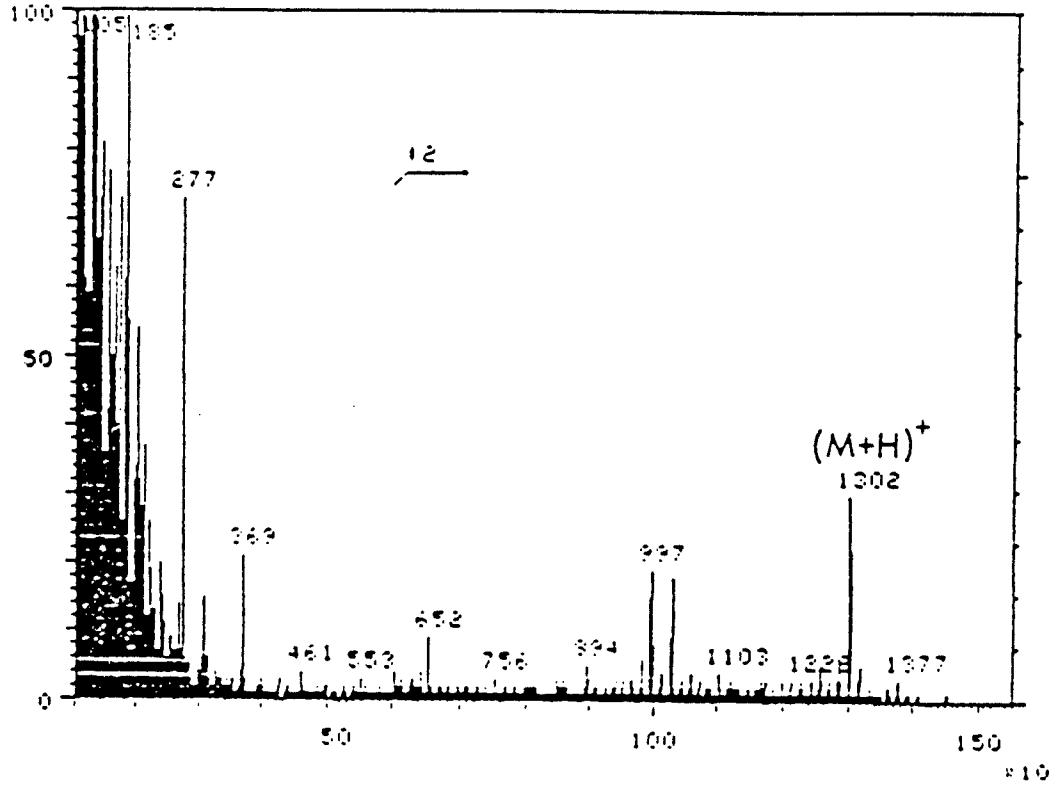

Figure 3. ^{1}H-NMR spectrum of glutathione-bound microcystin-LR.

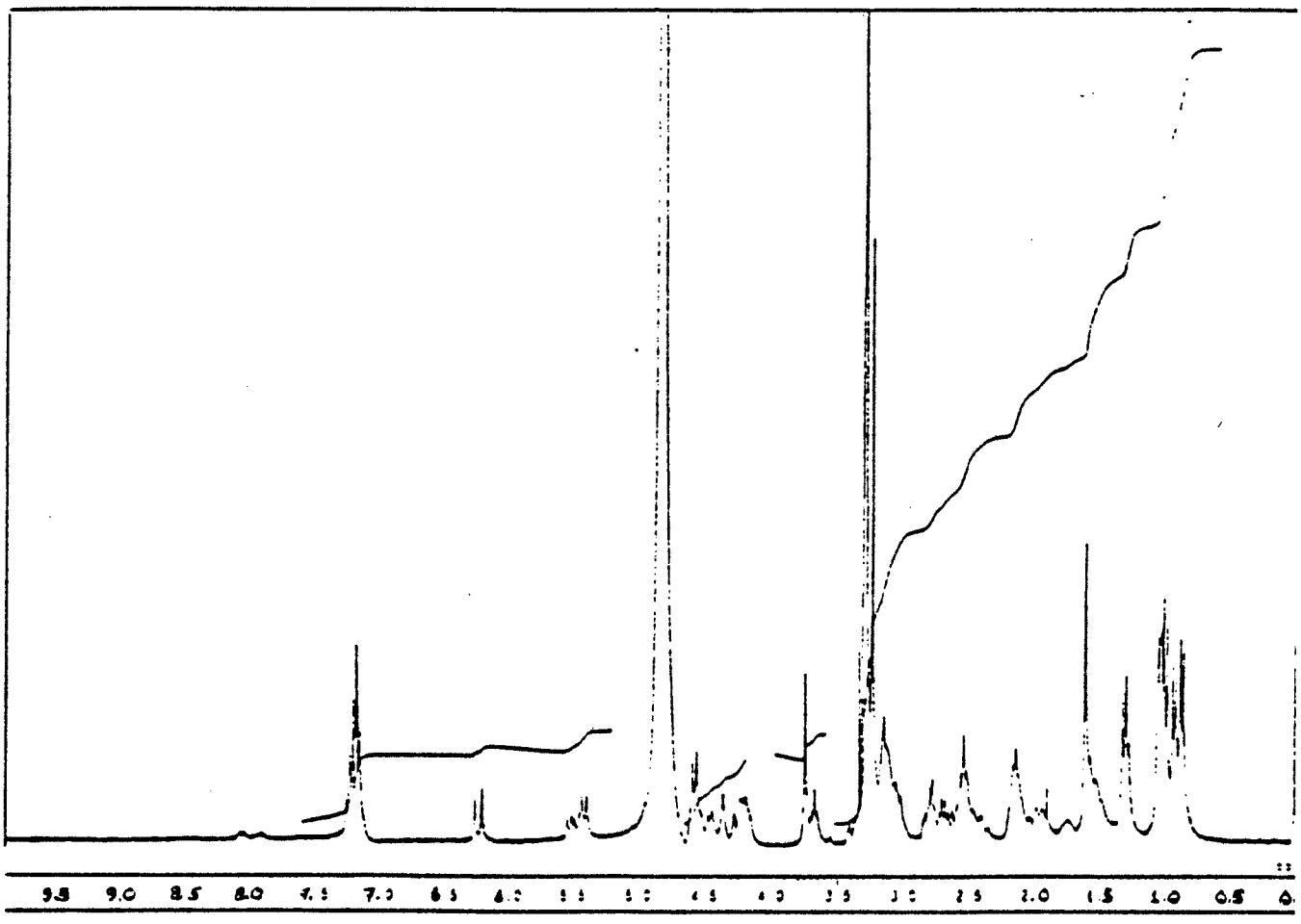

Figure 4. Relative survival over time in glutathione-depleted, toxin-treated mice. NAC = N-acetylcysteine, DEM = dicthylmaleate, BSO = buthionine sulfoximine. (N = 16 animals/group with the exception of N-acetylcysteine-treated animals where N = 10.)

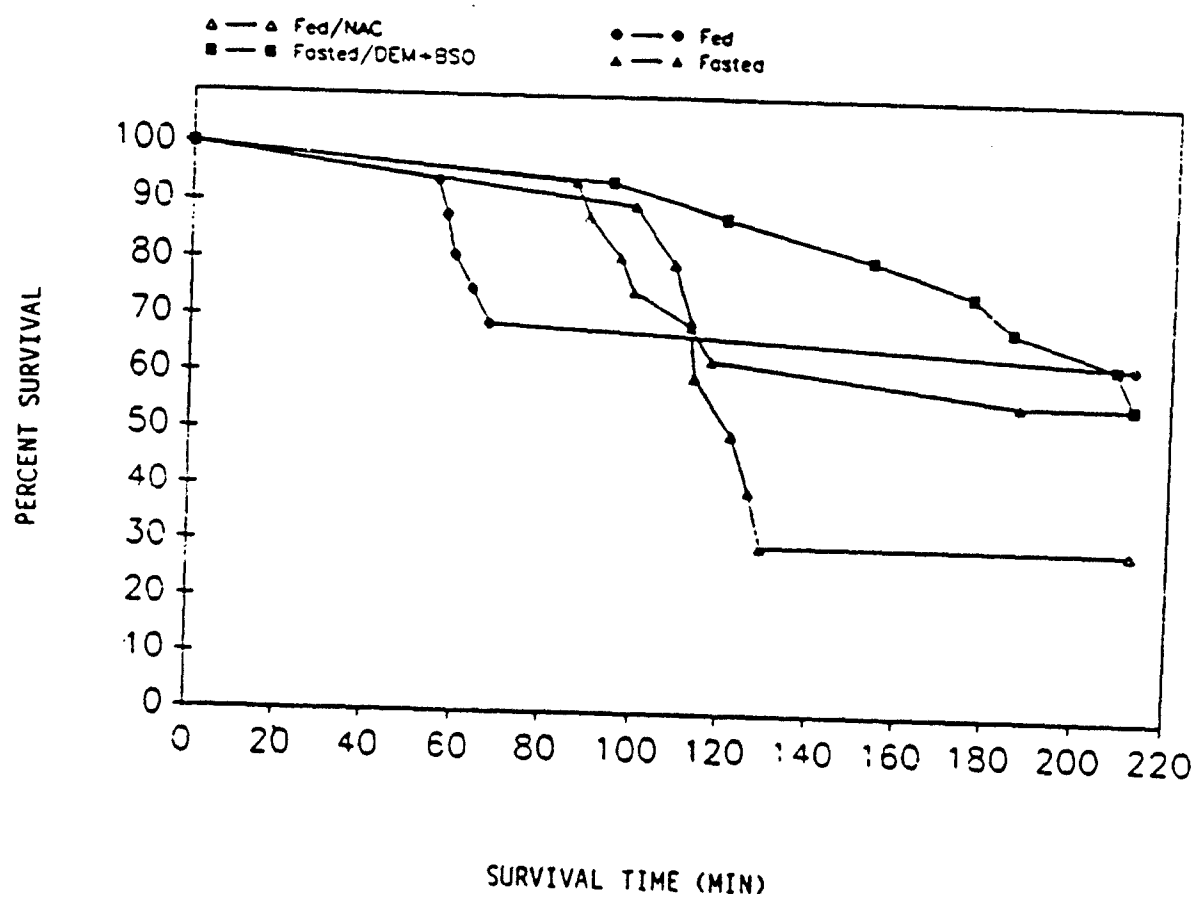

IV. FORMATION OF SYNTHETIC DERIVATIVES OF PEPTIDE TOXINS FOR STRUCTURE/TOXICITY RELATIONSHIP STUDIES

A. M. Dahlem, K.-I. Harada, M. Namikoshi, C. Chen, K. L. Rinehart

INTRODUCTION

Formation of derivatives of parent peptide toxins from cyanobacteria will yield products with altered toxicity and bioactivity and will provide insight into which portions of the cyclic peptide structure are essential for bioactivity.

In our previous experiments we have described the effects of saturation of the N-methyl dehydroalanine portion of MCLR on whole animal toxicity. We found that reduction of this portion of the molecule resulted in a slight decrease in the toxicity but that the compound remained potent and highly hepatotoxic (Dahlem et al., 1987). In other experiments, we saturated MCLR with hydrogen gas and a paladium catalyst and found that reduction of the molecule at the points of unsaturation in ADDA greatly reduced the observed toxicity (Dahlem, 1989).

The purpose of this study was to assess the effect of removal of the ADDA portion of the molecule on the resulting bioactivity of the product. In these experiments, the cyclic nature of the compound was preserved but the hydrophobic portion of the molecule was removed.

MATERIALS AND METHODS

Microcystin-LR (MCLR) was subjected to ozonolysis for 30 minutes then reduced with excess sodium borohydride to yield a cyclic peptide structure which lacked all points of unsaturation (Figure 1). Additional MCLR was first reduced with sodium borohydride to form the dihydro derivative which results

from hydrogen addition to the α,β-unsaturated N-methyl alanine then subjected to ozonolysis and reduced with sodium borohydride to yield another cyclic product which lacked points of unsaturation (Figure 2). The toxin derivatives were purified and separated from parent compounds by Bond Elut columns and HPLC and confirmed by FAB/MASS.

Male, Swiss Webster mice (Harlin Sprague-Dawley, Indianapolis, IN) were used in all toxicity trials. Animals were dosed intraperitoneally with the saline vehicle, parent toxin, or the appropriate purified toxin ozonolysis derivative and monitored for 24 hours. Animals which survived this observation period were killed by cervical dislocation. Survival times and whole body, liver, and kidney weights were recorded. Liver, kidneys, spleen, small and large intestines, and heart were examined grossly for lesions.

Sections of liver, lung, kidney, heart, spleen, and intestine were fixed by immersion in 10% neutral buffered formalin for histologic examination. After fixation, the sections were routinely processed, embedded in paraffin, cut at 4 to 6 μm and stained with hematoxylin and eosin.

RESULTS AND DISCUSSION

These derivatives caused no detected toxic effects and no treatment-related lesions were seen in any of the tissues examined, throughout the range of concentrations administered (Tables 2 and 3). A summary of the toxigenic potential of all derivatives formed to date is shown in Table 1. It appears that the alterations explored to date in the α,β-unsaturated amino acids result in decreases in toxicity but do not change the hepatospecific properties of the molecule; however, alterations in the ADDA moiety produce marked reductions in lethal toxicity and hepatic damage. These data demonstrate that ADDA is an essential component for the hepatotoxic properties of microcystin-LR.

Table 1. Comparative toxicity of synthetic derivatives of cyclic peptide toxins from cyanobacteria.

Toxin	Molecular Weight	LD_{100} (Min)
Nodularin	824	97 nM/kg
Dihydro-Nodularin	826	605 nM/kg
Microcystin-LR	994	90 nM/kg
Dihydro-Microcystin-LR	996	201 nM/kg
GSH-Microcystin-LR	1,301	461 nM/kg
Hexahydro-Microcystin-LR	1,000	> 2,000 nM/kg
Ozonolysis $Product_1$ of Microcystin-LR	800	> 16,000 nM/kg
Ozonolysis $Product_2$ of Microcystin-LR	799	> 16,000 nM/kg

Table 2. Dose range finding study for microcystin ozonolysis product1.

Toxin	Dose (mg/kg)	Surv Time (Min)	Liv Wt %	$\bar{X}$	SD	Kid Wt %	$\bar{X}$	SD	Spl Wt %	$\bar{X}$	SD	Lung Wt %	$\bar{X}$	SD
MCLR	0	1,440	5.62			1.68			0.32			1.78		
MCLR	0	1,440	6.05	5.84 ±	0.22	1.80	1.74 ±	0.06	0.45	0.39 ±	0.07	1.75	1.77 ±	0.02
MCLR	50	1,440	5.76			1.72			0.35			1.77		
MCLR	50	1,440	5.65	5.71 ±	0.06	1.95	1.84 ±	0.12	0.37	0.36 ±	0.01	1.85	1.81 ±	0.04
MCLR	100	147	9.73			2.00			0.35			1.30		
MCLR	100	150	9.65	9.69 ±	0.04	2.08	2.04 ±	0.04	----	----	----	1.88	1.59 ±	0.29
OZ	0	1,440	6.48			2.01			0.50			1.56		
OZ	0	1,440	5.71			1.60			0.35			2.17		
OZ	0	1,440	7.41			2.00			0.41			1.76		
OZ	0	1,440	6.53	6.53 ±	0.60	1.78	1.85 ±	0.17	0.35	0.40 ±	0.06	1.73	1.81 ±	0.22
OZ	100	1,440	5.78			1.90			0.40			1.56		
OZ	100	1,440	5.37	5.58 ±	0.21	1.77	1.84 ±	0.07	0.30	0.35 ±	0.05	1.97	1.77 ±	0.21
OZ	200	1,440	5.43			2.01			0.49			1.74		
OZ	200	1,440	6.54	5.99 ±	0.56	1.47	1.74 ±	0.27	1.38	0.44 ±	0.06	1.42	1.58 ±	0.16
OZ	400	1,440	6.01			1.76			0.43			2.18		
OZ	400	1,440	5.83	5.92 ±	0.09	1.72	1.74 ±	0.02	0.42	0.43 ±	0.01	1.88	2.03 ±	0.15
OZ	800	1,440	5.47			1.47			0.37			2.53		
OZ	800	1,440	5.56	5.52 ±	0.05	1.75	1.61 ±	0.14	0.41	0.39 ±	0.02	2.34	2.44 ±	0.10
OZ	1,600	1,440	5.74			1.69			0.41			1.59		
OZ	1,600	1,440	6.38	6.06 ±	0.32	1.91	1.80 ±	0.11	----	----	----	----	----	----
OZ	3,200	1,440	6.48			1.91			0.35			1.91		
OZ	3,200	1,440	6.65	6.57 ±	0.09	1.65	1.78 ±	0.13	0.48	0.42 ±	0.07	1.38	1.65 ±	0.27
OZ	6,400	1,440	6.08			1.64			0.41			1.93		
OZ	6,400	1,440	6.49	6.29 ±	0.21	1.73	1.69 ±	0.05	0.32	0.37 ±	0.05	2.11	2.02 ±	0.09
OZ	12,800	1,440	5.94			1.67			0.44			1.89		
OZ	12,800	1,440	6.12	6.03 ±	0.09	1.70	1.69 ±	0.02	0.42	0.43 ±	0.01	1.58	1.74 ±	0.16

Table 3. Dose range finding study for microcystin ozonolysis product$_2$.

Toxin	Dose (mg/kg)	Surv Time (Min)	Liv Wt %	$\bar{X}$	SD	Kid Wt %	$\bar{X}$	SD	Spl Wt %	$\bar{X}$	SD
MCLR	0	1,440	5.02			1.24			0.27		
MCLR	0	1,440	5.08	5.05	± 0.04	1.16	1.20	± 0.06	0.28	0.28	± 0.01
MCLR	50	1,440	5.20			1.25			0.32		
MCLR	50	1,440	5.04	5.12	± 0.11	1.27	1.26	± 0.01	0.37	0.35	± 0.04
MCLR	100	143	8.35			1.61			0.38		
MCLR	100	157	8.36	8.36	± 0.01	1.37	1.49	± 0.17	0.31	0.35	± 0.05
OZ	0	1,440	4.94			1.27			0.29		
OZ	0	1,440	4.94	4.94	± 0.00	1.30	1.29	± 0.02	0.32	0.31	± 0.02
OZ	100	1,440	5.24			1.12			0.32		
OZ	100	1,440	5.29	5.27	± 0.35	1.38	1.25	± 0.18	0.33	0.33	± 0.01
OZ	200	1,440	4.67			1.31			0.33		
OZ	200	1,440	5.09	4.88	± 0.30	1.35	1.33	± 0.03	0.32	0.33	± 0.01
OZ	400	1,440	5.25			1.28			0.25		
OZ	400	1,440	5.16	5.21	± 0.06	1.20	1.24	± 0.06	0.27	0/26	± 0.01
OZ	800	1,440	5.14			1.25			0.28		
OZ	800	1,440	5.14	5.14	± 0.00	1.31	1.28	± 0.04	0.41	0.35	± 0.09
OZ	1,600	1,440	5.71			1.38			0.29		
OZ	1,600	1,440	4.79	5.25	± 0.65	1.43	1.41	± 0.04	0.32	0.31	± 0.02
OZ	3,200	1,440	5.81			1.40			0.34		
OZ	3,200	1,440	5.63	5.72	± 0.13	1.21	1.31	± 0.13	0.33	0.34	± 0.01
OZ	6,400	1,440	6.04			1.24			0.28		
OZ	6,400	1,440	5.53	5.79	± 0.36	1.30	1.27	± 0.04	0.37	0.33	± 0.06
OZ	12,800	1,440	5.92			1.28			0.28		
OZ	12,800	1,440	5.46	5.69	± 0.33	1.37	1.33	± 0.06	0.35	0.32	± 0.05

Figure 1. Microcystin-LR ozonolysis product #1.

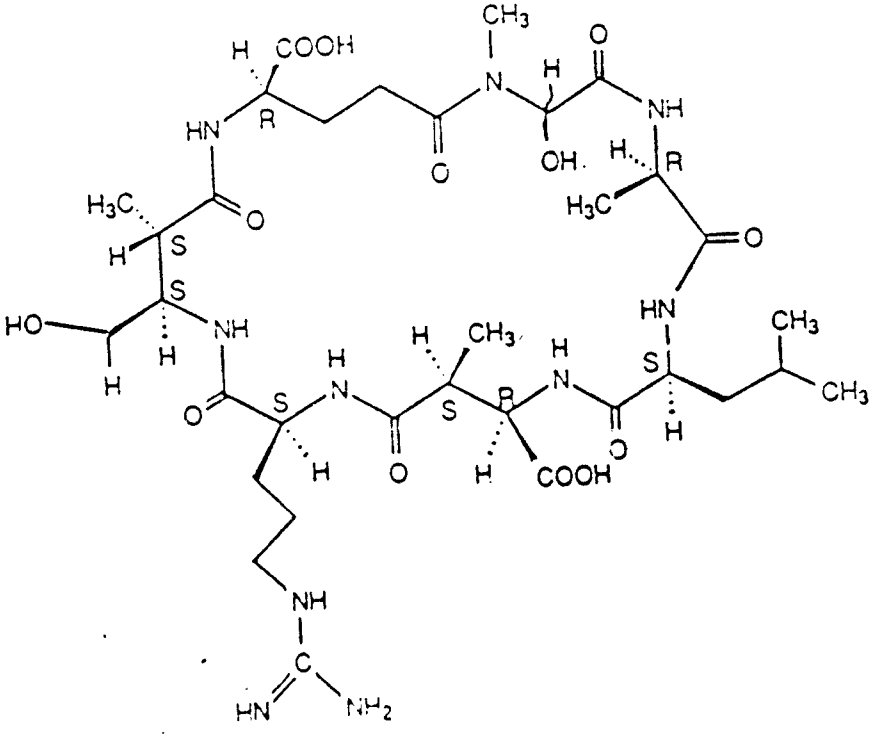

Figure 2. Microcystin-LR ozonolysis product #2.

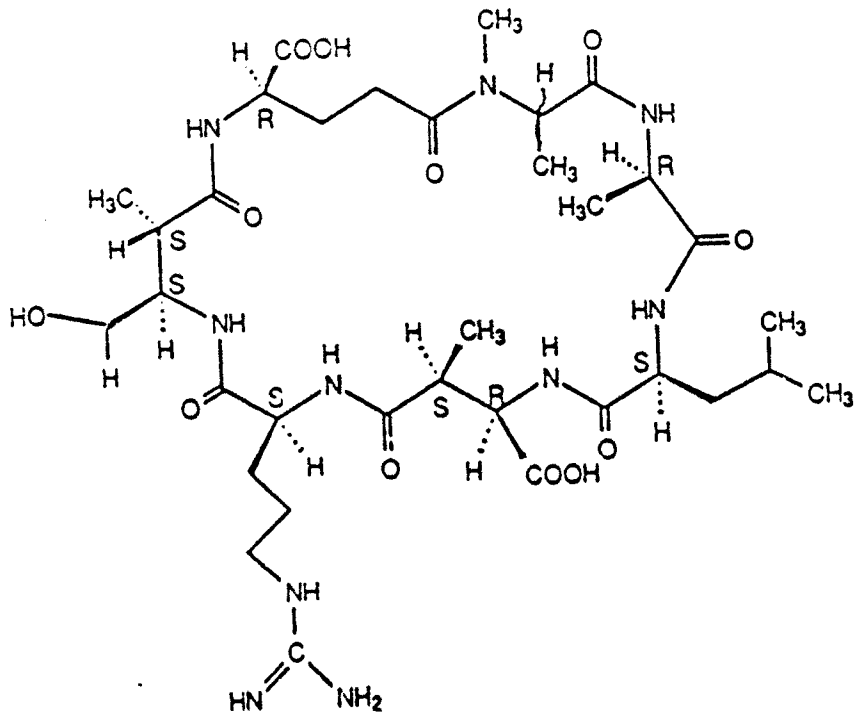

V. CYTOSKELETAL ALTERATIONS IN RAT HEPATOCYTES INDUCED IN VIVO AND IN VITRO BY MICROCYSTIN-LR, A HEPATOTOXIN FROM T-E BLUE-GREEN ALGA, MICROCYSTIS AERUGINOSA

Stephen B. Hooser, Mark S. Kuhlenschmidt, Wanda M. Haschek

ABSTRACT

Microcystin-LR (MCLR) is a cyclic heptapeptide hepatotoxin (MW = 994) produced by the blue-green alga, Microcystis aeruginosa. The morphologic effects of MCLR on rat hepatic parenchymal cells (hepatocytes) and nonparenchymal cells (primarily sinusoidal endothelial and Kupffer cells) in suspension were compared. Also evaluated were the effects of MCLR on actin filaments of hepatocytes in vivo and in primary monolayer cultures of hepatocytes in vitro. Alterations of actin filaments in hepatocytes exposed in vitro were compared to those induced by phalloidin and cytochalasin B. MCLR was added to suspensions of rat hepatic parenchymal and nonparenchymal cells at concentrations of 0.1, 1.0, or 10.0 µg/ml. The phosphate-buffered saline (PBS) vehicle was added to control cell suspensions. For studies in vivo, rats were given intraperitoneal injections of PBS (controls) or a lethal dose of MCLR (180 µg/kg) and killed at 5, 10, 20, 30, 45, and 60 minutes postdosing. Frozen liver sections were then stained with rhodamine phalloidin. The addition of MCLR to hepatocytes in suspension caused rapid (10 minutes), dose-dependent blebbing of the plasma membrane which progressed in extent and severity with time. In suspension, nonparenchymal cells and hepatocytes treated with PBS were unaffected. Primary hepatocyte cultures were treated with 0.1, 1.0, or 10.0 µg of MCLR/ml, 10.0 µg of phalloidin/ml or 10.0 µg of cytochalasin B/ml, fixed, and stained with rhodamine-labelled

phalloidin for filamentous actin. The number of cells affected by MCLR was dose dependent. Six hours postdosing with 0.1 µg of MCLR/ml, very few hepatocytes were affected. The number of cells having morphologic and actin filament changes increased, with greater than 75% of all cells affected by 6 hours after exposure to 1.0 and 10.0 µg of MCLR/ml. Over a period of 6 hours at 10 µg of MCLR/ml, there was a progression of lesions in the cultured hepatocytes. One hour after dosing, scattered cells had 1 or 2 small blebs in the plasma membrane with actin localized at their bases. Many hepatocyte blebs had one or more rays of actin extending from the actin localized at their bases to the tips. At 3 hours postdosing, affected cells were comprised of numerous plasma membrane blebs, each with a thickened ray of actin extending from the base to the tip. By 6 hours after initial exposure to MCLR, most of the cells were affected with numerous plasma membrane blebs and centrally condensed actin. Six hours postdosing with phalloidin, plasma membrane blebbing was evident and filamentous actin had aggregated into numerous, variably sized, intracytoplasmic foci. Also at 6 hours, cytochalasin B had caused hepatocyte plasma membrane blebbing and a change from a linear orientation of actin filaments to numerous, small foci of actin scattered throughout the cytoplasm. In vivo, hepatocyte actin filament alterations were present at 20 minutes after initial exposure to MCLR while morphologic alterations seen by H&E staining were not present until 30 minutes postdosing. Thus, in suspension, MCLR causes toxin-related plasma membrane blebbing in hepatocytes but not sinusoidal endothelial or Kupffer cells, indicating that hepatocytes and not nonparenchymal hepatic cells are the primary target cells. In hepatocyte culture, MCLR causes plasma membrane blebbing and cell deformation accompanied by rearrangement of actin filaments

which is distinct from that caused by phalloidin or cytochalasin D. Alterations in hepatocyte actin filaments also occur *in vivo* and precede other morphologic changes. The results of work both *in vitro* and *in vivo* suggest that morphologic lesions *in vivo* caused by microcystin-LR toxicosis are due to alterations in hepatocyte actin filaments with numerous secondary lesions occurring thereafter.

Studies with purified MCLR in rats and mice show that it is specifically toxic to the liver. However, the mechanism of action of MCLR is unknown. This toxicosis is characterized by rapid (within 30 minutes), progressive, centrilobular hepatocyte rounding, dissociation, and necrosis, with breakdown of the sinusoidal endothelium resulting in massive intrahepatic hemorrhage (Falconer et al., 1981; Hooser et al., 1988). Ultrastructurally, hepatocyte-to-hepatocyte separation, hepatocyte plasma membrane invagination, loss of plasma membrane microvilli, as well as subsequent sinusoidal endothelial breakdown, precede cellular degeneration and necrosis (Hooser et al., 1988). However, previous studies utilizing sequential scanning electron microscopy and transmission electron microscopy (TEM) of murine livers following intraperitoneal administration of an aqueous *M. aeruginosa* extract showed a progressive breakdown of sinusoidal endothelium, disappearance of the space of Disse, damage to hepatocyte membranes, and "necrotic changes" in hepatocyte cytoplasm (Falconer and Runnegar, 1981). Hence, some question remains as to the hepatic cell type which is initially affected by MCLR, hepatocytes or the nonparenchymal hepatic cells (primarily sinusoidal endothelial or Kupffer cells). Suspensions of hepatocytes treated with MCLR undergo rapid (5 minutes postdosing) plasma membrane blebbing without cell death (as indicated by morphology, intracellular enzyme release, or trypan

blue uptake) (Aune and Berg, 1986; Runnegar and Falconer, 1981, 1982, 1986). Based on light microscopic, TEM, and suspension findings, it has been hypothesized that cytoskeletal alteration was an early intracellular event in affected cells as it is with hepatocytes treated with phalloidin (prevents depolymerization of actin filaments) or cytochalasin B (prevents assembly of actin filaments) (Sager et al., 1986).

The objectives of this study were: 1) to identify the primary hepatic cell type(s) affected by MCLR in suspension, 2) to characterize morphologic changes and to determine whether there is an association between these and alterations in the arrangement of actin filaments within affected cultured hepatocytes, 3) to compare MCLR-related actin filament alterations to those caused by phalloidin and cytochalasin B in hepatocyte culture, and 4) to determine if MCLR also causes alterations of actin filaments in hepatocytes in vivo and whether these are related to the morphologic lesions seen by light microscopy.

MATERIALS AND METHODS

Animals

Male, 175 to 200 g Sprague-Dawley rats (Harlan Sprague-Dawley, Inc., Indianapolis) were obtained and allowed to acclimate for 2 weeks or longer before use. Animals had free access to a commercial laboratory animal ration and water and were maintained on a 12-hour light-dark cycle. Rats were not fasted prior to use.

Toxin

Microcystin-LR (MCLR) (approximately 95% pure) from Microcystis aeruginosa laboratory strain 7820 was produced and purified in our (W. W. Carmichael) laboratory by techniques that include methanol/butanol extraction of algal

cells, centrifugation, Sephadex filtration, and purification by high performance liquid chromatography (Krishnamurthy et al., 1986). Microcystin-LR was dissolved in phosphate buffered saline prior to use.

Hepatic Parenchymal and Nonparenchymal Cell Isolation

Rat hepatic parenchymal (hepatocytes) and nonparenchymal (primarily sinusoidal endothelial and Kupffer) cells were isolated by previously described collagenase perfusion methods (Kuhlenschmidt et al., 1982; Wanson and Mosselmans, 1980; Lafranconi et al., 1986). Centrifugation was used for hepatocyte isolation followed by pronase digestion of the supernatant and metrizamide gradient centrifugation to isolate nonparenchymal cells (Kuhlenschmidt et al., 1982; Wanson and Mosselman, 1980; Lafranconi et al., 1986). Nonparenchymal cells were identified by their size and morphology. The cell pellets were resuspended in Ham's F-10 medium containing (per 500 ml) 100 ml of fetal bovine serum, 0.3 ml of insulin and, if used for subsequent culturing, 1.0 ml of gentamicin (50 mg/ml) and 6 ml of a combination of penicillin (10,000 U/ml) and streptomycin (10 mg/ml).

Toxin Exposure, Cell Suspension, Culture and Fixation

For cell suspension studies, 2 ml of the cell suspensions (1×10^6 cells/ml) were placed in 5 ml cell suspension tubes to which were added 2 ml of phosphate-buffered saline (PBS; pH = 7.4), or 2 ml of MCLR in PBS at a final concentration of 0.1, 1.0, or 10.0 µg of MCLR/ml. The addition of PBS or MCLR was designated as time 0. The cells were incubated with mild agitation at 37°C. At 10, 20, and 30 minutes, aliquots of cells were removed for immediate microscopic examination or for fixation in 10% neutral-buffered formalin (Aune and Berg, 1986; Runnegar and Falconer, 1981, 1982).

For cell culture studies, hepatocytes suspended in complete Ham's F-10 medium were added to Lux 8-well tissue culture plates, each of which contained a 22-mm-square glass coverslip. The cells were initially seeded at a subconfluent concentration of 1×10^5 cells/ml and were allowed to spread for 24, 48, or 72 hours with changes of fresh media every 24 hours. The hepatocytes were incubated in a water-jacketed incubator at 37°C in air:CO_2, 95:5.

Seventy-two-hour monolayer cultured hepatocytes were treated with PBS or MCLR in PBS at a final concentration of 0.1, 1.0, or 10.0 µg/ml. At 6 hours (0.1 and 1.0 µg/ml) and at 1, 2, 3, 4, 5, and 6 hours (10.0 µg/ml) posttreatment, replicates of the cells had the media removed, were washed with PBS, fixed with fresh 3.7% paraformaldehyde in PBS and permeabilized with 0.5% Triton X-100.

Twenty-four-, 48-, and 72-hour cultured hepatocytes were treated with PBS, 10.0 µg MCLR/ml, 10.0 µg phalloidin/ml, or 10.0 µg cytochalasin B/ml. At 6 hours postdosing on each of the 3 days, replicates of the cells had the media removed, were washed with PBS, fixed with fresh 3.7% paraformaldehyde in PBS, and permeabilized with 0.5% Triton X-100 in PBS.

Lactate Dehydrogenase Determination

After 30 minutes of incubation with PBS or MCLR, the hepatocyte and nonparenchymal cell suspensions were centrifuged at 4°C (to stop cellular reactions) at 700 x g for 2 minutes (hepatocytes) or 1,500 x g for 15 minutes (nonparenchymal hepatic cells). The supernatant was removed and immediately frozen for subsequent LDH analysis and the cells were fixed with 10% neutral-buffered formalin. For the experiment involving exposure of 72-hour cultured hepatocytes to 10 µg of MCLR/ml or PBS for 1, 2, 3, 4, 5, or 6 hours,

the media was removed prior to washing with PBS and was immediately frozen for LDH determination.

Study of MCLR In Vivo

Twenty-one rats were randomly assigned to 7 groups of 3 rats each and given an intraperitoneal injection of a consistently lethal dose of MCLR (180 µg of MCLR/kg) or of PBS (controls). At 60 minutes following PBS administration (controls) or at 5, 10, 20, 30, 45, and 60 minutes following MCLR administration, the 3 rats from each time group were killed by ether inhalation, the livers removed and sectioned, and these sections covered with optimal cutting temperature fluid (a cryoprotectant) and frozen in liquid nitrogen. They were subsequently cryosectioned using a cryomicrotome and placed on slides. Adjacent liver sections from each rat were also fixed in 10% neutral buffered formalin and routinely processed, paraffin embedded, cut at 4 to 6 µ, and stained with hematoxylin and eosin.

Use of Rhodamine-Labelled Phalloidin for Visualization of Actin

Filamentous actin in cultured hepatocytes and in frozen liver sections was visualized by using rhodamine-labelled phalloidin (Molecular Probes, Eugene, OR) in accordance with a previously described procedure (Zachary et al., 1986). The frozen liver sections and the fixed, permeabilized hepatocytes on coverslips were stained with rhodamine-labelled phalloidin, and mounted on glass slides for examination with an epiluminescent fluorescence microscope and with direct luminescence light microscopy.

Photomicroscopy

Photomicrographs were taken with an Olympus BH2 fluorescent and incandescent illumination photomicroscope using Kodak TMAX 400 black and white film.

RESULTS

Cell Suspension

Hepatocytes in control incubations were unaffected by PBS treatment. Plasma membrane blebbing was observed, however, in MCLR-treated hepatocytes. The number and size of blebs increased in a dose and time-dependent manner. Scattered hepatocytes treated with MCLR at 0.1 µg/ml had multiple, medium to large, plasma membrane blebs at 30 minutes. Treatment with MCLR at 1.0 µg/mi resulted in many cells having a few plasma membrane blebs at 10 minutes with the majority of cells having such blebs by 30 minutes. Ten minutes posttreatment with MCLR at 10.0 µg/ml, almost all hepatocytes had multiple medium to large plasma membrane blebs. By 30 minutes, these blebs had frequently coalesced to form a rim around the original cell border. Hepatic nonparenchymal cells treated with either PBS or MCLR had no treatment-associated plasma membrane blebs at any toxin concentration at any of the observation times.

Cell Culture

Hepatocytes cultured for 72 hours and then treated with PBS had normal actin filaments (Figures 1 and 2). One hour after treatment with 10 µg of MCLR/ml, scattered hepatocytes had 1 or 2 plasma membrane blebs with an increased amount of actin at the bases of the blebs. In many of these cells, thickened rays of actin extended from a dense actin spot in the interior of the cell to the tip of the bleb (Figure 3). The frequency of affected cells increased until at 4 hours, many hepatocytes had several plasma membrane blebs, each with an increased amount of actin at its base and one or more thick rays of actin extending from the base to the tip of the bleb (Figures 4 and 5). By 6 hours, the majority of hepatocytes were affected. These had

extensively blebbed plasma membranes which occasionally coalesced to form a rim around the original cell border and the actin in these cells was aggregated in the center of the cells into a single, intensely staining spot (Figures 6 and 7). No elevation of LDH was noted at any time point as compared to PBS controls.

The frequency of the morphologic changes in MCLR-treated hepatocytes cultured for 72 hours was dose-dependent. Six hours after treatment with MCLR at 0.1 µg/ml, a few scattered cells were affected as described above. At a MCLR concentration of 1.0 µg/ml, many hepatocytes were affected but not to the extent of those treated with 10.0 µg of MCLR/ml.

Six hours postdosing with PBS, 24-hour cultured hepatocytes had no actin filament changes; however, the cells were still rounded, had not spread out, had diffuse staining with rhodamine-phalloidin and few linearly organized actin filaments. The filamentous actin in those hepatocytes treated for 6 hours with 10.0 µg of MCLR/ml was aggregated in the centers of the cells into single, intensely staining spots identical to those in hepatocytes cultured for 72 hours prior to exposure as described in the first paragraph of this section. Replicate 24-hour hepatocytes treated with 10.0 µg of phalloidin/ml had numerous plasma membrane blebs, but when stained with rhodamine-phalloidin, there were many variably sized aggregations of actin scattered throughout the cytoplasm (Figure 8). Replicate 24-hour hepatocytes treated with 10.0 µg of cytochalasin B/ml were similar to those treated with phalloidin, however, the actin aggregations located throughout the cytoplasm were more uniform in size and smaller (Figure 9). The number of cultured hepatocytes responding to phalloidin treatment was related to the age of the cells. Approximately 1/2 of the 24-hour-old cells were affected as described above. With 48-hour-old

cells, less than 1/5 of all cells were affected, while with 72-hour-old cultures, almost no hepatocytes were affected by 10.0 µg of phalloidin/ml. Neither MCLR nor cytochalasin B showed this hepatocyte age-dependent effect.

Morphologic and Cytoskeletal Effects in Livers of Intact Rats

Morphologic lesions seen with light microscopy in formalin-fixed, hematoxylin- and eosin-stained sections were similar to those reported previously (Hooser et al., 1988) except that no lesions were seen until 30 minutes postdosing. Thirty minutes postdosing with 180 µg of MCLR/kg, there was disassociation and rounding of 5 to 10 rows of hepatocytes adjacent to central veins, with mild hemorrhage present in some areas (Figure 10). This lesion progressed in extent and severity until at 60 minutes postdosing, there was hepatocyte-to-hepatocyte disassociation and rounding with hemorrhage and hepatocyte fragmentation and necrosis involving entire liver lobules except for a rim of periportal hepatocytes 10 to 15 cells wide.

In rhodamine-phalloidin stained, frozen liver sections of PBS-treated rats, a normal pattern of marginated actin was seen in hepatocytes (Figure 11), as it was in MCLR-treated animals at 5 and 10 minutes postdosing. However, at 20 minutes after addition of MCLR, centrilobular and a few midzonal hepatocytes had 5 to 15 small, discrete aggregations of actin within their cytoplasm (Figure 12). Forty-five minutes postdosing, midzonal hepatocytes were affected with marked aggregation of actin (Figure 13). This lesion progressed in extent and severity until at 60 minutes the majority of periportal hepatocytes were also affected. By this time, in many centrilobular and midzonal hepatocytes the intracytoplasmic filamentous actin had aggregated into a single, dense focus. This actin aggregation was quite prominent in hepatocytes immediately adjacent to normal-appearing hepatocytes (Figures 14 and 15).

DISCUSSION

In suspension, hepatocytes but not sinusoidal endothelial or Kupffer cells had morphologic changes caused by MCLR. Presumably this is because cellular uptake of MCLR occurs by a hepatocyte-specific bile acid carrier similar to that responsible for phalloidin uptake into hepatocytes (Frimmer, 1982; Faulstich, 1986). Hepatocytes in suspension are protected from MCLR induced toxicity when competitors of bile acid carriers are added prior to toxin administration (Runnegar et al., 1981). The lack of such plasma membrane carriers in other cell types would account for the liver and hepatocyte specificity of MCLR. Unlike phalloidin, the addition of MCLR to hepatocytes in suspension reportedly does not cause an increase of polymerized actin nor does it cause a decrease of polymerized actin as does cytochalasin B (Runnegar et al., 1986). In the present study, we have demonstrated that the effects of MCLR on the arrangement of filamentous actin within hepatocytes are distinctly different from those of phalloidin, or cytochalasin B. In addition, we found that the effect of phalloidin on cultured hepatocytes decreases with the age of the cells but that they remain sensitive to the effects of MCLR. This decrease could be due to one of the following reasons: 1) there are reduced numbers of the bile acid carrier which carries phalloidin into the cell and that MCLR is carried in by other bile acid carriers so that the cells are still affected by MCLR, or 2) there is an intracellular change which renders the hepatocytes insensitive to the effects of phalloidin but which does not alter sensitivity to MCLR. Whether the changes in actin filaments represent a direct interaction of MCLR with actin or whether these filamentous changes are secondary to other intracellular effects of MCLR remains to be elucidated. However, it is evident that, whatever the mechanism of action of MCLR, its

effects are distinct from those of phalloidin or cytochalasin B. These findings suggest that although MCLR and phalloidin may enter hepatocytes by similar membrane carriers, the resulting lesions are due to different intracellular mechanisms.

Early in our studies, it was noted that freshly isolated hepatocytes in suspension responded much more rapidly to the addition of MCLR than did cultured hepatocytes (1/2 versus 6 hours before approximately 100% of the cells were affected). The reason(s) for this difference remain unknown at this time but could be due to: a decline in numbers of hepatocyte plasma membrane receptors for MCLR (if there is a receptor) in cultured cells, a decline of some other as yet undiscovered intracellular receptor or protein in cultured hepatocytes which is necessary for toxicity, or perhaps the poor organization of actin filaments in suspended hepatocytes as opposed to the well-organized actin filaments and stress fibers in cultured hepatocytes could account for this difference. Although hepatocytes in suspension react to MCLR more rapidly than do cultured hepatocytes, we chose to examine actin filaments in 72 hours cultured cells because alterations in the well organized actin filaments of cultured cells were much easier to discern than in poorly organized actin filaments in hepatocytes less than 24 hours old.

Both in suspension, up to 30 minutes postdosing and in cultured cells up to 6 hours postdosing, there was no leakage of intracellular LDH from MCLR-treated hepatocytes as compared to PBS treated control cells. This would indicate that actin filament alterations and morphologic changes occur before plasma membrane damage and leakage.

We have found that changes in hepatocyte actin filaments <u>in vivo</u> precede morphologic lesions seen by H&E staining and that these actin filament changes

progress to aggregation of actin into a single dense spot just as is seen with cultured hepatocytes *in vitro*. Thus, we have shown that similar changes in actin filaments are seen in hepatocytes *in vitro* and *in vivo*.

It is concluded that MCLR principally affects hepatocytes rather than nonparenchymal cells and causes redistribution and an aggregation of actin filaments within hepatocytes. This disruption of the structural support of the cell and aggregation of the intracellular actin into a single area most likely accounts for the plasma membrane blebbing that occurs *in vitro*, as well as hepatocyte disassociation, plasma membrane invagination, and loss of microvilli *in vivo*.

Figure 1. PBS treated, normal, 72-hour cultured hepatocytes 6 hours postdosing. 250-X.

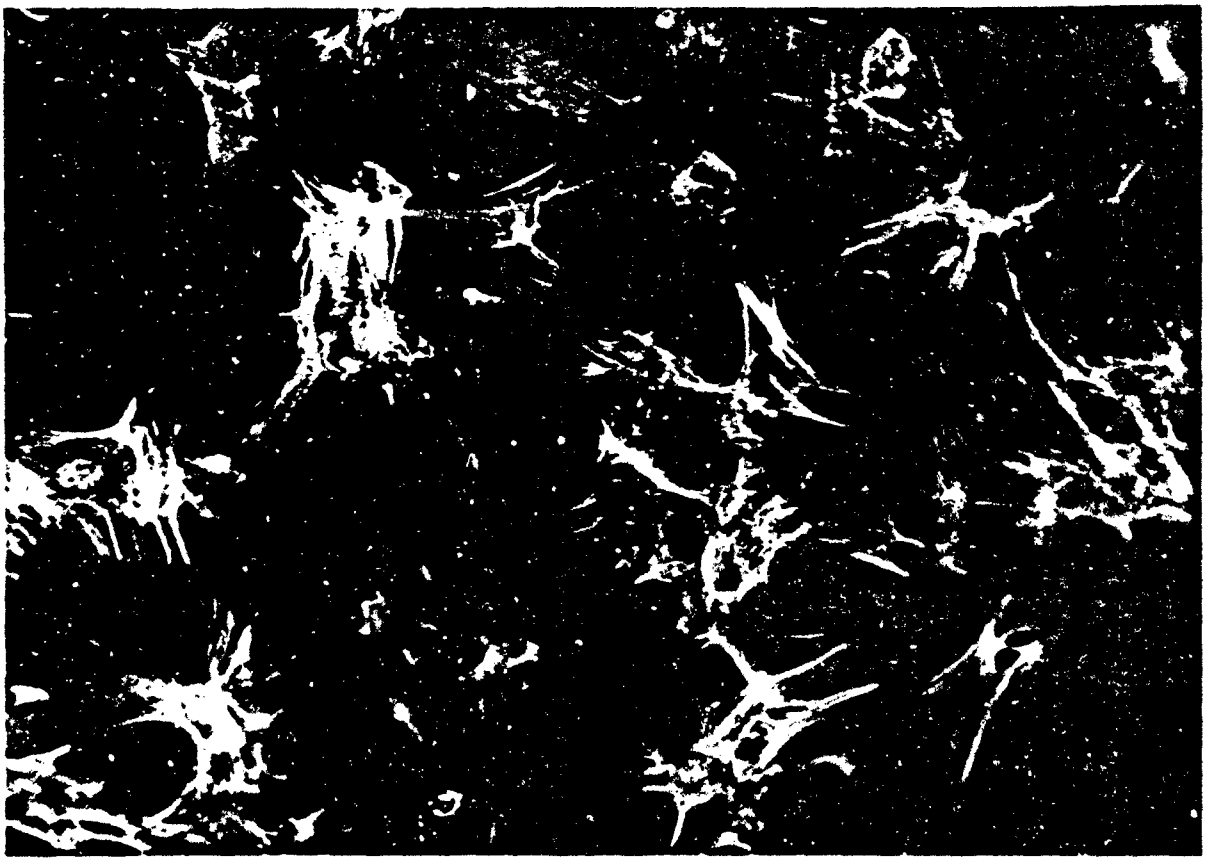

Figure 2. PBS treated, normal, 72-hour cultured hepatocytes 6 hours postdosing. 500-X.

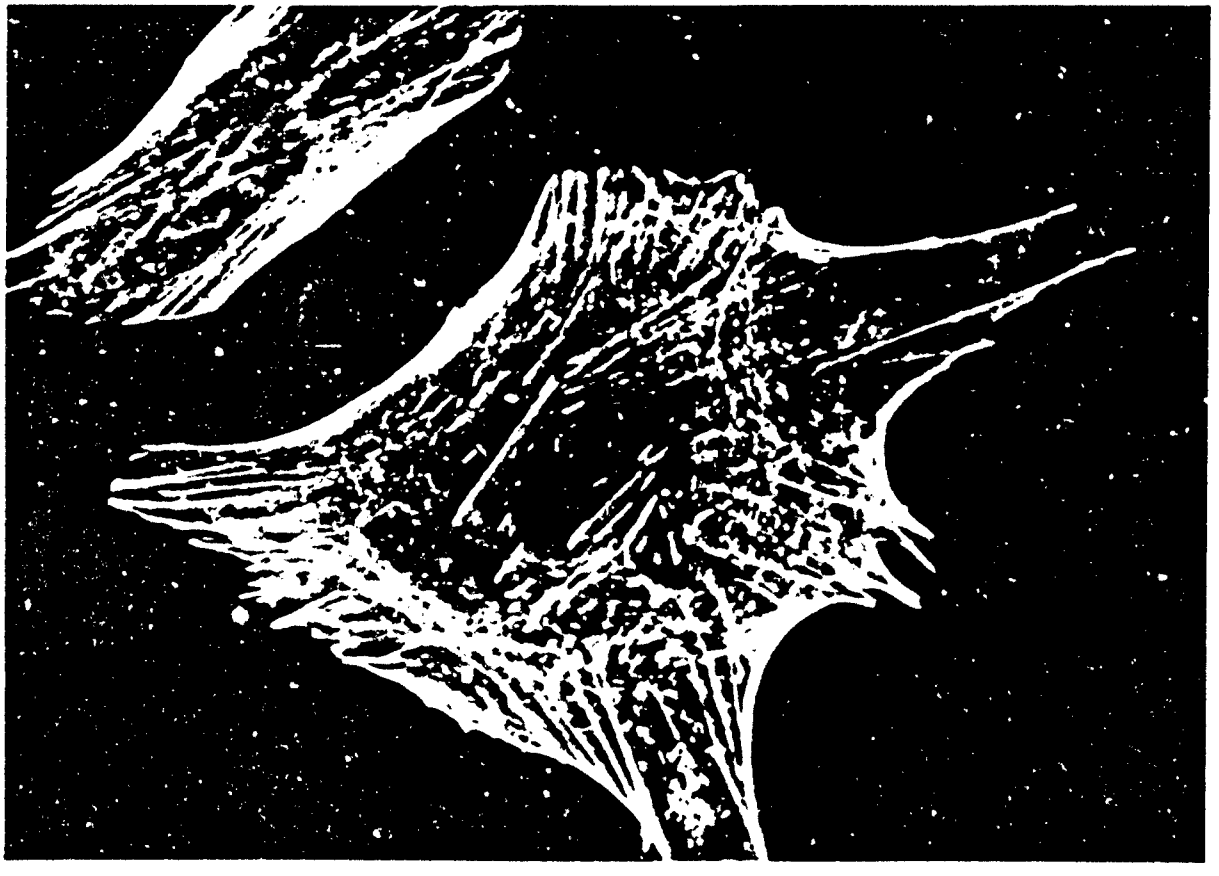

Figure 3. Seventy-two-hour, cultured hepatocytes 1 hour after treatment with 10.0 μg of MCLR/ml. Several plasma membrane blebs contain large, thick actin filaments which extend from the bases to the tips of the blebs. 500-X.

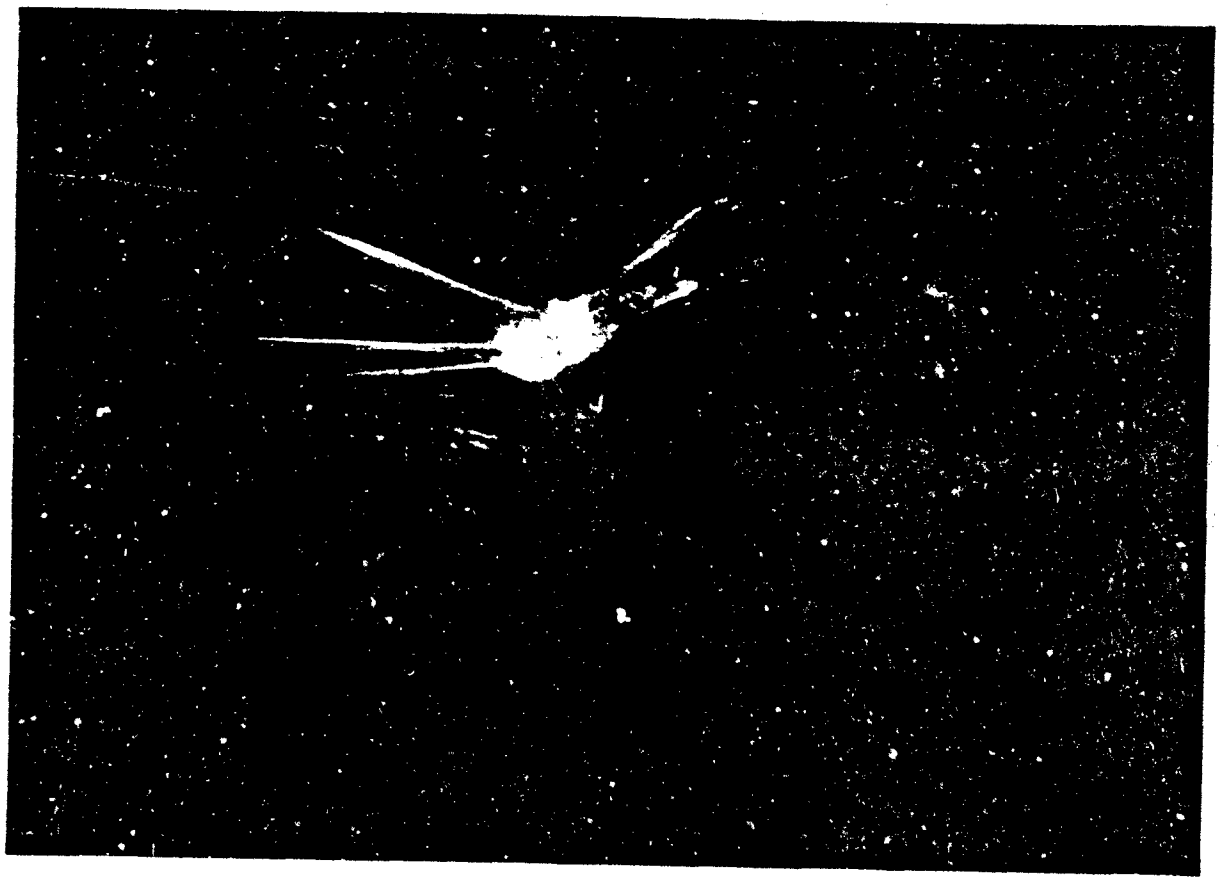

Figure 4. Seventy-two-hour, cultured hepatocytes 3 hours after treatment with 10.0 μg of MCLR/ml. Actin is aggregating beneath the plasma membrane with thickened actin filaments extending out to the tips of the blebs. 500-X.

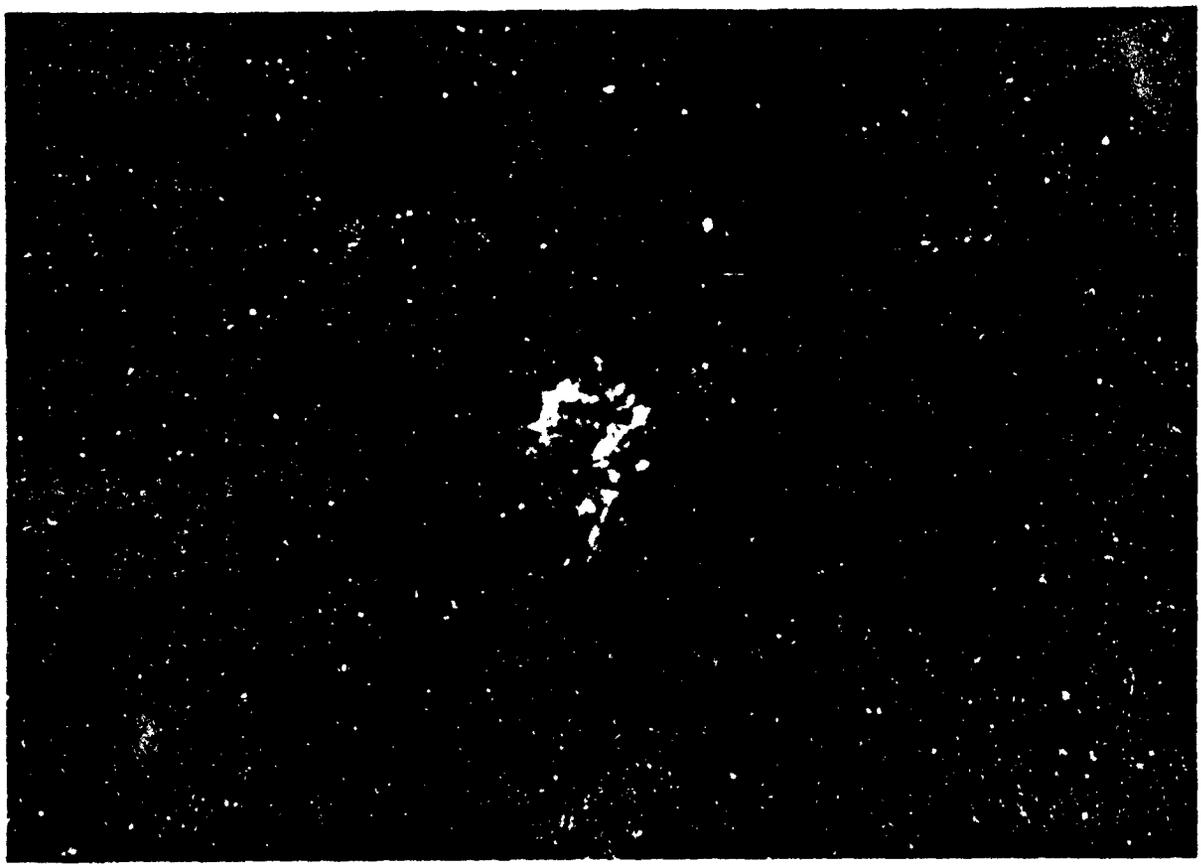

Figure 5. Seventy-two-hour, cultured hepatocytes 4 hours after treatment with 10.0 µg of MCLR/ml. Actin is aggregating in the center of the cell with thickened actin filaments extending out to the tips of the blebs. 500-X.

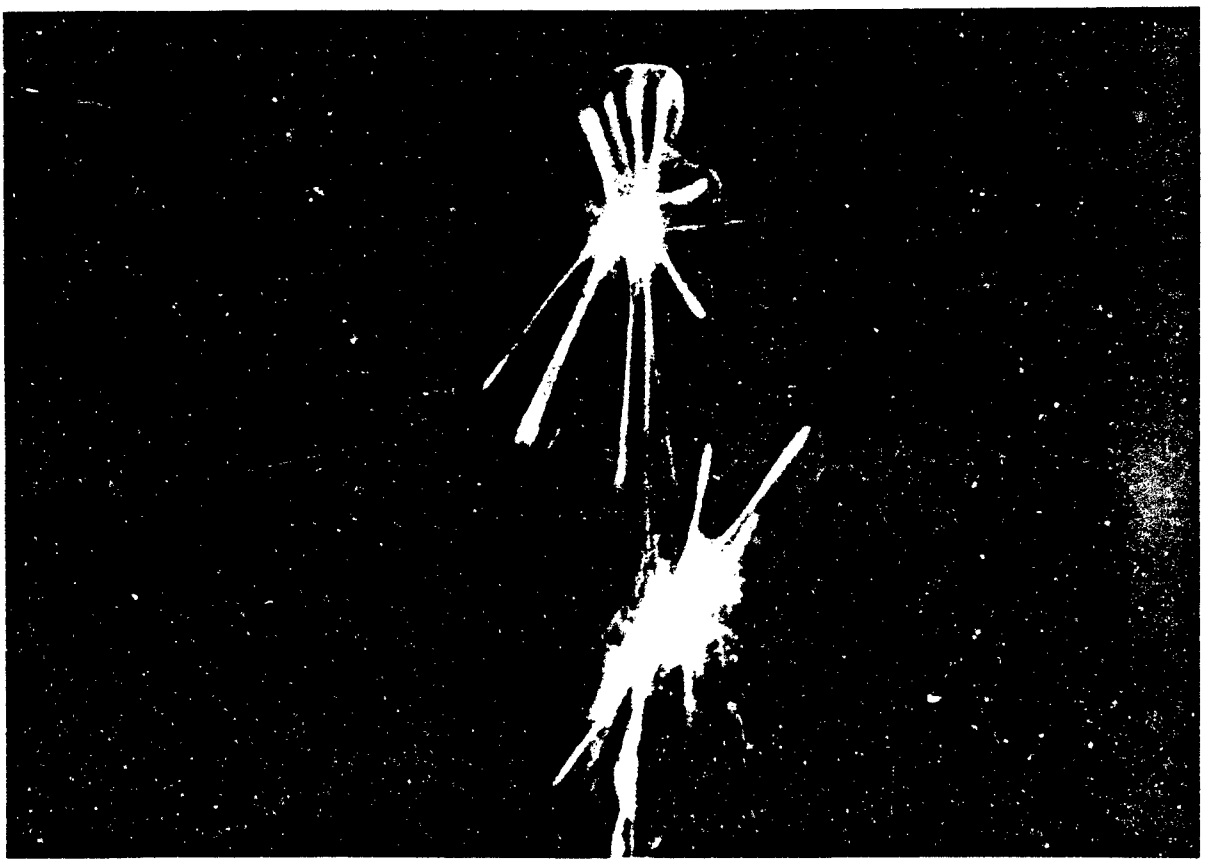

Figure 6. Seventy-two-hour, cultured hepatocytes 6 hours after treatment with 10.0 µg/ml of MCLR. Almost all cells are affected. 100-X.

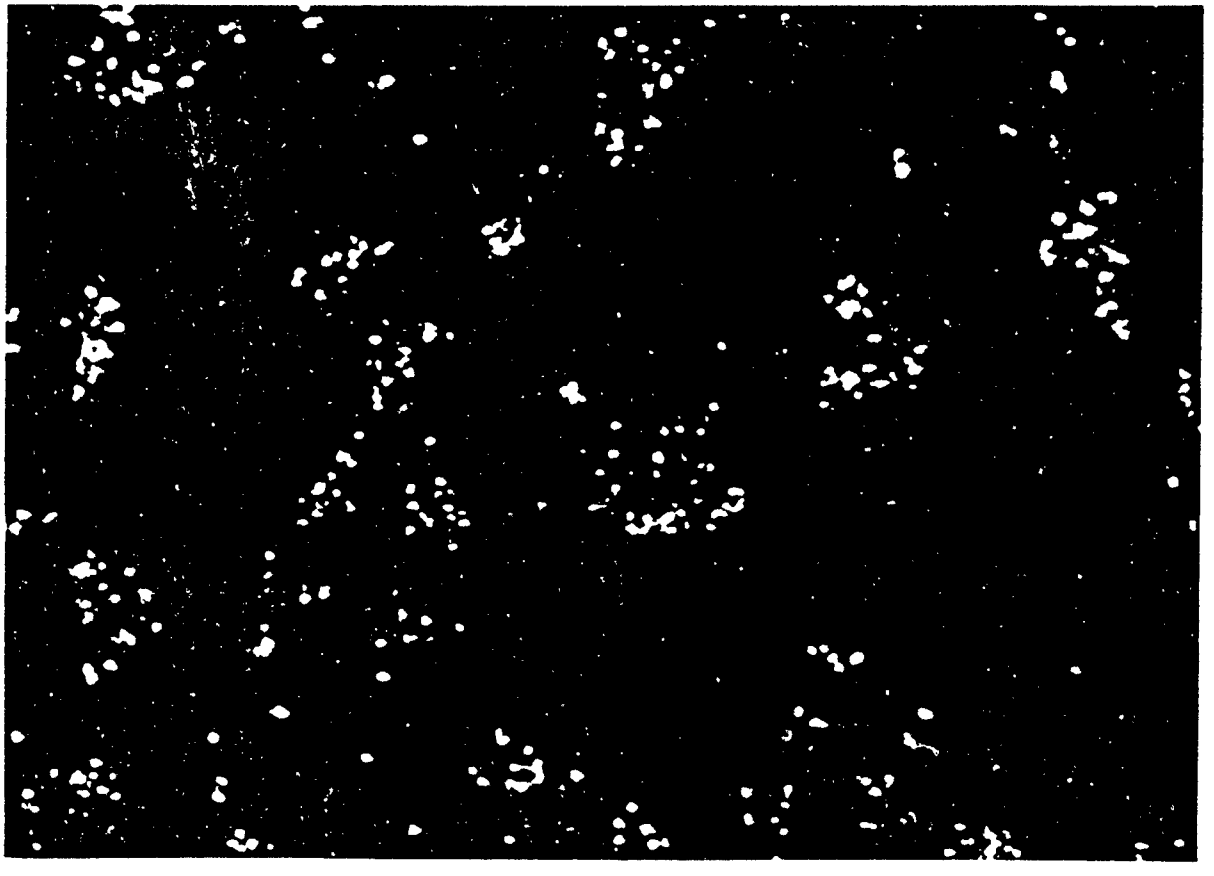

Figure 7. Seventy-two-hour, cultured hepatocytes 6 hours after treatment with 10.0 µg/ml of MCLR. Most of the intracellular actin has aggregated into a single spot and there is extensive blebbing of the plasma membranes. 500-X.

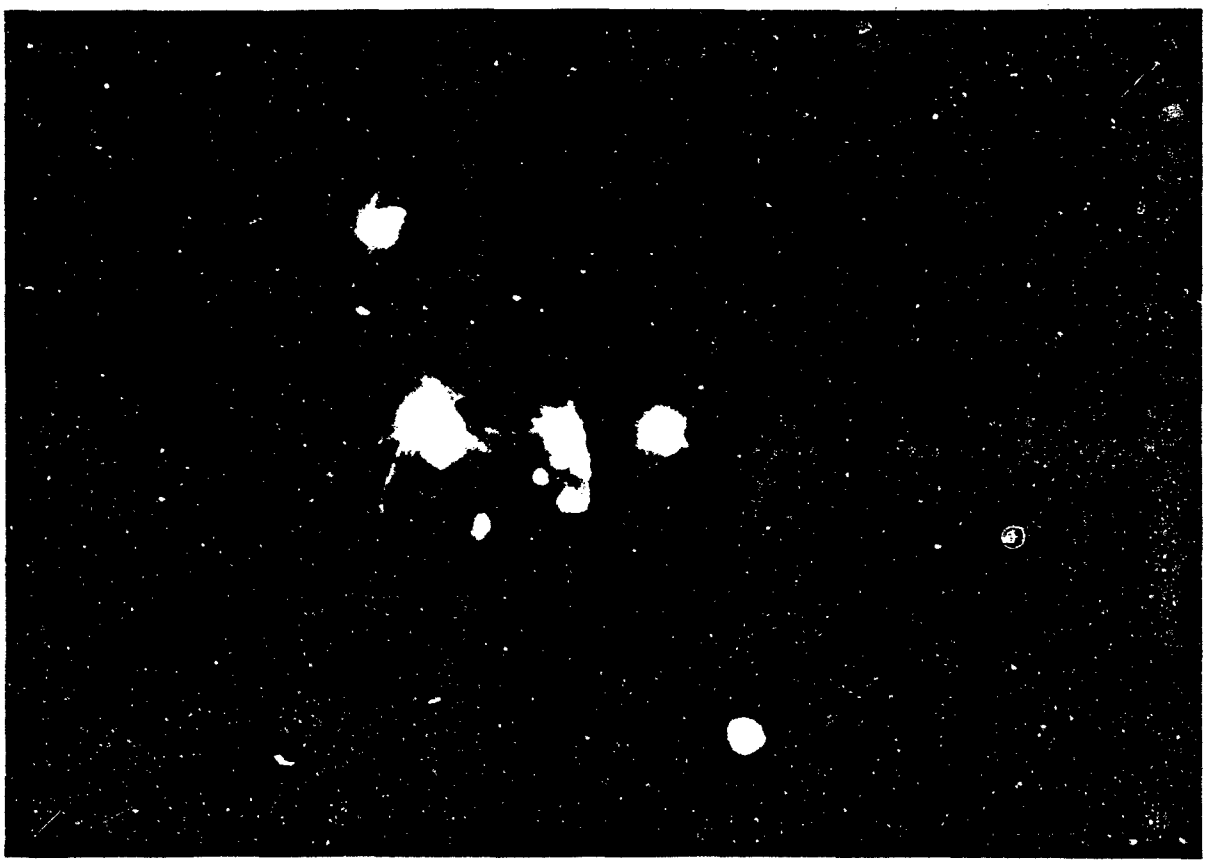

Figure 8. Twenty-four hour, cultured hepatocytes 6 hours after treatment with 10.0 µg of phalloidin/ml. Intracellular actin has aggregated into many, variably sized foci located throughout the cytoplasm. 500-X.

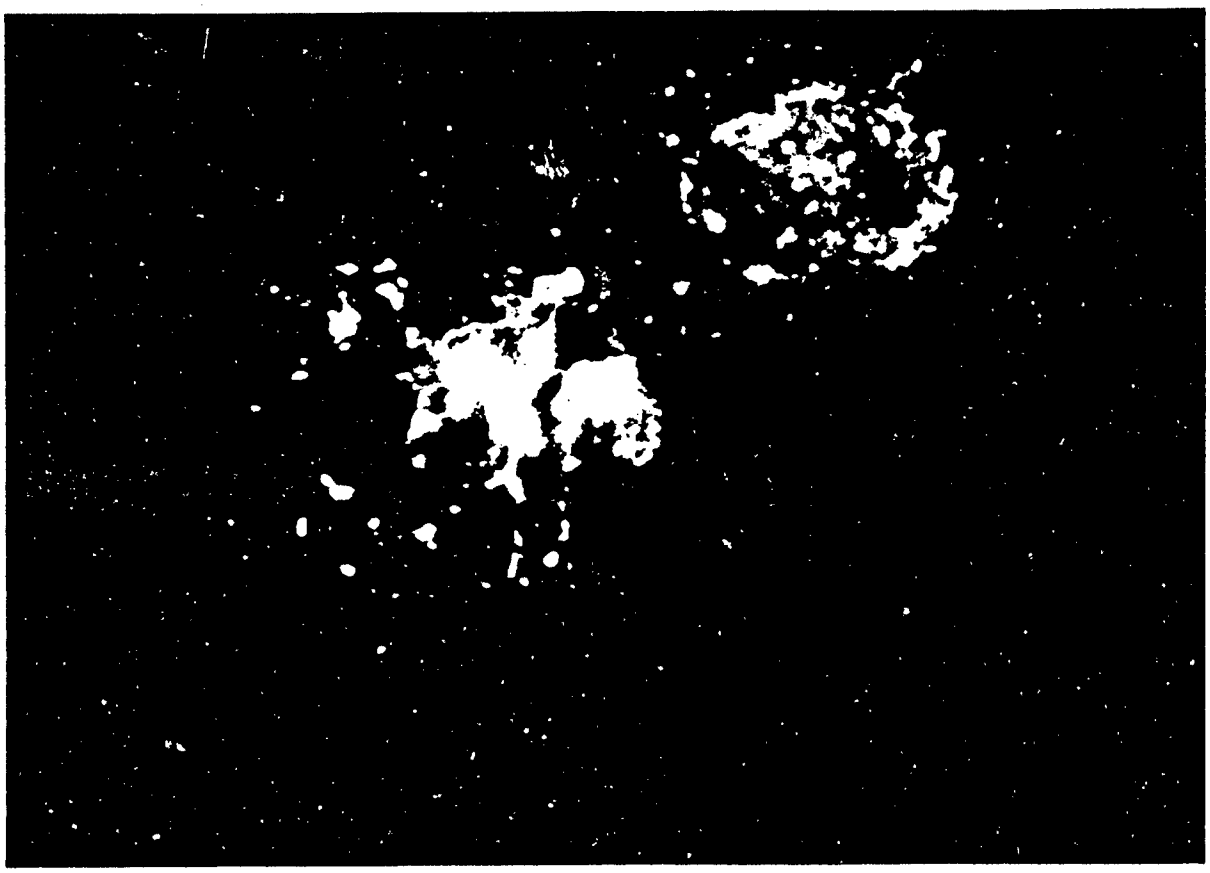

Figure 9. Twenty-four-hour, cultured hepatocytes 6 hours after treatment with 10.0 µg of cytochalasin B/ml. Intracellular actin has aggregated into many, small foci located throughout the cytoplasm. 500-X.

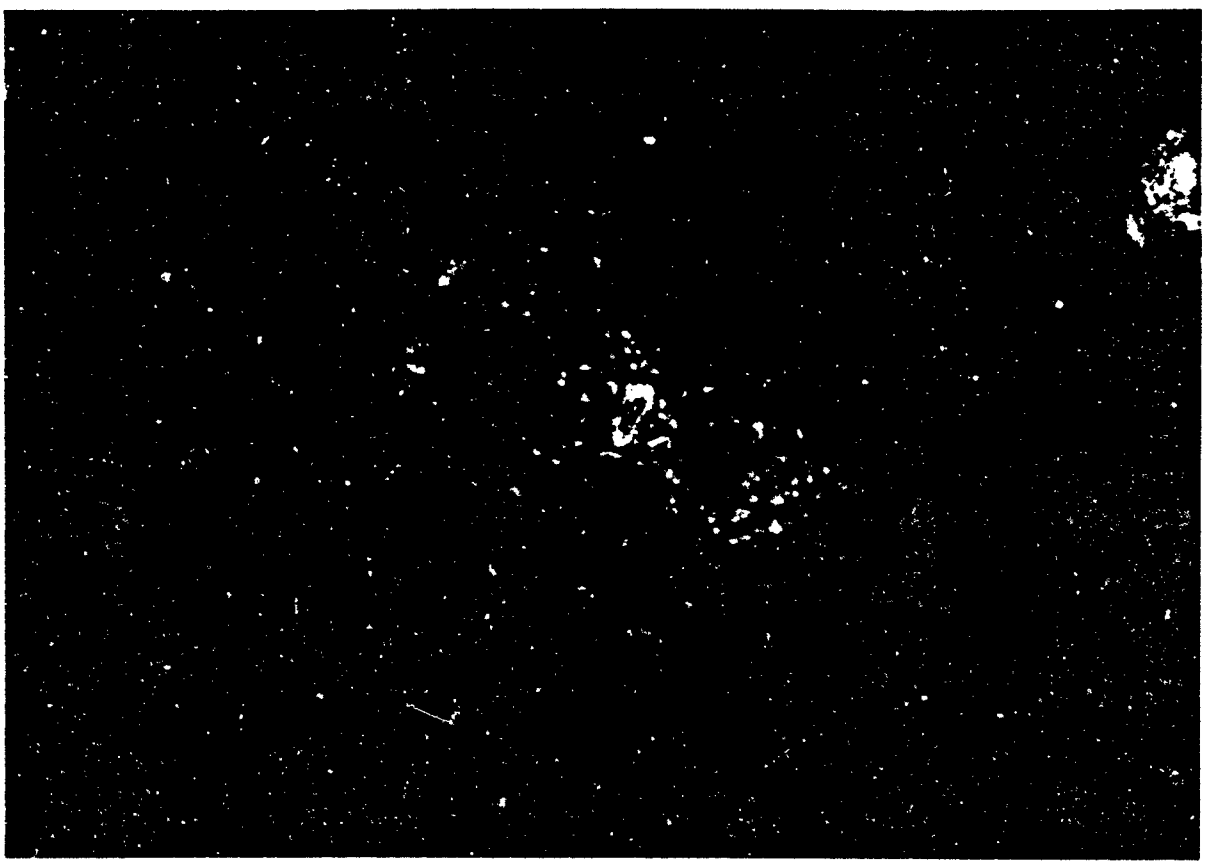

Figure 10. Formalin-fixed rat liver 30 minutes postdosing with 180 µg of MCLR/kg. There is rounding of hepatocytes adjacent to the central vein. 500-X. H&E.

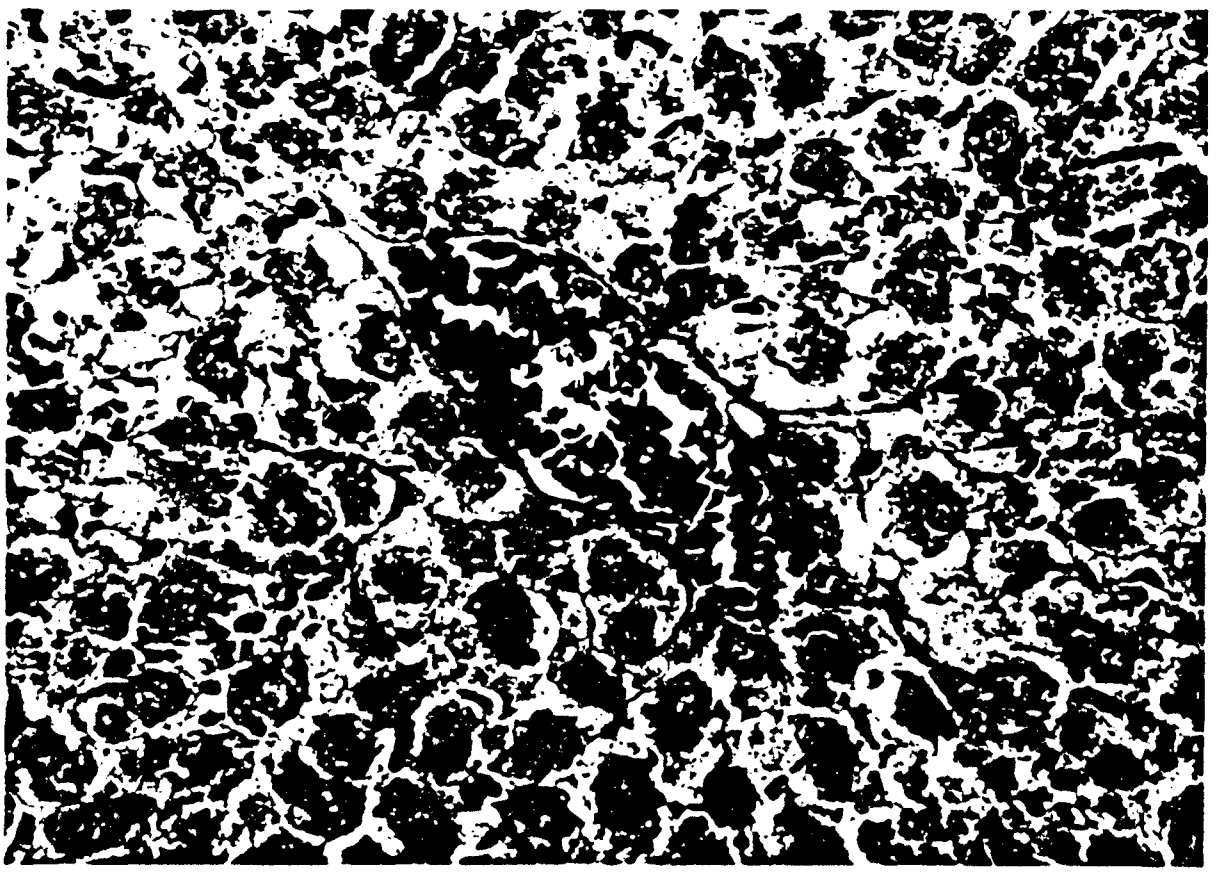

Figure 11. Rhodamine-phalloidin stained, frozen liver section 60 minutes postdosing with PBS. There is a normal pattern of actin staining at the margins of the hepatocytes. 500-X.

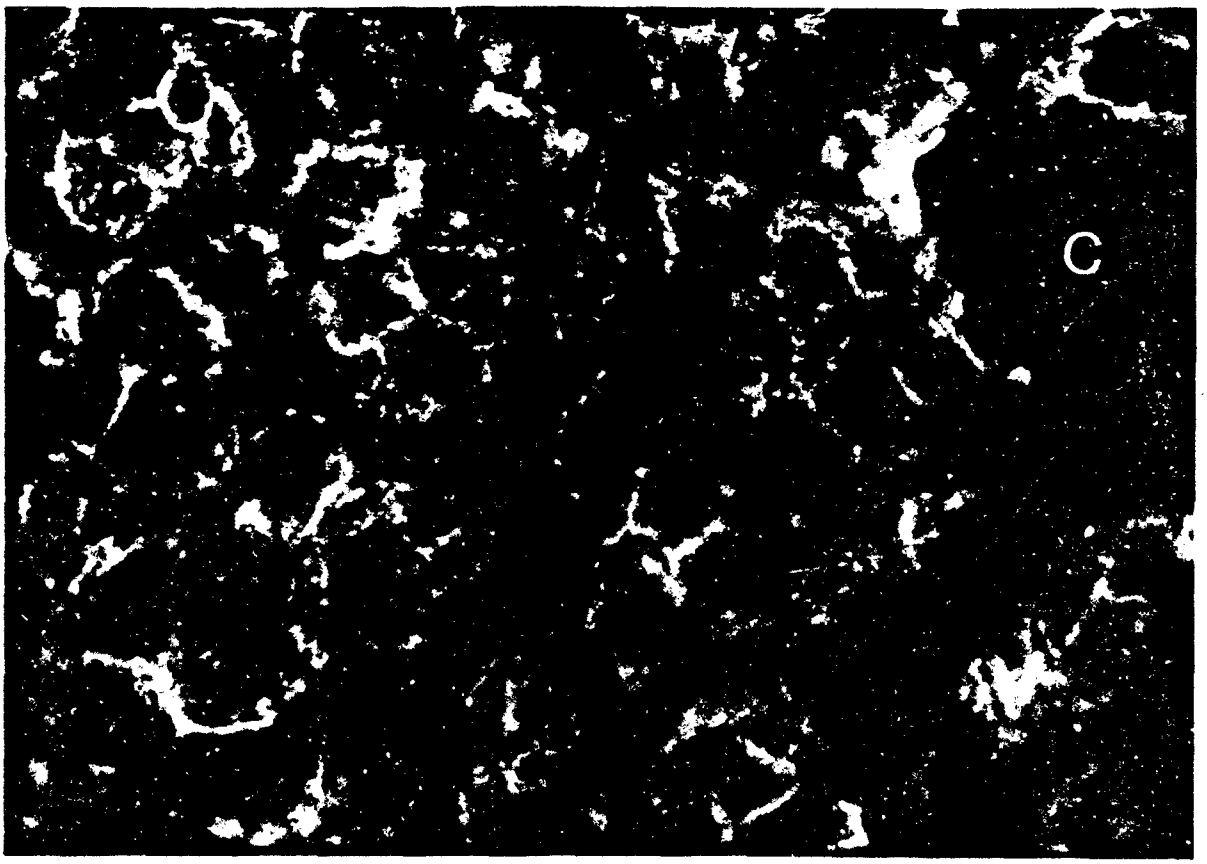

Figure 12. Rhodamine-phalloidin stained, frozen liver section 20 minutes postdosing with 180 µg of MCLR/kg. Hepatocytes adjacent to the central vein (c) have small, discrete aggregations of actin within their cytoplasm. 500-X.

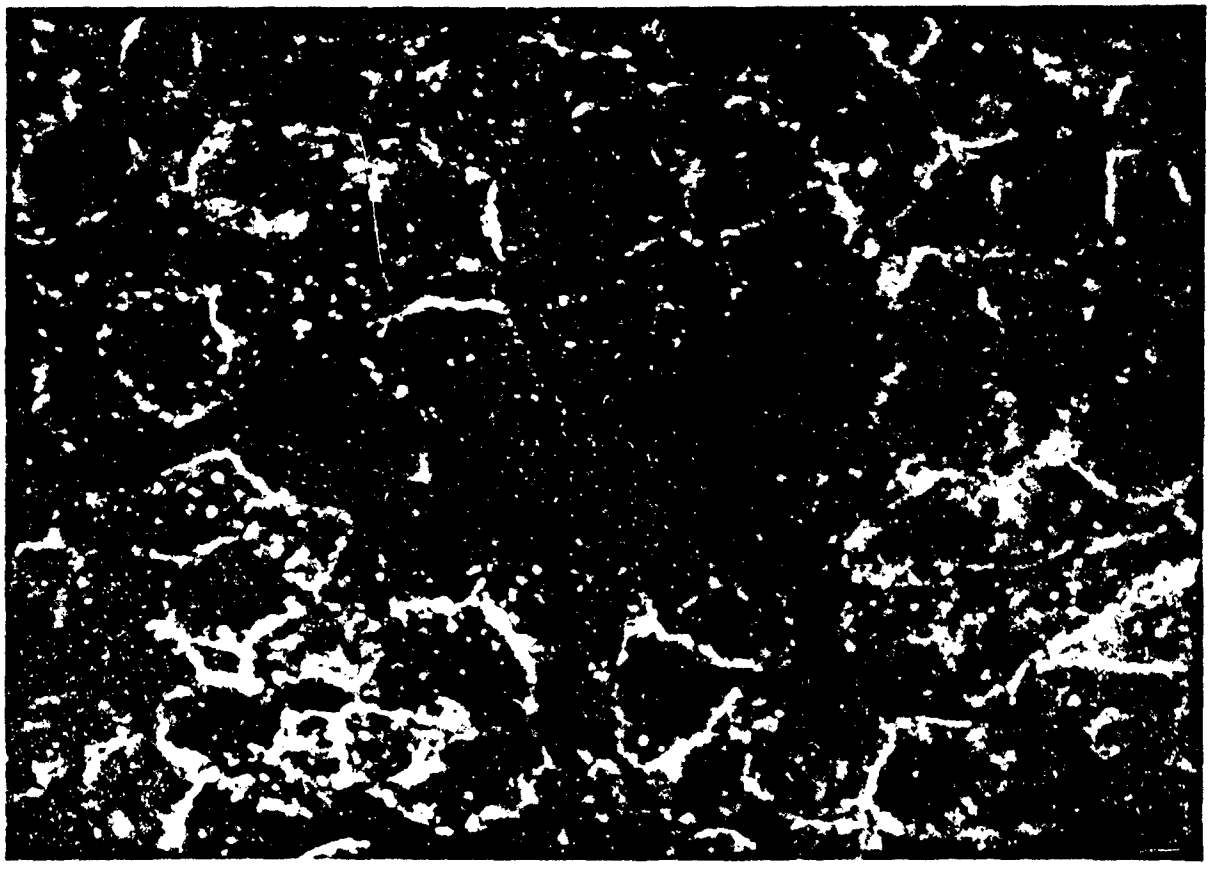

Figure 13. Rhodamine-phalloidin stained, frozen liver section 45 minutes postdosing with 180 µg of MCLR/kg. Midzonal hepatocytes on right appear normal while those on left have lost marginal actin and the actin is now aggregated in numerous, variably sized foci. 500-X.

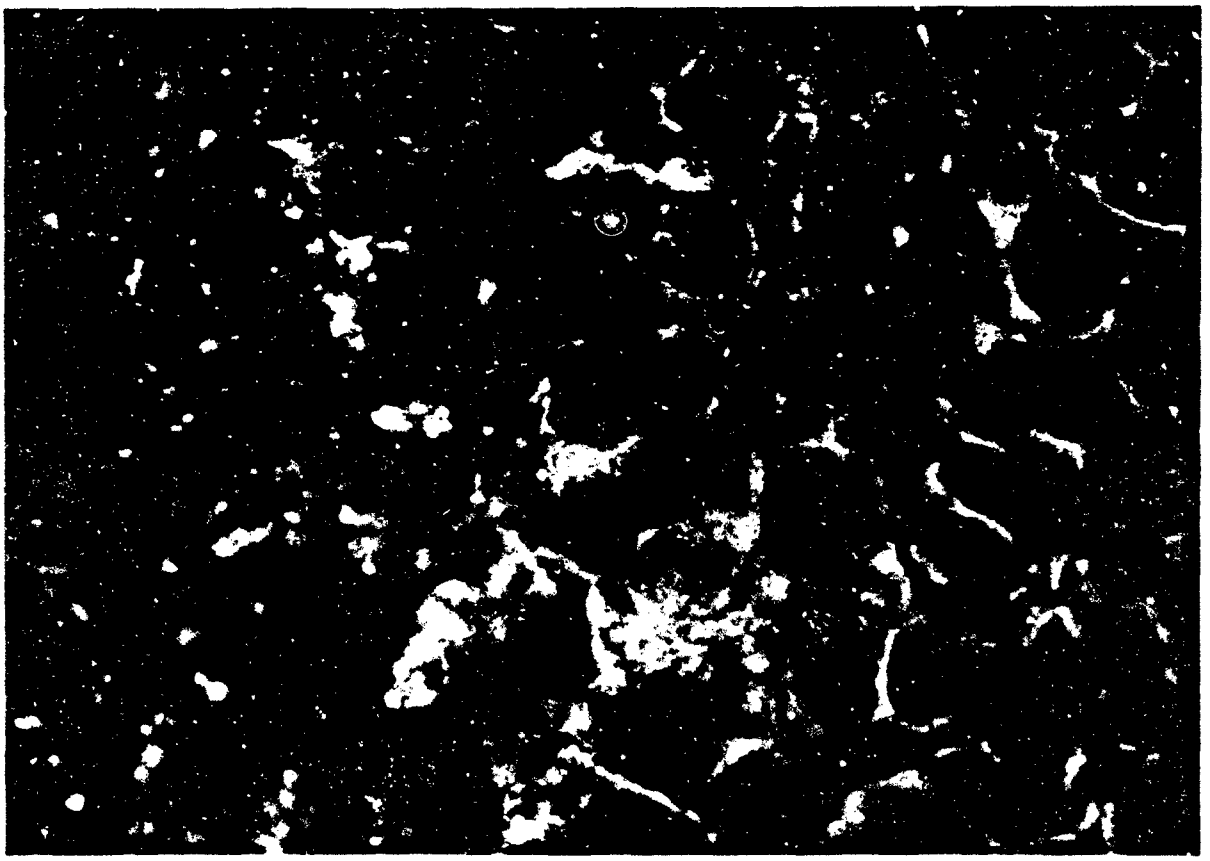

Figure 14. Rhodamine-phalloidin stained, frozen liver section 60 minutes postdosing with 180 µg of MCLR/kg. By this time, the lesion has progressed from the central regions to the periportal regions. Only a few normal appearing hepatocytes immediately adjacent to the portal vein (P) can be seen. 250-X.

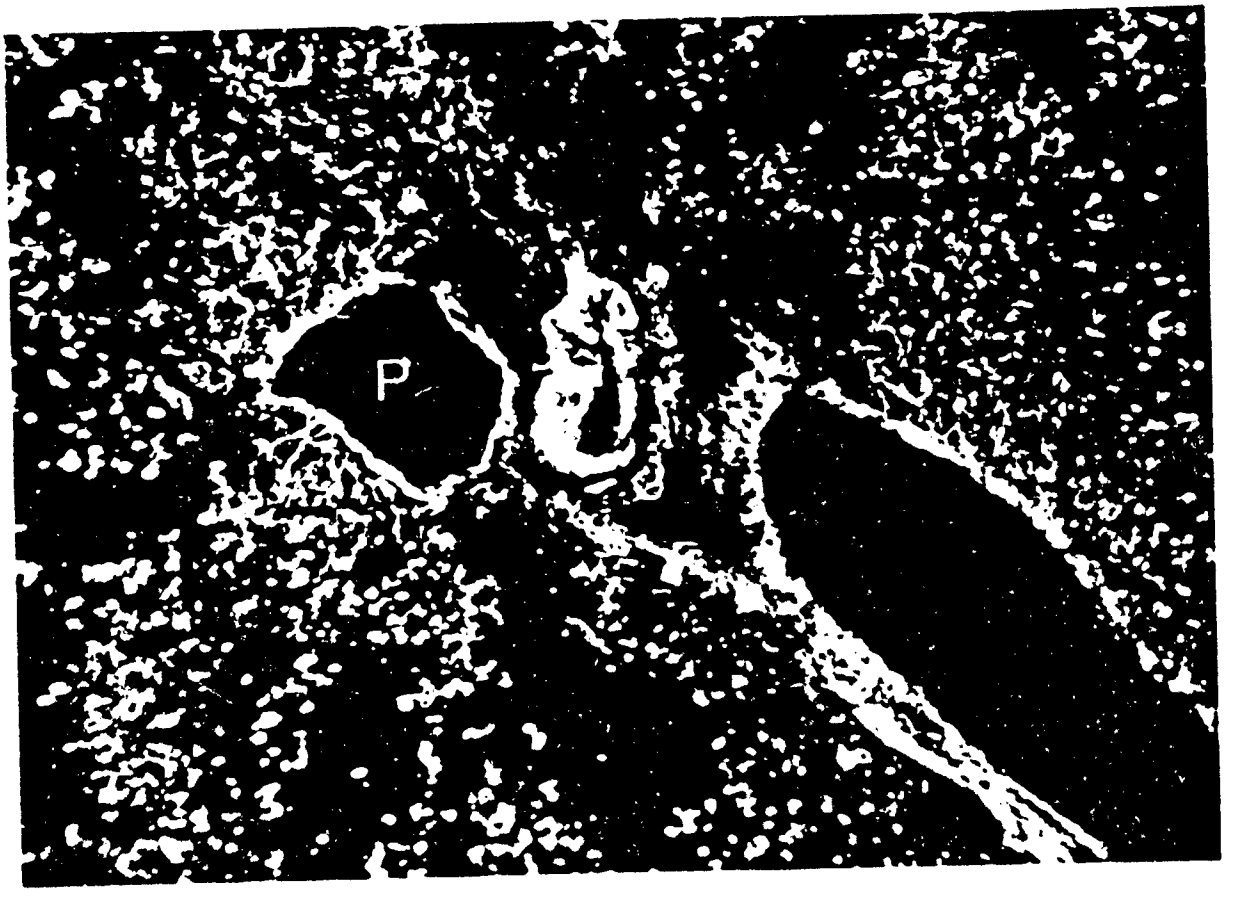

Figure 15. Rhodamine-phalloidin stained, frozen liver section 60 minutes postdosing with 180 µg of MCLR/kg. Hepatocytes close to the portal triad (p) contain a single, dense actin aggregation and have lost the actin at their margins. A few hepatocytes still appear unaffected with normal, marginal staining of filamentous actin. 500-X.

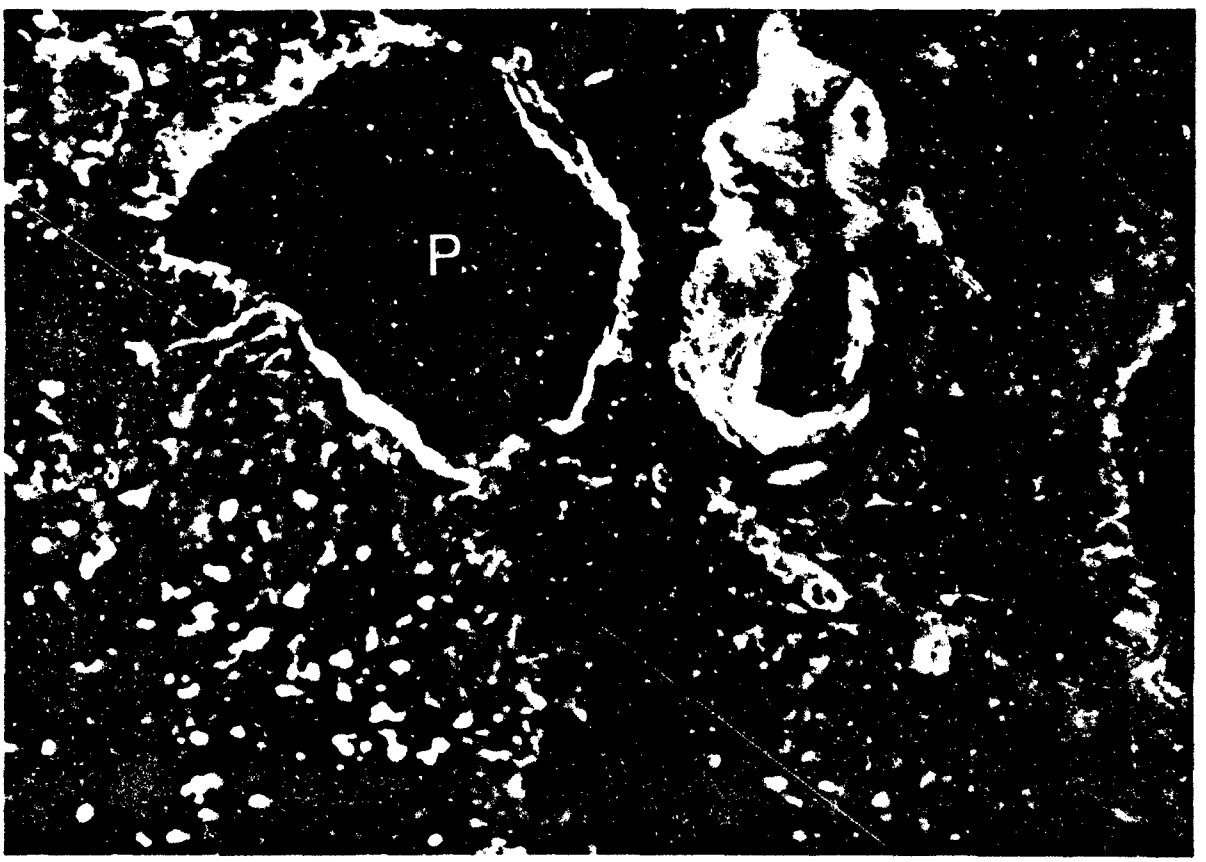

VI. THE EFFECTS OF MICROCYSTIN-LR ON HEMODYNAMIC, CLINICAL PATHOLOGIC, AND BLOOD-GAS PARAMETERS IN SWINE

Randall A. Lovell and Kenneth R. Holmes

INTRODUCTION

The microcystins are a family of hepatotoxic monocyclic heptapeptides produced by M. aeruginosa and other cyanobacteria (blue-green algae). Most aspects of the structure of microcystin-LR (MCLR; cyanoginosin-LR), the most studied member of the microcystin family, have been elucidated recently (Elleman et al., 1978; Botes et al., 1982, 1985). The toxin likely gains entrance into hepatocytes (Runnegar and Falconer, 1982) via organic anion (bile-acid) carriers. Blebbing of hepatocytes is one of the first effects of microcystins in vitro (Runnegar et al., 1981; Runnegar and Falconer, 1986). Although the cause of acute death following microcystin administration has been attributed to hemorrhagic shock (Ostensvik et al., 1981; Runnegar and Falconer, 1982; Sasner et al., 1984; Theiss and Carmichael, 1986) caused by primary effects of microcystin on the liver, Slatkin et al. (1983) surmised that the presence of "atypical pulmonary thrombi" lead to pulmonary congestion, right heart failure, and centrilobular hepatic necrosis and hemorrhage. The major goals of this study were to determine the primary cause(s) of death following MCLR administration in swine and to identify processes which differentiate lethal from sublethal toxicoses.

MATERIALS AND METHODS

The animals, materials, and methods used in this study were described in the 1987 Annual Report for the contract on pages 97-99.

Hematology, Serum Chemistry, and Blood Gas Measurements

Complete blood counts (3 ml) [includes red (RBC) and white (WBC) blood cell counts, differential white blood cell counts, platelet counts, hemoglobin, and hematocrit], serum chemistry profiles (10 ml) [includes creatinine (CRE), urea nitrogen (UN), total protein (TP), albumin, calcium, phosphorus (P), sodium, potassium, chloride (Cl), magnesium (Mg), glucose, cholesterol, total bilirubin (TB), alanine aminotransferase (ALT), aspartate aminotransferase (AST), alkaline phosphatase (AP), gamma glutamyl transferase (GGT), lactate dehydrogenase (LDH), creatinine phosphokinase (CPK),[1] arginase (ARG; Mia and Koger, 1978), and bile acids],[2] blood gases and electrolytes (3 ml; anaerobically collected) [includes PH, pCO_2, total CO_2, pO_2, O_2 saturation, O_2 content, base excess base (BE_B), base excess extracellular fluid (BE_{ECF}), standardized bicarbonate (SBC), bicarbonate (HCO_3-), hematocrit (Hct), hemoglobin (Hb), sodium (Na), potassium (K), ionized calcium (iCa), and normalized calcium (nCa')],[3] and blood lactate concentrations[4] (1 ml) were followed over time. The aortic catheter was flushed as above after each blood sample was obtained. All catheters were periodically flushed to maintain patency.

Statistical Analysis

A nested analysis of variance patterned on a univariate repeated measures analysis (Wilkinson, 1988) was used to identify significant differences (α = 0.05) due to treatment, time, or treatment*time interaction for the clinical pathology, blood-gas, and hemodynamic data. Prior to statistical analysis, all postdosing values (except electrolytes) were subtracted from the predose mean of that animal. The model used was: corrected response (corresp) = constant + treatment (trt) + subjects in control group (subl) + subjects in

toxic-sublethal dose group (sub2) + subjects in lethal dose group (sub3) + time + trt*time. Corresp, trt, subl-3, time, and trt*time represent the corrected response (postdosing value minus mean predose value), the treatment, the subjects within each treatment, the time after MCLR administration, and the treatment*time interaction, respectively. Since the majority of any changes in the electrolyte data occurred terminally, the electrolyte data was analyzed using both the untransformed data (respons- replaces corresp in the above model) and the transformed data. Analysis of the untransformed data was chosen because it provided a more conservative estimate of electrolyte changes. The number of surviving animals in the lethal dose group decreased with time which prevented the use of a repeated measures analysis. Data from terminal blood samples in the lethal dose group (collected at 57, 60, 85, 138, and 178 minutes, respectively) were analyzed as though they were taken at the next scheduled time point (90, 90, 90, 150, and 210 minutes) for the clinical pathology and blood-gas parameters.

Comparisons between treatment groups at postdosing time points were performed using linear contrast at a level of $\alpha = 0.05$ (Wilkinson, 1988), except at the time points where only 1 pig was alive in the lethal dose group. These included the 300-minute time point for blood-gas and clinical pathology parameters and the 186-, 198-, 210-, 222-, 236-, 248-, 260-, 272-, 284-, and 194-minute time points for hemodynamic and organ perfusion parameters. The denominator of the F statistic in these contrasts was the error (time) term in the nested ANOVA analysis. At the time points where only 1 pig was alive in the lethal dose group, 1-way analysis of variance (Wilkinson, 1988) was used to determine statistical significance between the lethal dose group and the other 2 groups. Due to the small sample size and a desire to increase power, α was set at 0.15 in these analyses.

RESULTS

Hemodynamic Effects

Mean central venous pressure (CVP; Figure 1) in the lethal dose group was significantly less than controls at 15 minutes (12- to 18-minute mean) after MCLR administration. At 21 minutes, mean portal venous pressure (PVP; Figure 2) was significantly increased in the lethal dose group when compared to controls. The 3 pigs in the lethal group with the highest predosing portal venous pressures had the largest increases in portal venous pressure and the shortest survival times. The PVP of the lethal dose group was significantly increased in comparison to the toxic-sublethal dose group at 21 minutes. From 180 to 300 minutes, the PVP was not significantly different between the toxic-sublethal and lethal dose groups.

In the toxic-sublethal dose group, the hemodynamic parameters exhibited the same direction of change as the lethal dose group when compared to the controls, but these changes except the aortic mean pressure (AOM), which was significantly decreased at 15 minutes, took longer to become significantly different (liver perfusion = 39 minutes, renal perfusion = 51 minutes, CVP = 57 minutes, and PVP = 162 minutes) and were not of as great a magnitude. The toxic-sublethal dose group AOM was not significantly lower than control AOM the last hour of the study.

Hematology, Serum Chemistry, and Blood-Gas Effects

Clinical pathology, blood-gas, and complete blood count parameters (Table 1) in the lethal dose group which were significantly different from the control group by 45 minutes included: a) lactate (Figure 3), bile acids (Figure 4), K (Figure 5), pO_2 (Figure 6), O_2 saturation, and TB (all increased); and b) Hct, platelet count (Figure 7), HCO_3-, pCO_2 (Figure 8), and

BE_B (all decreased). By 90 minutes, significant increases (lethal vs control) in ARG (Figure 9), UN, P, and CRE were present as well as significant decreases in glucose (Figure 10) and pH (Figure 11). At 150 minutes, ALT, AST (Figure 12), ALP, LDH, and CPK (Figure 13) were significantly increased (lethal vs control). At 150 minutes in the toxic-sublethal group, bile acid concentrations were significantly higher and platelet counts were significantly lower than controls. Significant decreases (lethal dose group vs control dose group) in serum Hb, SBC, and BE_{ECF} were observed at the 5 postdosing time points (except serum Hb at 300 minutes).

Serum concentrations of Na, Cl, Mg, iCa, and nCa were within normal ranges, although there was a trend over time toward lower iCa and nCa and higher Mg concentrations in the lethal dose group. The WBC blood cell counts exhibited wide variability, and no significant changes were observed in comparison to the controls. There were no significant treatment-related changes in TP, albumin, GGT, cholesterol, and RBC among the groups.

DISCUSSION

Ostensvik et al. (1981), Berg and Soli (1985b), and Theiss and Carmichael (1986) have measured aortic blood pressure in anesthetized rats after a lethal parenteral dose of MCLR or a microcystin extract. They found that aortic blood pressures steadily declined to values which were less than 50% of predosing values, often by 45 to 60 minutes postdosing. Our findings concerning a fall in aortic blood pressure are in close agreement with those in rats, except with the pig the decrease was often more precipitous.

Theiss and Carmichael (1986) found no significant changes in either jugular or portal venous pressures during the course of their rat study. The concommitant decrease in central venous pressure and increase in portal venous

pressure in the swine of this study indicates, however, that there is a partial blockage or blood flow through the liver to the posterior vena cava. Although our central and portal venous pressure findings differ from those of Theiss and Carmichael (1986) and may be due to differences in species, dose, anesthetics, and survival time, the data of neither study is compatible with a backup of pressure from a failing heart (Fox, 1986; Bonagura and Hamlin, 1986) as the cause of the hepatic lesions as suggested by Slatkin et al. (1983). The findings of this study indicate that there is a partial obstruction of blood flow through the liver to the caudal vena cava in swine administered a lethal dose.

No previous studies were found where blood-gas parameters were measured following microcystin administration. Our findings indicate that the lungs were functioning properly since the lethal dose group had the highest arterial pO_2 and lowest pCO_2 after dosing. Tachypnea was observed in the lethal dose group, and this was likely in response to a metabolic acidosis (decreased pH, HCO_3-, and BE_B and increased lactate) and a marked fall in AOM (Brobst, 1983).

Clinical pathology parameters have been followed in sheep (Konst et al., 1965; Main et al., 1977; McInnes et al., 1983; Jackson et al., 1984), cattle (Konst et al., 1965; Stowe et al., 1981; Galey et al., 1987; Cook et al., 1988), mice (Mason and Wheeler, 1942, Falconer et al., 1981; Slatkin et al., 1983; Adams et al., 1985), and rats (Jones and Carmichael, 1984; Berg and Soli, 1985a; Theiss and Carmichael, 1986; LeClaire et al., 1988) after microcystin administration. Marked increases in liver-related parameters including AST, ALT, AP, GGT, bile acids, LDH, ARG, TB, bromosulfophthalein clearance time, glutamate dehydrogenase, iditol dehydrogenase, and ornithine carbamyl transferase have been reported. Changes in clinical pathology

parameters not necessarily related to liver damage include increases in CPK, lactate, urine hemoglobin, and urea nitrogen. Decreases have occurred in platelet count, inorganic phosphorus, and calcium.

The clinical pathologic parameter which provided the most marked, early indication of acute hepatic damage/dysfunction in the MCLR-dosed swine of this study was serum bile acid concentration. Bile acids were increased 40X by 45 minutes and 15X by 150 minutes in the lethal and toxic-sublethal dose groups, respectively. Significant increases in liver-related enzymes (ARG, AST, LDH, AP) in the serum required 90 to 150 minutes to occur, which suggests that hepatocyte membrane disruption occurs after the onset of inadequate liver perfusion. The longer the survival time in this study, the greater was the magnitude of increase in serum activities of enzymes potentially released from the liver and muscle (AST and LDH) as well as the mild increase in one considered to be muscle specific (CPK). This seems to indicate that mild muscle damage as well as liver damage is contributing to the increases in AST and LDH (Duncan and Prasse, 1977). Also, the longer the survival time in this study, the greater was the decrease in glucose concentrations and the lesser the decrease in hematocrit. Significant decreases in hematocrit and platelet counts and increases in lactate occurred by 45 minutes postdosing in the lethal group and are consistent with hemorrhage and shock.

The decreased renal perfusion, as described in the 1987 report for this contract, and mild renal damage as documented by others are the most likely cause(s) for the significant increases in BUN, CRE, and PHOS. Tubular nephrosis has been reported previously in several species (Ashworth and Mason, 1946; Louw and Smit, 1950; Konst et al., 1965; Elder et al., 1985) and is likely secondary to hypoxia and hepatic emboli, although direct microcystin

effects cannot be ruled out. Reduced ability of the kidney to excrete hydrogen ions, hepatocyte leakage, and especially metabolic acidosis resulting in the exchange of extracellular hydrogen ions for intracellular K probably accounts for the terminal hyperkalemia (Brobst, 983; Duncan and Prasse, 1977).

Although right or left heart failure can elevate hydrostatic pressures which may lead to centrilobular hepatic necrosis and congestion, it usually takes several days to weeks to develop, and significant decreases in platelet counts and increases in arterial pO_2 are not commonly associated with the syndrome (Fox, 1986; Bonagura and Hamlin, 1986; Robbins and Contran, 1979). In conclusion, the hemodynamic, organ perfusion, blood-gas, and clinical pathology findings of the present study indicate that the liver is the target organ for MCLR. Death is apparently caused by hypovolemic shock, partial blockage of blood flow through the liver, hepatic failure, hypoglycemia, and/or hyperkalemia.

FOOTNOTES

[1]Hitachi 705, Boehringer Mannheim Diagnostics, Indianapolis, IN.

[2]Enzabil, NYCOMED AS Diagnostics, Oslo, Norway.

[3]Stat Profile 1 Analyzer, Nova Biomedical, Newton, MA.

[4]Lactate Procedure No. 826-UV, Sigma Diagnostics, St. Louis, MO.

Table 1. Changes in selected clinical pathologic, blood-gas, and complete blood count parameters which had significant ($p \leq 0.05$) treatment or treatment*time effects.

				CHANGE FROM PREDOSE VALUES				
PARAMETER	P VALUES	TRT GRP	Predose Mean ± SEM	45 Min Mean ± SEM	90 Min Mean ± SEM	150 Min Mean ± SEM	210 Min Mean ± SEM	300 Min Mean ± SEM
Alanine Aminotransferase (IU/L)	TRT<0.001 TIME<0.001 TRT*TIME<0.001	VEH	26 ± 4.3	1 ± 1.7^a	2± 1.7^a	-3 ± 2.1^a	3± 1.2^a	-1± 1.5^a
		TOX	25 ± 4.6	1 ± 1.8^a	4± 1.8^a	11 ± 6.2^b	16± 7.4^b	25± 8.2^b
		LET	39 ± 4.5	1 ± 1.2^a	12± 5.9^a	75 ± 4.7^c	120±31.0^c	104 ^{c}
Alkaline Phosphatase (IU/L)	TRT=0.043 TIME<0.001 TRT*TIME=0.032	VEH	274 ± 44.0	9± 7.6^a	26±14.8^a	-6±17.4^a	18±24.6^a	14±11.3^a
		TOX	383 ± 34.8	29± 8.3^a	81±30.1^a	79±59.8^b	103±57.0^b	180±65.2^b
		LET	358 ± 42.5	39±12.4^a	89±17.0^a	147±14.2^b	190± 5.0^b	328 ^{b}
Arginase (IU/L)	TRT=0.059 TIME=0.014 TRT*TIME=0.036	VEH	0 ± 0.0	0 ± 0.0^a	1± 0.8^a	2± 1.2^a	3± 2.0^a	3± 1.1^a
		TOX	1 ± 1.2	-0 ± 1.6^a	3± 3.3^a	26±24.9^a	30±21.9^a	36±23.2^{ab}
		LET	0 ± 0.0	24 ±15.7^a	92±28.1^b	103±27.1^b	35±10.0^a	75 ^{b}
Bile Acids (uM/L)	TRT=0.064 TIME<0.001 TRT*TIME=0.041	VEH	5 ± 2.8	6 ± 2.4^a	10± 9.2^a	11±12.0^a	4± 4.4^a	7± 7.6^a
		TOX	4 ± 1.8	15 ± 2.5^a	32± 8.1^a	61±16.9^b	60±19.4^b	82±28.7^b
		LET	3 ± 2.3	120 ±82.7^b	162±65.4^b	150±42.8^c	179±19.5^c	218 ^{c}
Total Bilirubin (mg/dL)	TRT<0.001 TIME=0.001 TRT*TIME<0.001	VEH	0.5 ± 0.18	0.0±0.07^a	0.0±0.09^a	0.0±0.07^a	-0.0±0.05^a	-0.2±0.09^a
		TOX	0.4 ± 0.07	0.1±0.06^{ab}	0.2±0.06^a	0.2±0.09^a	0.2±0.10^b	0.3±0.12^b
		LET	0.3 ± 0.07	0.2±0.05^b	0.4±0.05^b	0.6±0.07^b	0.8±0.10^c	0.9 ^{c}
Aspartate Aminotransferase (IU/L)	TRT<0.001 TIME<0.001 TRT*TIME<0.001	VEH	40 ± 10.1	10 ± 4.0^a	18± 6.1^a	20±9.0^a	29± 9.1^a	37±13.9^a
		TOX	41 ± 8.5	6 ± 2.8^a	50±22.0^a	212±110^a	343± 156^b	541± 222^b
		LET	47 ± 1.5	53 ±24.7^a	283±64.1^a	2217±429^b	3065± 237^c	4034 ^{c}
Lactate Dehydrogenase (IU/L)	TRT<0.001 TIME<0.001 TRT*TIME<0.001	VEH	446 ± 63.6	34±15.4^a	54±25.5^a	2±38.5^a	56±36.2^a	55±48.9^a
		TOX	460 ± 69.4	-10±27.3^a	110±55.6^a	248± 125^a	367± 216^a	628± 350^b
		LET	460 ± 68.4	95±72.9^a	282±85.4^a	2136± 360^b	2777± 457^b	4038 ^{c}
Creatinine Phosphokinase (IU/L)	TRT=0.196 TIME<0.001 TRT*TIME=0.002	VEH	1207 ± 209	408± 124^a	658± 243^a	593±363^a	867± 390^a	804± 333^a
		TOX	1466 ± 307	292± 55^a	670± 237^a	757±406^a	1196± 403^a	2020± 542^b
		LET	1873 ± 166	437± 189^a	735± 313^a	1205± 39^b	2256± 333^b	3189 ^{b}
Glucose (mg/dL)	TRT=0.002 TIME=0.325 TRT*TIME=0.095	VEH	77 ± 11.2	0 ± 3.4^a	-1± 8.4^a	-2±11.7^a	13 ± 6.6^a	14± 4.5^a
		TOX	91 ± 10.6	8 ±10.9^a	8±10.2^a	10± 8.0^a	2 ± 9.1^a	12±13.3^a
		LET	98 ± 11.0	-12 ±12.5^a	-39±13.2^b	-36±10.1^b	-44 ± 2.5^b	-74 ^{b}
Lactate (mg/dL)	TRT<0.001 TIME<0.001 TRT*TIME<0.001	VEH	8.4± 0.40	1.2±0.76^a	3.2±1.53^a	2.7±1.36^a	1.1±0.45^a	0.3±0.44^a
		TOX	10.7± 1.03	0.6±1.40^a	2.7±1.33^a	6.9±1.81^a	14.3±4.53^a	20.9±6.95^b
		LET	9.0± 0.86	25.9±12.7^b	61.7±19.4^b	75.7±24.7^b	76.4±31.4^b	101.7 ^{c}

VEH = vehicle control group; 0 µg/kg MCLR
TOX = toxic-sublethal group; 25 µg/kg MCLR
LET = lethal group; 72 µg/kg MCLR
Means with different letters are significantly different ($p<.05$)

Table 1. Continued

PARAMETER	P VALUES	TRT GRP	Predose Mean ± SEM	CHANGE FROM PREDOSE VALUES 45 Min Mean ± SEM	90 Min Mean ± SEM	150 Min Mean ± SEM	210 Min Mean ± SEM	300 Min Mean ± SEM
Potassium **	TRT=0.002	VEH	3.93±.118[a]	4.26±.139[a]	4.53±.115[a]	4.43±.139[a]	4.40±.241[a]	4.09±.040[a]
(mmol/L)	TIME=0.004	TOX	3.98±.157[a]	4.03±.104[a]	3.94±.145[a]	3.70±.159[a]	3.82±.117[a]	3.94±.099[a]
	TRT*TIME=0.002	LET	4.10±.065[a]	5.67±1.05[b]	5.52±.801[b]	5.85±1.11[b]	6.97±2.44[b]	5.94 [b]
Inorganic	TRT=0.031	VEH	9.6 ± .33[a]	9.6 ± .41[a]	9.1 ± .51[a]	9.3 ± .33[a]	9.2 ± .38[a]	9.3± .38[a]
Phosphorus **	TIME<0.001	TOX	9.4 ± .48[a]	9.8 ± .63[a]	10.4± .60[a]	9.8 ± .68[a]	9.8 ± .62[a]	10.0± .73[a]
(mg/dL)	TRT*TIME<0.001	LEH	9.3 ± .66[a]	10.0± .99[a]	11.6± .66[b]	12.9± .78[b]	15.1±.45[b]	13.0 [b]
Creatinine	TRT<0.001	VEH	0.85 ±.096	.05±.029[a]	.03 ±.111[a]	-.05±.065[a]	.13±.048[a]	.10±.000[a]
(mg/dL)	TIME<0.001	TOX	0.97 ±.105	-.02±.017[a]	.08 ±.065[a]	.07±.120[a]	.12±.140[a]	.28±.122[a]
	TRT*TIME<0.001	LET	0.97 ±.099	.13±.088[a]	.37 ±.086[b]	.67±.033[b]	.95±.050[b]	1.60 [b]
Blood Urea	TRT=0.067	VEH	9.1± 1.31	0.7±0.31[a]	1.4±0.36[a]	0.3±1.10[a]	2.6±0.55[a]	2.6±1.43[a]
Nitrogen	TIME<0.001	TOX	11.9± 2.43	0.2±1.37[a]	2.7±1.25[ab]	1.8±1.63[a]	2.5±1.51[a]	5.9±2.07[ab]
(mg/dL)	TRT*TIME<0.001	LET	12.0± 1.25	1.1±0.69[a]	3.8±0.26[b]	7.0±0.75[b]	10.2±0.20[b]	13.5 [b]
Platelet	TRT=0.005	VEH	496 ±103.4	-8±10.3[a]	-12±15.5[a]	-15±34.2[a]	-36±41.7[a]	-25±21.5[a]
Count	TIME=0.114	TOX	663 ± 99.9	-50±22.6[a]	-84±50.3[a]	-143±47.5[b]	-151±53.7[b]	-101±53.6[ab]
(X 1000)	TRT*TIME=0.919	LET	581 ± 25.8	-248±63.4[b]	-317±33.8[b]	-242±82.8[c]	-310±70.0[c]	-260 [b]
Bicarbonate	TRT<0.001	VEH	24.9±0.33	-2.0±0.73[a]	-1.6±0.59[a]	-1.9±0.64[a]	-2.6±0.92[a]	-3.0±0.17[a]
(mmol/L)	TIME<0.001	TOX	23.1±0.62	-0.7±1.04[a]	-2.3±0.89[a]	-3.2±0.95[a]	-3.7±1.54[a]	-4.9±1.35[a]
	TRT*TIME<0.001	LET	26.8±0.62	-7.5±2.14[b]	-10.5±2.8[b]	-12.5±1.9[b]	-14.8±4.6[b]	-16.5 [b]
Arterial	TRT=0.268	VEH	7.40±.012	.01±.016[ab]	.02±.015[a]	.03±.021[a]	.04±.016[a]	.07±.021[a]
pH	TIME=0.420	TOX	7.41±.014	-.01±.009[a]	.02±.015[a]	.02±.014[a]	.02±.017[ab]	.02±.017[b]
	TRT*TIME=0.001	LET	7.42±.006	.05±.032[b]	-.06±.051[a]	-.09±.055[b]	-.04±.025[b]	-.08 [c]
Corrected pCO_2	TRT=0.002	VEH	39.8±1.74	-3.7±1.15[a]	-3.6±1.69[a]	-4.7±1.42[a]	-6.7±1.79[a]	-9.4±2.04[a]
Carbon Dioxide	TIME<0.001	TOX	36.7±1.56	-0.5±1.92[a]	-4.7±1.43[a]	-6.1±1.18[a]	-7.5±2.25[a]	-8.9±1.67[a]
(mm Hg)	TRT*TIME=0.002	LET	41.6±1.05	-13.5±4.5[b]	-12.9±3.6[b]	-15.2±4.2[b]	-21.9±7.6[b]	-22.1 [b]
Base Excess	TRT<0 001	VEH	1.1±0.22	-1.2±0.80[a]	-0.5±0.50[a]	-0.6±0.76[a]	-0.7±0.79[a]	-0.6±0.32[a]
Blood	TIME<0.001	TOX	0.1±0.60	-0.5±0.91[a]	-1.3±0.92[a]	-1.9±0.88[a]	-2.5±1.31[a]	-3.7±1.19[b]
(mmol/L)	TRT*TIME<0.001	LET	3.3±0.62	-5.6±1.56[b]	-9.9±3.12[b]	-12.2±2.6[b]	-13.1±4.7[b]	-15.0 [c]
Corrected pO_2	TRT=0.016	VEH	71.4±9.67	-2.0±1.80[a]	-0.3±5.02[a]	-2.4±5.86[a]	6.5±2.67[a]	8.5±5.62[a]
Oxygen	TIME<0.001	TOX	75.1±3.47	0.7±3.07[a]	-1.4±3.34[a]	1.5±3.41[a]	9.7±4.54[ab]	13.2±5.56[a]
(mm Hg)	TRT*TIME=0.042	LET	75.3±1.60	16.6±9.42[b]	16.3±7.22[b]	24.8±12.5[b]	13.1±4.75[b]	37.1 [b]
Hematocrit	TRT=0.011	VEH	30.0±0.82	2.5±1.44[a]	3.8±1.65[a]	4.0±1.08[a]	2.0±1.47[a]	1.5±1.19[a]
(%)	TIME=0.917	TOX	28.5±1.43	1.7±0.92[a]	1.7±1.38[a]	1.5±0.42[a]	2.3±1.05[a]	2.7±0.99[a]
	TRT*TIME=0.487	LET	32.0±0.37	-4.3±1.56[b]	-3.3±1.89[b]	-2.3±1.76[b]	-2.0±4.00[b]	2.0 [a]

VEH = vehicle control group; 0 µg/kg MCLR
TOX = toxic-sublethal group; 25 µg/kg MCLR
LET = lethal group; 72 µg/kg MCLR
** = statistical analysis of untransformed data--not change from predose
Means with different letters are significantly different ($p<.05$)

Figure 1. Six- and 12-minute means ± standard error of the change from the predose mean for central venous pressures in gilts intravenously administered a lethal (72 µg/kg; n = 6 and decreases with time) or toxic-sublethal (25 µg/kg; n = 6) dose of microcystin-LR or the normal saline vehicle (n = 3).

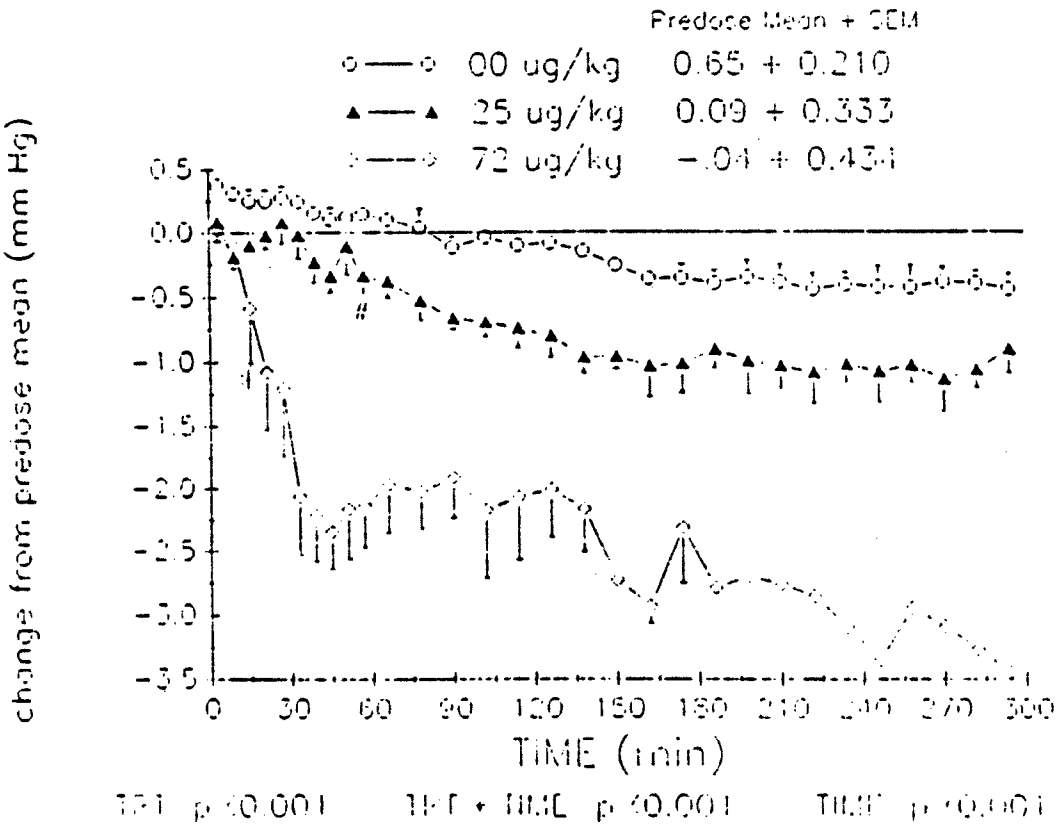

*Indicates the time point where the lethal group is significantly different than both the control and toxic-sublethal groups ($p < 0.05$).

#Indicates the time point where the toxic-sublethal group is significantly different than controls ($p < 0.05$).

Figure 2. Six- and 12-minute means ± standard error of the change from the predose mean for portal venous pressures in gilts intravenously administered a lethal (72 µg/kg; n = 6 and decreases with time) or toxic-sublethal (25 µg/kg; n = 5) dose of microcystin-LR or the normal saline vehicle (n = 4).

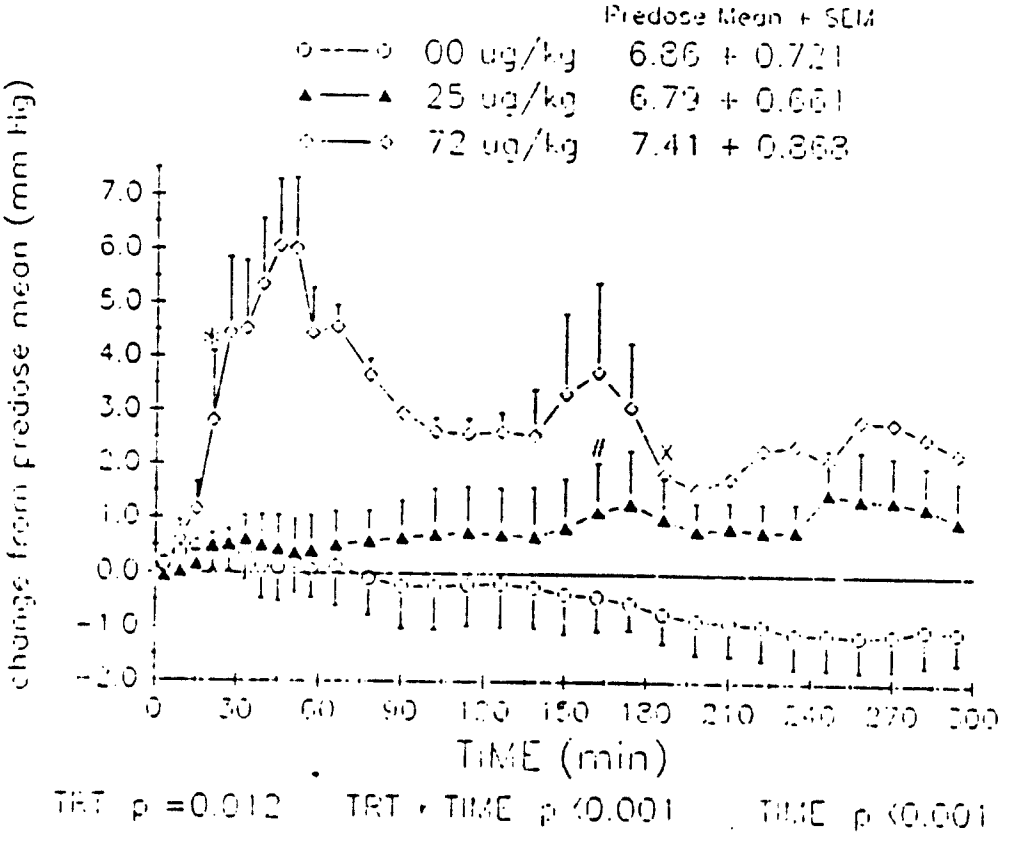

*Indicates the time point where the lethal group is significantly different than both the control and toxic-sublethal groups ($p < 0.05$).

#Indicates the time point where the toxic-sublethal group is significantly different than controls ($p < 0.05$).

XIndicates the time point where the toxic-sublethal group is no longer significantly different than the lethal group ($p < 0.05$).

Figure 3. Means ± standard error of the change from the predose mean for serum lactate concentrations in gilts intravenously administered a lethal (72 µg/kg; n = 6 and decreases with time) or toxic-sublethal (25 µg/kg; n = 6) dose of microcystin-LR or the normal saline vehicle (n = 4; 00 µg/kg).

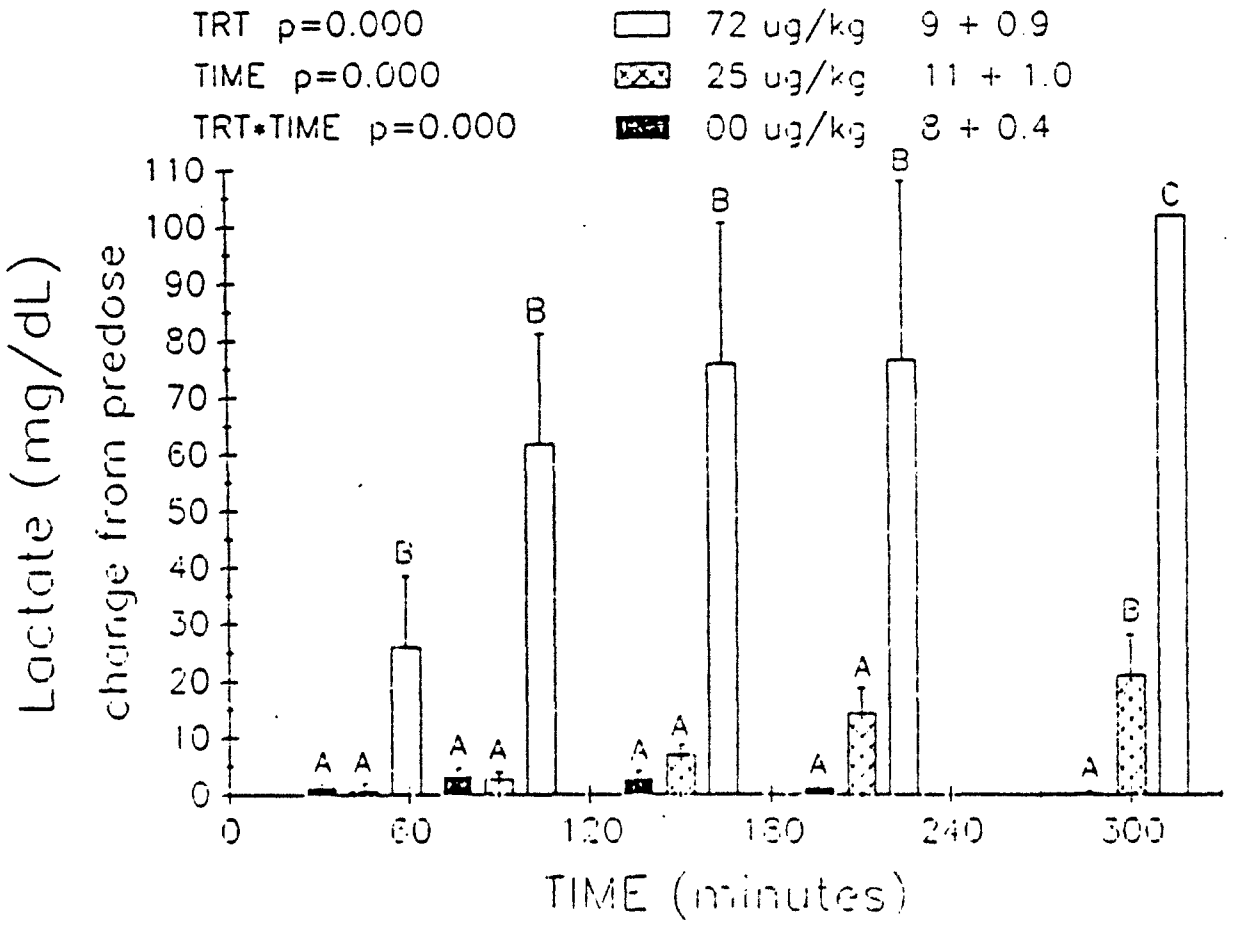

Note: The numbers to the right of the treatment group symbols represent the predose mean ± standard deviation.

Figure 4. Means ± standard error of the change from the predose mean for serum bile acid concentrations in gilts intravenously administered a lethal (72 µg/kg; n = 6 and decreases with time) or toxic-sublethal (25 µg/kg; n = 6) dose of microcystin-LR or the normal saline vehicle (n = 4; 00 µg/kg).

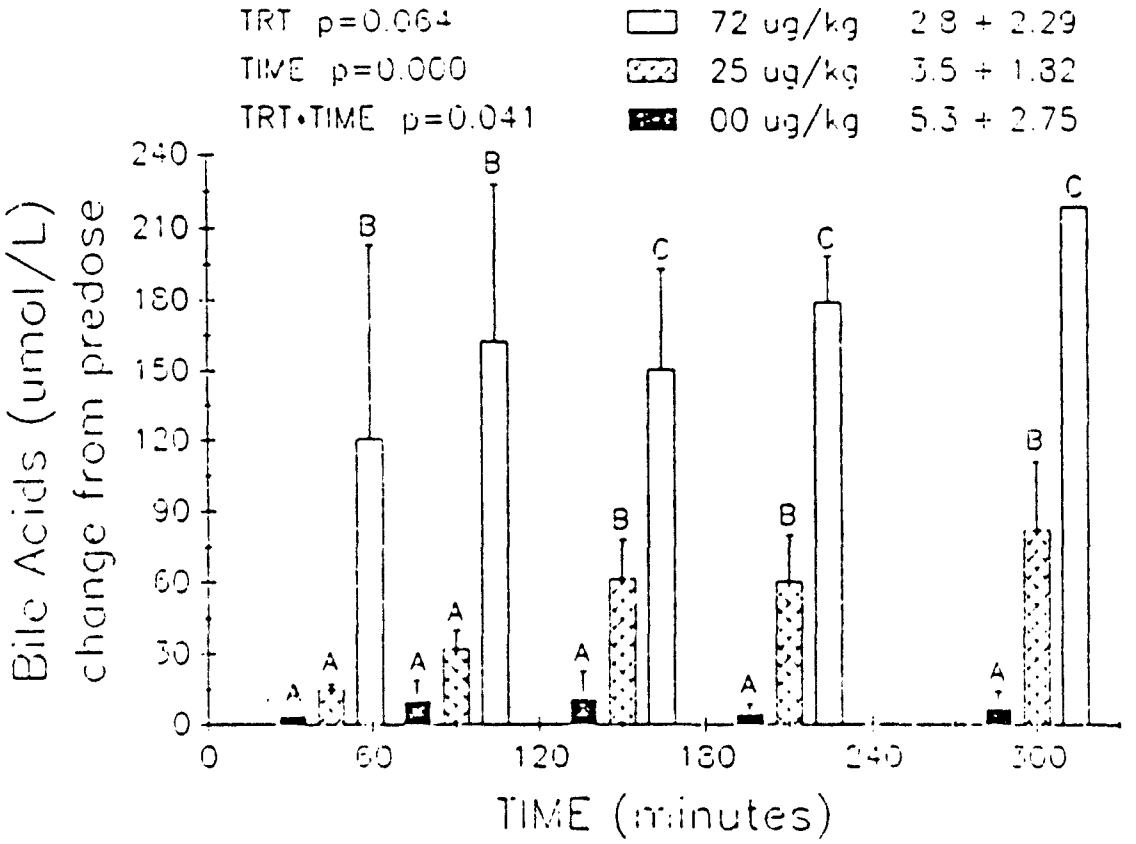

Note: The numbers to the right of the treatment group symbols represent the predose mean ± standard deviation.

Figure 5. Changes in serum potassium concentrations in the 6 gilts intravenously administered a lethal dose (72 µg/kg) of microcystin-LR.

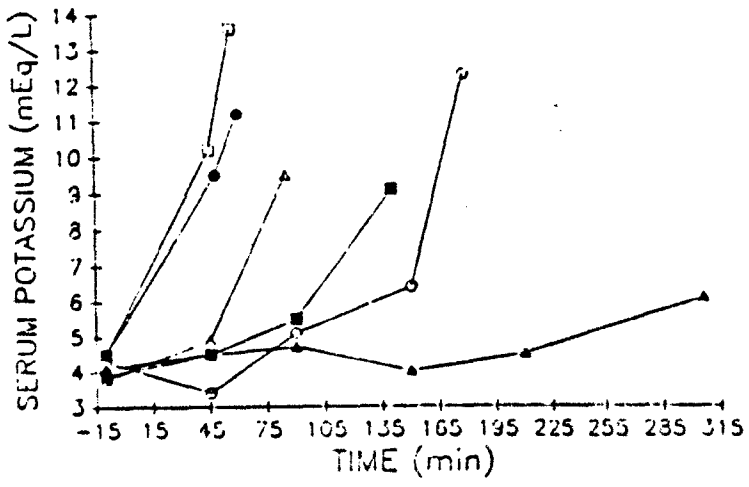

Note: No serum potassium concentrations in gilts intravenously administered a toxic-sublethal (25 µg/kg; n = 6) dose of microcystin-LR or the normal saline vehicle (n = 4) exceed 5.5 mEq/L as measured by the Hitachi 705.[1]

Figure 6. Means ± standard error of the change from the predose mean for tonometer-corrected arterial partial pressures of oxygen (pO_2) in gilts intravenously administered a lethal (72 µg/kg; n = 6 and decreases with time) or toxic-sublethal (25 µg/kg; n = 6) dose of microcystin-LR or the normal saline vehicle (n = 4; 00 µg/kg)

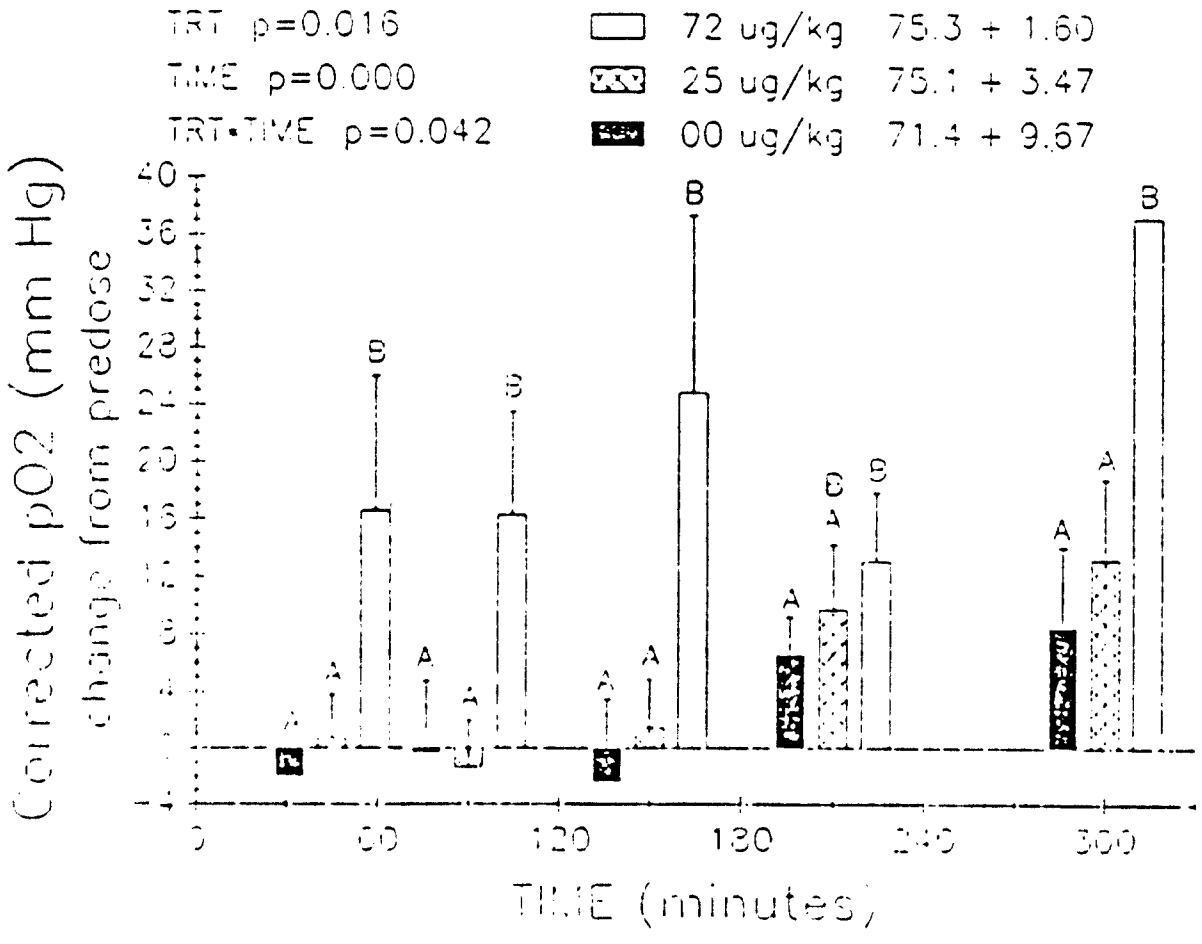

Note: The numbers to the right of the treatment group symbols represent the predose mean ± standard deviation.

Figure 7. Means ± standard error of the change from the predose mean for platelet counts in gilts intravenously administered a lethal (72 µg/kg; n = 6 and decreases with time) or toxic-sublethal (25 µg/kg; n = 6) dose of microcystin-LR or the normal saline vehicle (n = 4; 00 µg/kg).

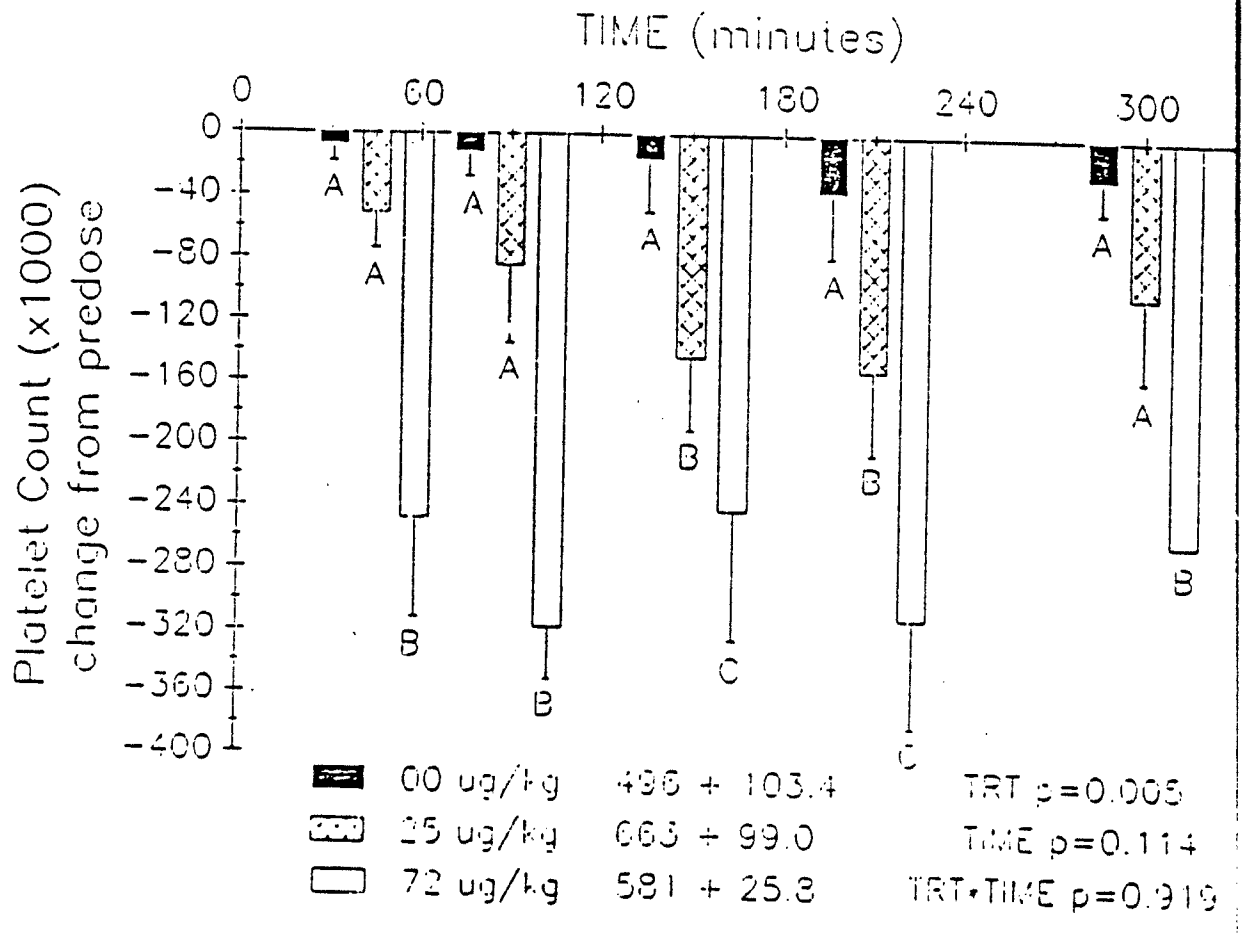

Note: The numbers to the right of the treatment group symbols represent the predose mean ± standard deviation.

Figure 8. Means ± standard error of the change from the predose mean for tonometer-corrected arterial partial pressures of carbon dioxide (pCO_2) in gilts intravenously administered a lethal (72 µg/kg; n = 6 and decreases with time) or toxic-suplethal (25 µg/kg; n = 6) dose of microcystin-LR or the normal saline vehicle (n = 4; 00 µg/kg).

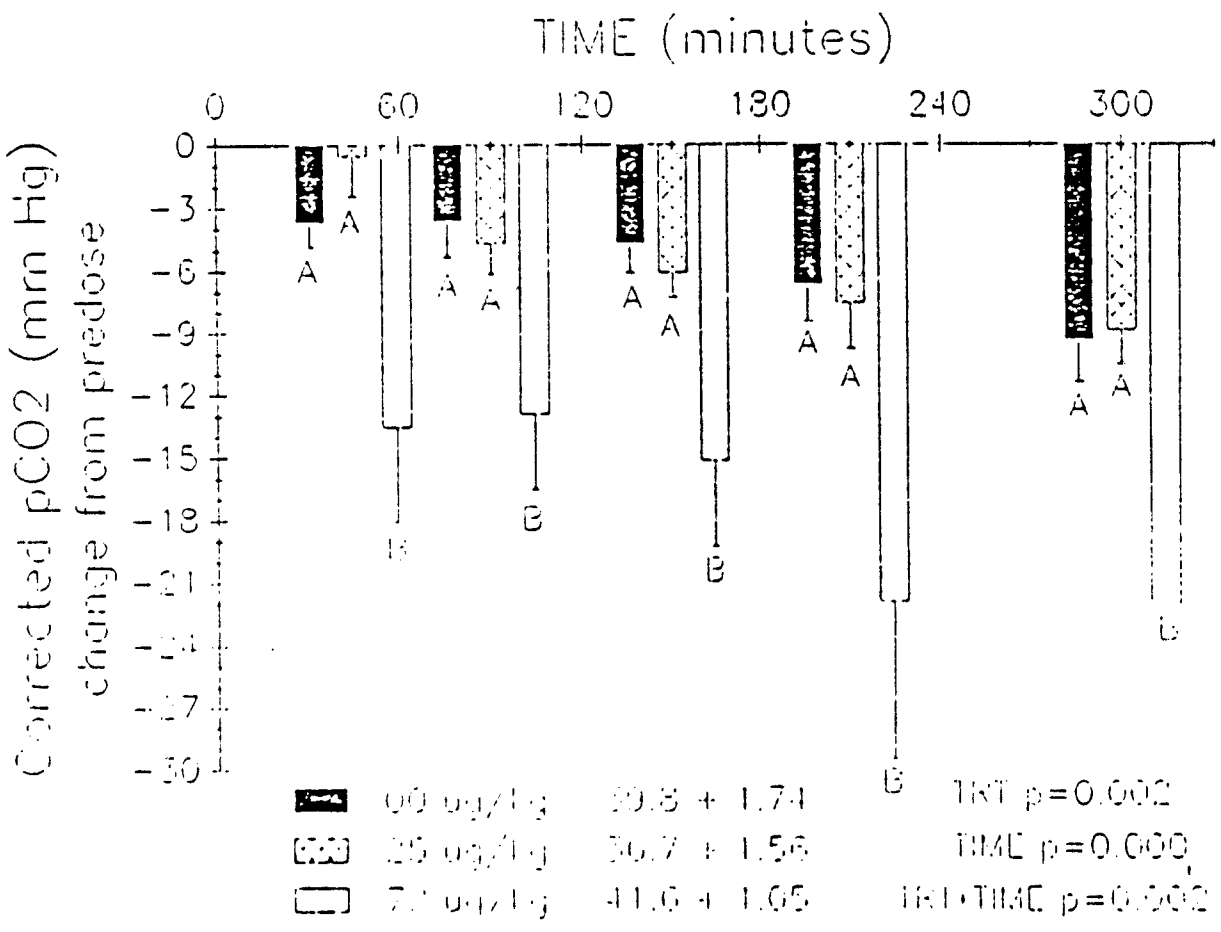

Note: The numbers to the right of the treatment group symbols represent the predose mean ± standard deviation.

Figure 9. Means ± standard error of the change from the predose mean for serum arginase activities in gilts intravenously administered a lethal (72 µg/kg; n = 6 and decreases with time) or toxic-sublethal (25 µg/kg; n = 6) dose of microcystin-LR or the normal saline vehicle (n = 4; 00 µg/kg).

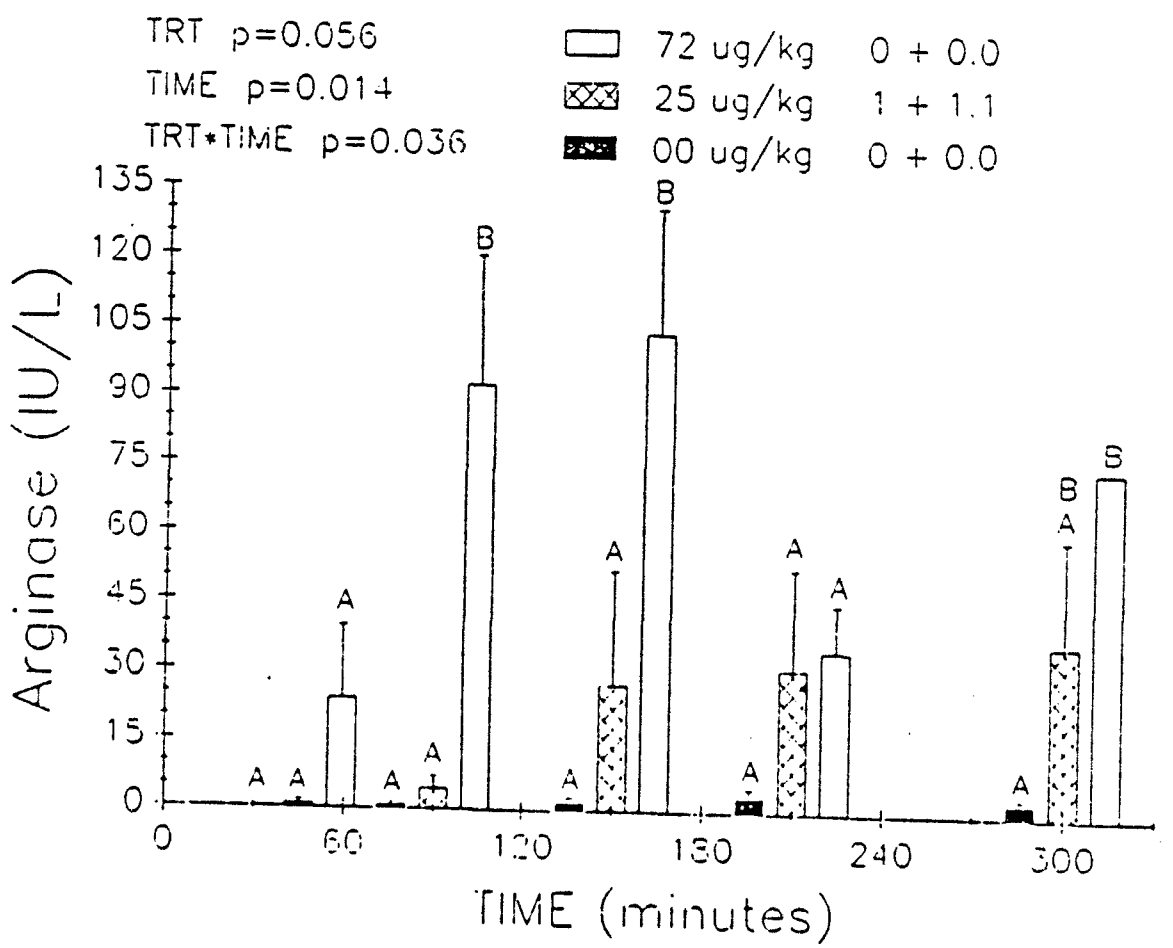

Note: The numbers to the right of the treatment group symbols represent the predose mean ± standard deviation.

Figure 10. Means ± standard error of the change from the predose mean for serum glucose concentrations in gilts intravenously administered a lethal (72 µg/kg; n = 6 and decreases with time) or toxic-subletnal (25 µg/kg; n = 6) dose of microcystin-LR or the normal saline vehicle (n = 4; 00 µg/kg).

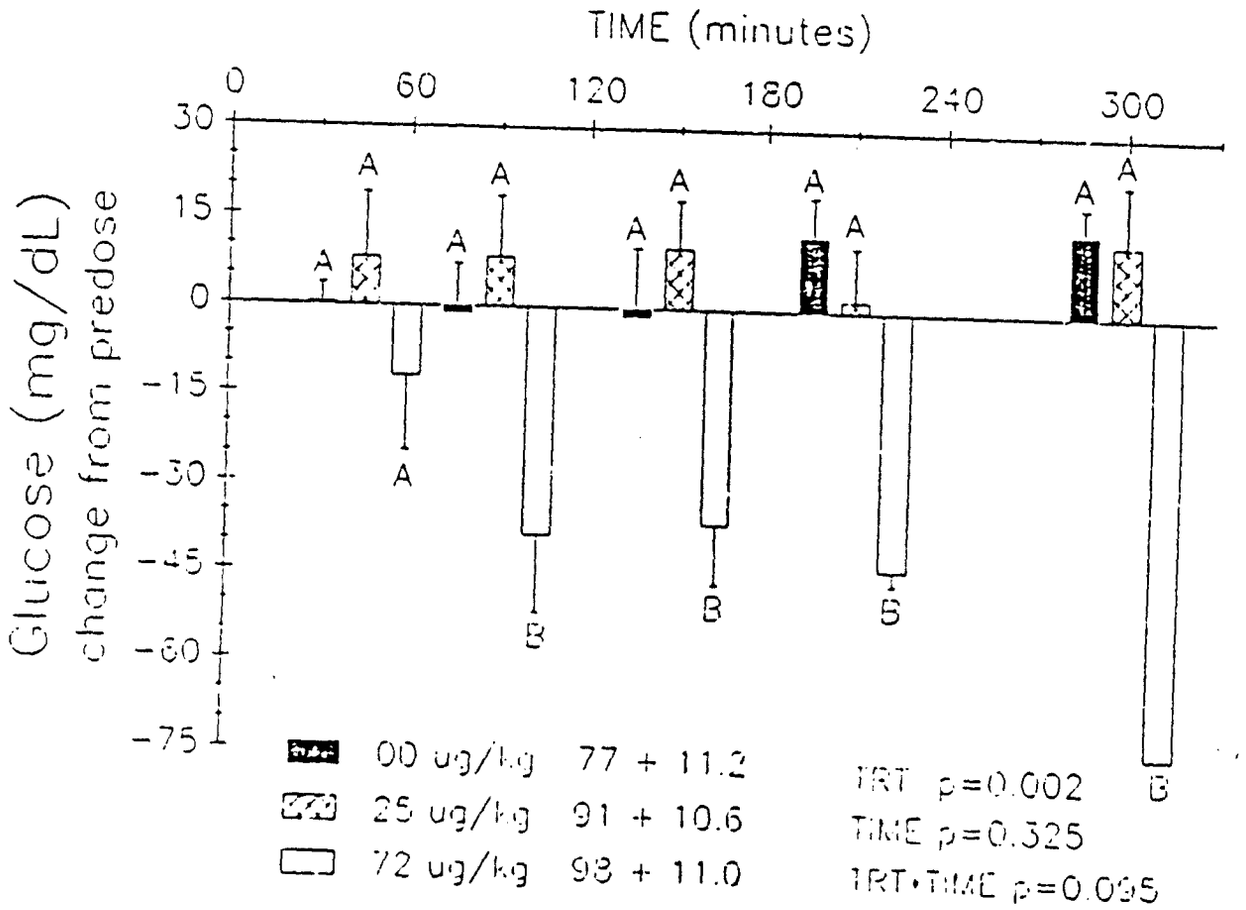

Note: The numbers to the right of the treatment group symbols represent the predose mean ± standard deviation.

Figure 11. Means ± standard error of the change from the predose mean for arterial pH in gilts intravenously administered a lethal (72 µg/kg; n = 6 and decreases with time) or toxic-sublethal (25 µg/kg; n = 6) dose of microcystin-LR or the normal saline vehicle (n = 4; 00 µg/kg).

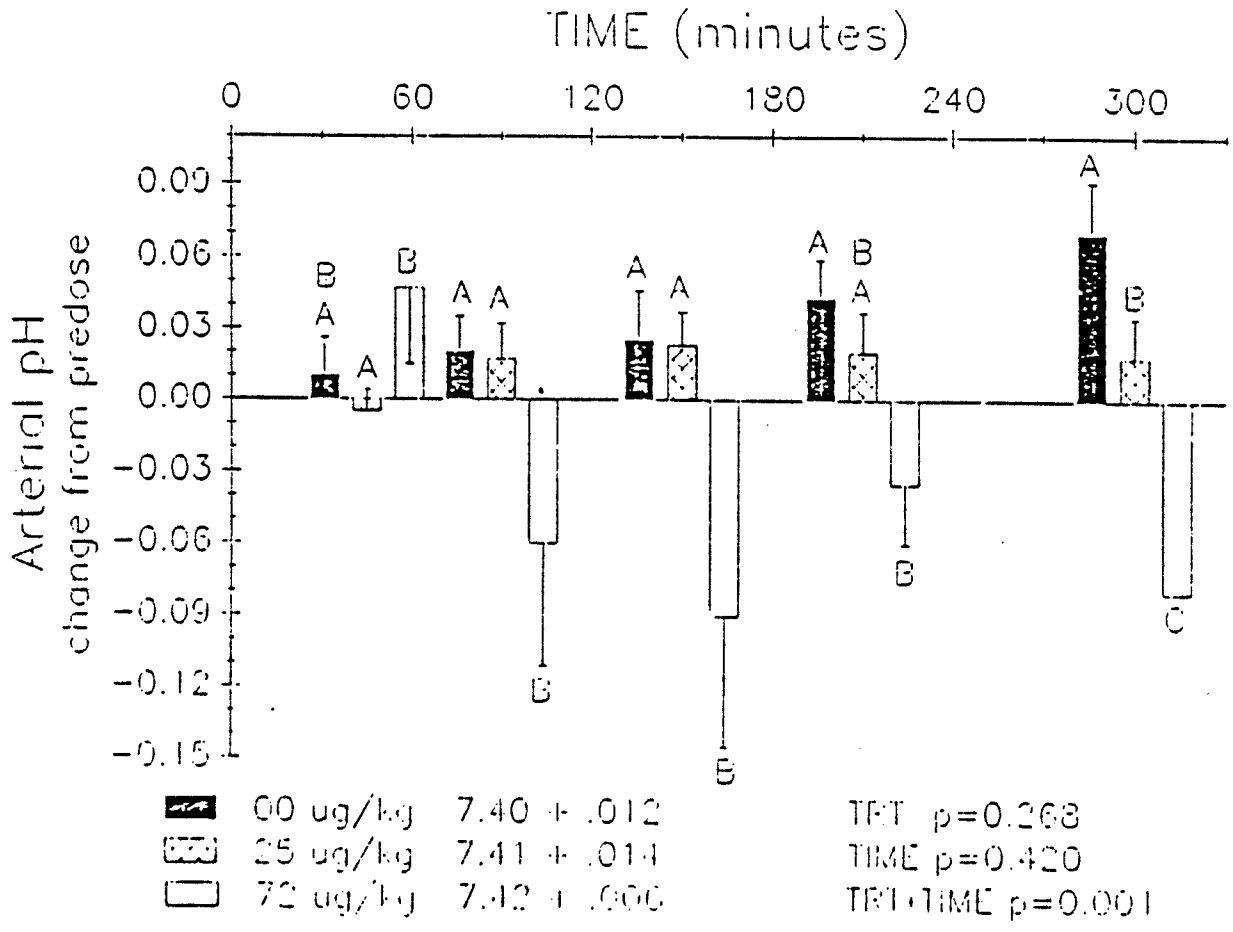

Note: The numbers to the right of the treatment group symbols represent the predose mean ± standard deviation.

Figure 12. Means ± standard error of the change from the predose mean for serum aspartate aminotransferase activities in gilts intravenously administered a lethal (72 µg/kg; n = 6 and decreases with time) or toxic-sublethal (25 µg/kg; n = 6) dose of microcystin-LR or the normal saline vehicle (n = 4; 00 µg/kg).

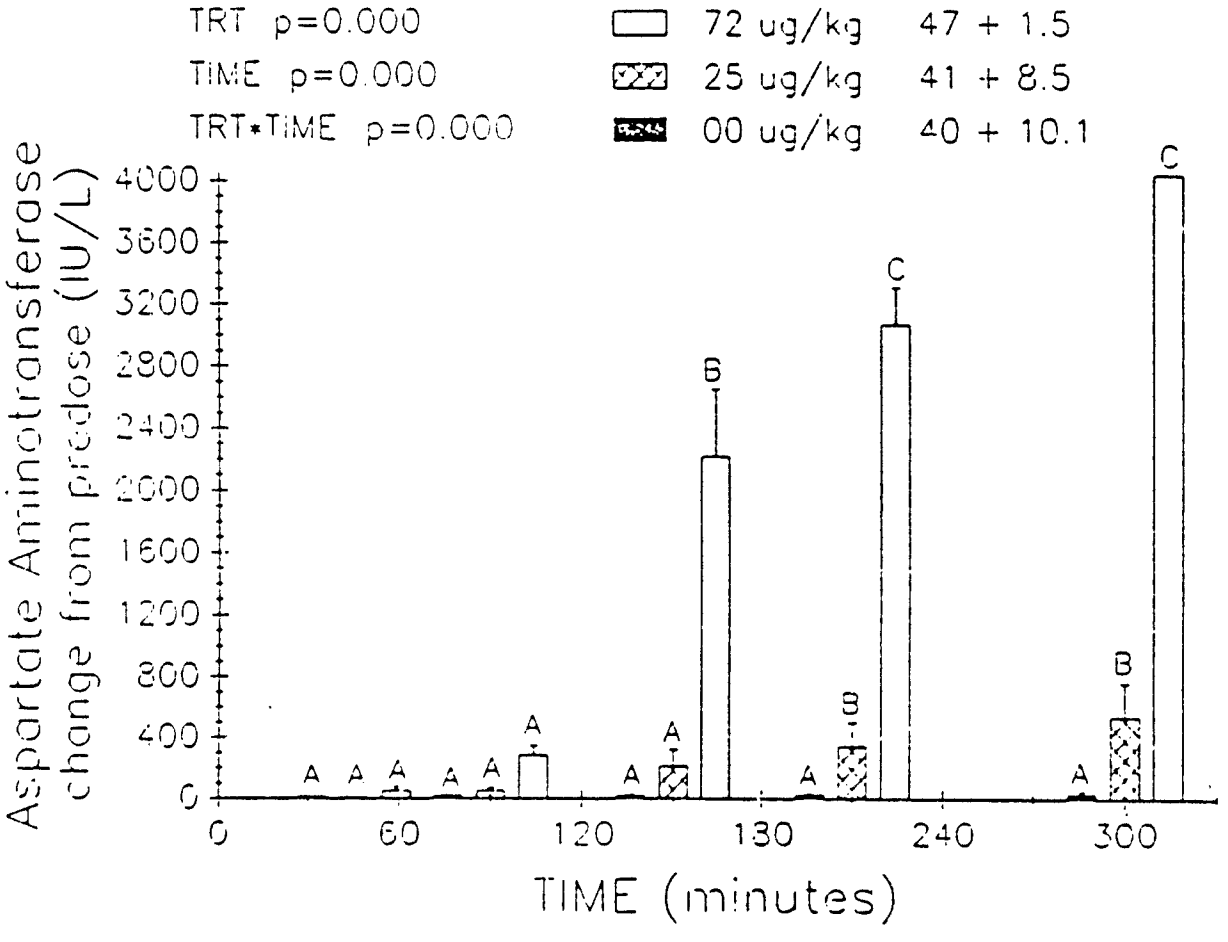

Note: The numbers to the right of the treatment group symbols represent the predose mean ± standard deviation.

Figure 13. Means ± standard error of the change from the predose mean for serum creatinine phosphokinase activities in gilts intravenously administered a lethal (72 µg/kg; n = 6 and decreases with time) or toxic-sublethal (25 µg/kg; n = 6) dose of microcystin-LR or the normal saline vehicle (n = 4; 00 µg/kg).

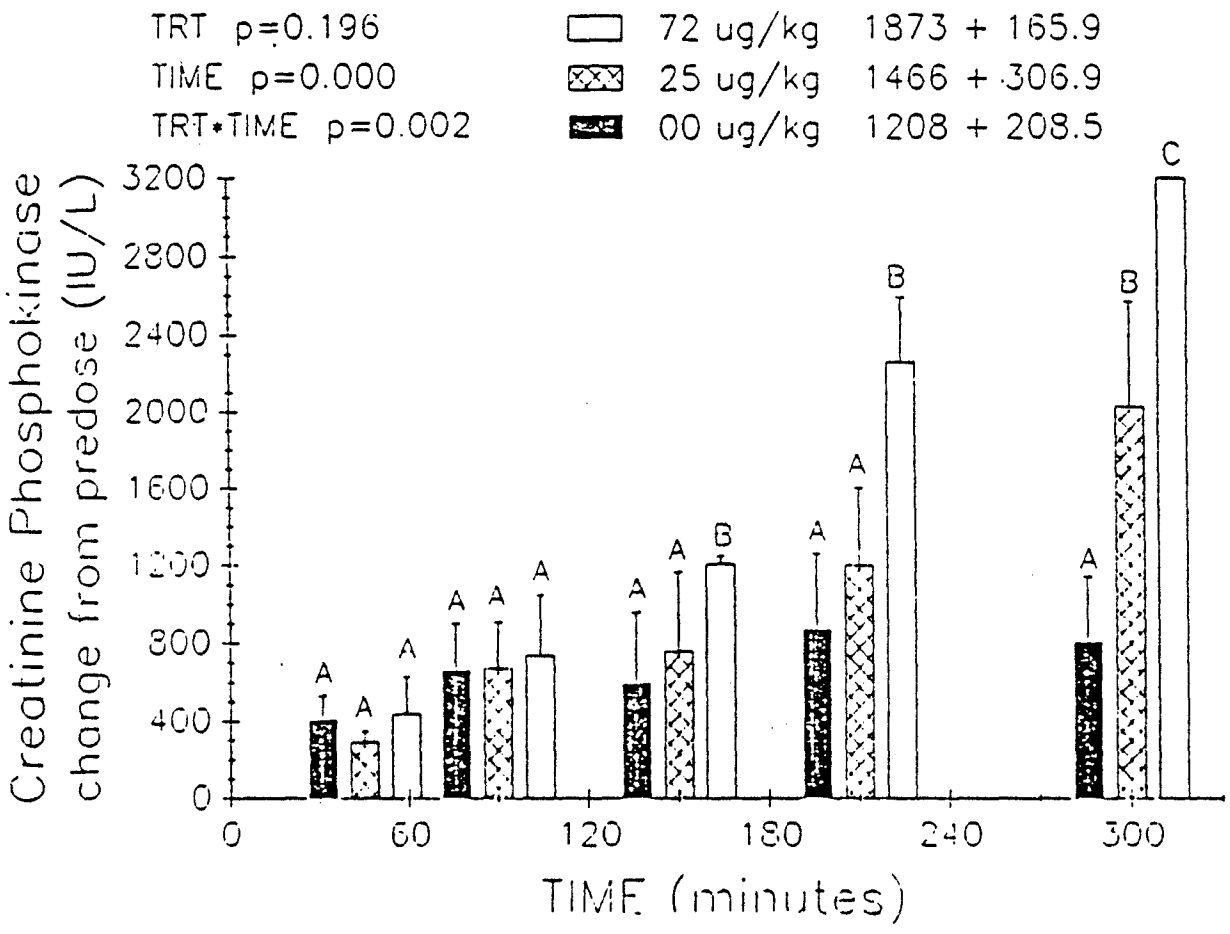

Note: The numbers to the right of the treatment group symbols represent the predose mean ± standard deviation.

VII. REFERENCES

Adams, W. H., Stoner, R. D., Adams, D. G., Slatkin, D. N., and Siegelman, H. W. (1985) Pathophysiologic effects of a toxic peptide from Microcystis aeruginosa. Toxicon 23:441.

Asaoka, K., and Takahashi, K. (1981) An enzymatic assay of reduced glutathione using glutathione S-aryltransferase with O-dinitrobenzene as a substrate. J. Biochem. 90:1237.

Ashworth, C. T., and Mason, M. F. (1946) Observations on the pathological changes produced by a toxic substance present in blue-green algae (Microcystis aeruginosa). Am. J. Path. 22:369.

Aune, T., and Berg, K. J. (1986) Use of freshly prepared rat hepatocytes to study toxicity of blooms of the blue-green alga Microcystis aeruginosa and Oscillatoria agardhii. J. Toxicol. Environ. Health 19:325.

Berg, K., and Soli, N. E. (1985a) Toxicity studies with the blue-green alga Oscillatoria agardhii from two eutrophic Norwegian lakes. Acta Vet. Scand. 26:363.

Berg, K., and Soli, N. E. (1985b) Effects of Oscillatoria agardhii toxins on blood pressure and isolated organ preparations. Acta Vet. Scand. 26:374.

Bonagura, J. D., and Hamlin, R. L. (1986) Treatment of heart disease: An overview. In: R. W. Kirk (ed.), Current Veterinary Therapy IX: Small Animal Practice, Vol. 9. W. B. Saunders, Philadelphia, pp. 319.

Botes, D. P., Viljoen, C. C. Kruger, H., Wessels, P. L., and Williams, D. H. (1982) Configuration assignments of the amino acid residues and the presence of N-methyldehydroalanine in the toxins from the blue-green alga, Microcystis aeruginosa. Toxicon 20(6):1037.

Botes, D. P., Wessels, P. L., Kruger, H., Runnegar, M. T. C., Santikarn, S., Smith, R. J., Barna, J. C. J., and Williams, D. H. (1985) Structural studies on cyanoginosins -LR, -YR, -YA, and -YM, peptide toxins from Microcystis aeruginosa. J. Chem. Soc. Perkin Trans. I, pp. 2747.

Brobst, D. (1983) Pathophysiologic and adaptive changes in acid-base discrders. J. Am. Vet. Med. Assoc. 183:773.

Brooks, W. P., and Codd, G. A. (1987a) Distribution of Microcystis aeruginosa peptide toxin and interactions with toxic microsomes. Pharmacol. Toxicol. 60:187.

Brooks, W. P., and Codd, G. A. (1987b) Extraction and purification of toxic peptides from natural blooms and laboratory isolates of the cyanobacterium Microcystis aeruginosa. Let. Appl. Micro. 2:1.

Carmichael, W. W. (1981) Freshwater blue-green algae (cyanobacteria) toxins--a review. In: W. W. Charmichael (ed.), The Water Environment: Algal Toxins and Health. Plenum Press, New York, pp. 1.

Carmichael, W. W. (1988) Toxins of freshwater algae. In: A. T. Tu (ed.), Handbook of Natural Toxins, Vol. 3 (Marine Toxins and Venoms). Marcel Dekker, New York, pp. 121.

Cook, W. O., Lovell, R. A., Dahlem, A. M., Carmichael, W. W., and Beasley, V. R. (1988) Hepatotoxicosis in cattle due to microcystin-LA produced by the freshwater blue-green algae Microcystis aeruginosa. N. Cent. Region, Vet. Lab. Diagn. Meeting, Roseville, MN, June 7-8, p. 27.

Corcoran, G. B., Racz, W. J., Smith, C. V., and Mitchell, J. R. (1985) Effects of N-acetylcysteine on acetaminophen covalent binding and hepatic necrosis in mice. J. Pharmacol. Exper. Therap. 232:864.

Corcoran, G. B., and Wong, B. K. (1986) Role of glutathione in prevention of acetaminophen-induced hepatotoxicity by N-acetyl-L-cysteine *in vivo*: Studies with N-acetyl-D-cysteine in mice. J. Pharmacol. Exper. Therap. 238:54.

Cote, L.-M., Lovell, R. A., Jeffery, E. H., Carmichael, W. W., and Beasley, V. R. (1986) Failure of blue-green algae (*Microcystis aeruginosa*) hepatotoxin to alter *in vitro* mouse liver enzymatic activity. Proc. 8th Rocky Mountain Regional Meeting of the American Chemical Society, July 25-28, Denver, CO.

Dahlem, A. M., Harada, K.-I., Harvis, C. A., Rinehart, K. L., Munro, M. H. G., Blunt, J. W., Mulligan, P. E., and Beasley, V. R. (1987) Structure/toxicity relationship of the dehydroamino acid from a cyclic peptide hepatotoxin produced by blue-green algae. The Toxicologist 7:153 (#6:2), Abstracts of the 26th Annual Meeting of the Society of Toxicology, Washington, DC.

Dahlem, A. M. (1989) Structure/toxicity relationships and fate of low molecular weight peptide toxins from cyanobacteria. PhD Thesis, University of Illinois.

Dahlem, A. M., Hassan, A. S., Swanson, S. P., Carmichael, W. W., and Beasley, V. R. (1989) A model system for studying the bioavailbaility of intestinally administered microcystin-LR, a hepatotoxin from the cyanobacterium *Microcystis aeruginosa*. Pharmacol. Toxicol. 64:177.

Drew, R., and Miners, J. O. (1984) The effects of buthionine sulphoximine (BSO) on glutathione depletion and xenobiotic biotransformation. Biochem. Pharmacol. 33:2989.

Duncan, J. R., and Prasse, K. W. (1977) Veterinary Laboratory Medicine Clinical Pathology. Iowa State University Press, Ames, Iowa.

Elleman, T. C., Falconer, I. R., Jackson, A. R. B., and Runnegar, M. T. (1978) Isolation, characterization and pathology of the toxin from a Microcystis aeruginosa (= Anacystis cyanea) bloom. Aust. J. Biol. Sci. 31:209.

Estrela, J. M., Saez, G. T., Such, L., and Vina, J. (1983) The effect of cysteine and N-acetylcysteine on rat liver glutathione (GSH). Biochem. Pharmacol. 32:3483.

Falconer, I. R., Jackson, A. R. B., Langley, J., and Runnegar, M. T. (1981) Liver pathology in mice by the blue-green alga Microcystis aeruginosa. Aust. J. Biol. Sci. 34:179.

Falconer, I. R., Beresford, A. M., and Runnegar, M. T. C. (1983) Evidence of liver damage by a toxin from a bloom of the blue-green alga Microcystis aeruginosa. Med. J. Aust. 1:511.

Falconer, I. R., Buckley, T., and Runnegar, M. T. C. (1986) Biological half-life, organ distribution and excretion of ^{125}I-labeled toxic peptide from the blue-green alga Microcystis aeruginosa. Aust. J. Biol. Sci. 39:17.

Faulstich, H., and Münter, K. (1986) New aspects of phalloidin poisoning. Klin. Wochenschr. 64(Suppl. VII):66.

Fox, P. R. (1986) Cor pulmonale. In: R. W. Kirk (ed.), Current Veterinary Therapy IX: Small Animal Practice, Vol. 9. W. B. Saunders, Philadelphia, pp. 313.

Frimmer, M. (1982) Organotropism by carrier-mediated transport. Trends Pharmacol. Sci. 3:395.

Galey, F. D., Beasley, V. R., Carmichael, W. W., Kleppe, G., Hooser, S. B., and Haschek, W. M. (1987) Blue-green algae (Microcystis aeruginosa) hepatotoxicosis in dairy cows. Am. J. Vet. Res. 48:1415.

Green, T., and Lock, E. A. (1984) The metabolism of xenobiotic conjugates and renal injury. In: P. H. Bach and E. A. Lock (eds.), Renal Heterogeneity and Target Cell Toxicity. Proceedings of the Second International Symposium on Nephrotoxicity, John Wiley and Sons, 135.

Harada, K.-I., Suzuki, M., Dahlem, A. M., Beasley, V. R., Carmichael, W. W., and Rinehart, K. L. (1988) Improved method for purification of toxic peptides produced by cyanobacteria. Toxicon 26:443.

Hawkins, P. R., Runnegar, M. T., and Jackson, A. R. B. (1985) Severe hepatotoxicity caused by the tropical cyanobacterium (blue-green alga) Cylindrospermiosis raciborskii (Woloszynska) Seenya and Subba Raju isolated from a domestic water supply reservoir. Appl. Environ. Micro. 50:1292.

Hazelton, G. A., Hjelle, J. J., and Klaassen, C. D. (1986) Effects of cysteine prodrugs on acetaminophen-induced hepatotoxicity. J. Pharmacol. Exper. Therap. 237:341.

Hooser, S., Beasley, V., Lovell, R., Carmichael, W., and Haschek, W. (1988) Toxicity of microcystin-LR, a cyclic heptapeptide hepatotoxin from Microcystis aeruginosa in rats and mice. Vet. Path. 26:246.

Hooser, S. B., Beasley, V. R., Carmichael, W. W., Lovell, R. A., and Haschek, W. M. (1989) Toxicity of microcystin LR, a cyclic heptapeptide toxin from Microcystis aeruginosa in rats and mice. Vet. Pathol. 26:246.

Hooser, S., Beasley, V., Basgall, E., Carmichael, W., Haschek, W. (1990) Microcystin-LR induced ultrastructural changes in rats. Vet. Path. 26:9.

Igwe, O. J. (1986) Biologically active intermediates generated by the reduced glutathione conjunction pathway--Toxicological implications. Biochem. Pharmacol. 35:2987.

Jackson, A. R. B., McInnes, A., Falconer, I. R., and Runnegar, M. T. C. (1984) Clinical and pathological changes in sheep experimentally poisoned by the blue-green alga Microcystis aeruginosa. Vet. Pathol. 21:102.

Jones, C. L. A., and Carmichael, W. W. (1984) Comparison of hepatotoxins from the cyanobacteria Anabaena flos-aquae and Microcystis aeruginosa. Fed. Am. Soc. Exper. Biol. J. 43:579, #1716.

Konst, H., McKercher, P. D., Gorham, P. R., Robertson, A., and Howell, J. (1965) Symptoms and pathology produced by toxic Microcystis aeruginosa NRC-1 in laboratory and domestic animals. Can. J. Comp. Med. Vet. Sci. 29:221.

Krishnamurthy, T., Carmichael, W. W., and Sarver, E. W. (1986) Toxic peptides from freshwater cyanobacteria (blue-green algae). I. Isolation, purification and characterization of peptides from Microcystis aeruginosa and Anabaena flos-aquae. Toxicon 24:865.

Kuhlenschmidt, M. S., Schmell, E., Slife, G. W., Kuhlenschmidt, T. B., Seiber, F., Lee, Y.-C., and Roseman, S. (1982) Studies on the intercellular adhesion of rat and chicken hepatocytes--Conditions affecting cell-cell specificity. J. Biol. Chem. 257:3157.

Lafranconi, W. M., Glatt, H., and Oesch, F. (1986) Xenobiotic metabolizing enzymes of rat liver nonparenchymal cells. Toxicol. Appl. Pharmacol. 84:500.

LeClaire, R. D., Lawrence, W. B., Bostian, K. A., and Mereish, K. A. (1988) Acute toxicity of microcystin-LR in the rat: A comparative dose-response study using serum chemistries and mortality as indices. Toxicologist 8:221.

Louw, P. G. J., and Smit, J. D. (1950) The active constituents of the poisonous algae, Mycrocystis toxica Stephens; with a note on experimental cases of algae poisoning in small animals. S. Afr. Indust. Chem. 4:62.

Main, D. C., Berry, P. H., Peet, R. L., and Robertson, J. P. (1977) Sheep mortalities associated with the blue-green alga Nodularia spumigena. Aust. Vet. J. 53:578.

Mason, M. F., and Wheeler, R. E. (1942) Observations upon the toxicity of blue-green algae. Am. Soc. Biol. Chem. 36th Ann. Meeting, Boston. Fed. Proc. 1:124.

McInnes, A., Jackson, A. R. B., Falconer, I. R., and Runnegar, M. T. C. (1983) The clinical pathology of sheep experimentally poisoned with the blue-green alga Microcystis aeruginosa. Toxicon 3:281.

Mia, K. S., and Koger, H. D. (1978) Direct colormetric determination of serum arginase in various domestic animals. Am. J. Vet. Res. 39:1381.

Ostensvik, O., Skulberg, O. M., and Soli, N. E. (1981) Toxicity studies with blue-green algae from Norwegian inland waters. In: W. W. Carmichael (ed.), The Water Environment: Algal Toxins and Health. Plenum Press, New York, p. 315.

Robbins, S. L., and Cotran, R. S. (1979) Pathologic Basis for Disease. W. B. Saunders Company, Philadelphia, p. 1000.

Runnegar, M. T., and Falconer, I. R. (1981) Isolation, characterization and pathology of the toxin from the blue-green alga Microcystis aeruginosa. In: W. W. Carmichael (ed.), The Water Environment: Algal Toxins and Health. Plenum Press, New York, p. 325.

Runnegar, M. T., Falconer, I. R., and Silver, J. (1981) Deformation of isolated rat hepatocytes by a peptide hepatotoxin from the blue-green alga, Microcystis aeruginosa. Naunyn-Schmiediberg's Arch Pharmacol. 317:268.

Runnegar, M. T. C., and Falconer, I. R. (1982) The in vivo and in vitro biological effects of the peptide hepatotoxin from the blue-green alga, Microcystis aeruginosa. S. Afri. J. Sci. 78:363.

Runnegar, M. T. C., and Falconer, I. R. (1986) Effect of toxin from the cyanobacterium Microcystis aeruginosa on ultrastructural morphology and actin polymerization in isolated hepatocytes. Toxicon 24:109.

Runnegar, M. T. C., Falconer, I. R., Buckley, T., and Jackson, A. R. B. (1986) Lethal potency and tissue distribution of ^{125}I-labelled toxic peptides from the blue-green alga Microcystis aeruginosa. Toxicon 24:506.

Runnegar, M. T. C., Andrews, J., Gerdes, R. G., and Falconer, I. R. (1987) Injury to hepatocytes induced by a peptide toxin from the cyanobacterium Microcystis aeruginosa. Toxicon 25:1235.

Sager, P. R., Syversen, T. L., Clarkson, T. W., Cavanagh, J. B., Elgsaeter, A., Guldberg, H. C., Lee, S. D., Lichtman, M. A., Mottet, N. K., and Olmsted, J. B. (1986) Structure and function of the cytoskeleton. In: T. Clarkson, P. Sager, T. Syverson (eds.), The Cytoskeleton: A Target for Toxic Agents. Plenum Press, New York, pp. 3.

Sasner, J. J., Jr., Ikawa, M., and Foxall, T. L. (1984) Studies on Aphanizomenon and Microcystis toxins. In: E. P. Ragelis (ed.), Seafood Toxins. Am. Chem. Soc. Symp. Series 262, Washington, DC, p. 391.

Savides, M. C., Oehme, F. W., and Leipold, H. W. (1985) Effects of various antidotal treatments on acetaminophen toxicosis and biotransformation in cats. Am. J. Vet. Res. 46:1485.

Sipes, I. G., and Gandolfi, A. J. (1986) Biotransformation of toxicants. In: C. D. Klaassen, M. O. Amdur, and J. D. Doull (eds.), Toxicology: The Basic Science of Poisons. Macmillan Publishing Co., New York, p. 64.

Skulberg, O. M., Codd, G. A., and Carmichael, W. W. (1984) Toxic blue-green algal blooms in Europe: A growing problem. Ambio 13:244.

Slatkin, D. N., Stoner, R. D., Adams, W. H., Kycia, J. H., and Siegelman, H. W. (1983) Atypical pulmonary thrombosis caused by a toxic cyanobacterial peptide. Science 220:1383.

Stowe, C. M., Monson, E., Abdullah, A. S., and Barnes, D. (1981) Blue-green algae poisoning (Microcystis aeruginosa) in a dairy herd. Bovine Clinics 1:6.

Sun, J. D., Ragsdale, S. S., Benson, J. M., and Henderson, R. F. (1985) Effects of the long-term depletion of reduced glutathione in mice administered L-buthionine-S,R,-sulfoximine. Fund. Appl. Toxicol. 5:913.

Theiss, W. C., and Carmichael, W. W. (1986) Physiological effect of a peptide toxin produced by the freshwater cyanobacteria (blue-green algae) Microcystis aeruginosa strain 7820. In: P. S. Steyn and R. Vleggaar (eds.), Mycotoxins and Phycotoxins, Bioactive Molecules, Vol. I. Elsevier, Amsterdam, p 353.

Viña, J., Romero, F. J., Estrela, J. M., and Viña, J. R. (1980) Effect of acetaminophen (paracetamol) and its antagonists on glutathione (GSH) content in rat liver. Biochem. Pharmacol. 29:1968.

Walker, R. M., Racz, W. J., and McElligott, T. F. (1985) Acetaminophen-induced hepatic congestion in mice. Hepatology 5:233.

Wanson, J. C., and Mosselmans, R. (1980) Coculture of adult rat hepatocytes and sinusoidal cells: A new experimental model for the study of ultrastructural and functional properties of liver cells. In: H. Popper, F. Gudat, L. Bianchi, W. Reutter (eds.), Communications of Liver Cells. MTP Press, Ltd., Lancaster, England, pp. 239.

Wilkinson, L. (1988) SYSTAT: The system for statistics. Systat, Inc., Evanston, IL.

Zachary, J. M., Cleveland, G., Kwock, L., Laurence, T., Weissman, R. M., Nabell, L., Fried, F. A., Staab, E. V., Risinger, M. A., and Lin, S. (1986) Actin filament organization of the Dunning R3327 rat prostatic adenocarcinoma system: Correlation with metastatic potential. Cancer Res. 46:926.

ANATOXINS

I. ANATOXIN-A(S)

W. O. Cook

A. Stability of Anatoxin-a(s) Using Human Plasma Cholinesterase In Vitro

INTRODUCTION

A structure for anatoxin-a(s) has recently been proposed (Figure 1) (Matsunaga et al., 1989). At the time of this study, however, the structural work was still underway. Absolute purity of anatoxin-a(s) [antx-a(s)] solely by conventional analytical techniques. In addition, it will be difficult to characterize the stability of the toxin over time until the reliability of analytical methods is well established. Since the toxin was known to be a cholinesterase (ChE) innibitor and ChE inhibition has been proposed as its primary mechanism of action (Mahmood and Carmichael, 1986, 1987), a ChE assay system was used to assess the stability of antx-a(x) in vitro.

We have hypothesized that antx-a(s) is stable when frozen in a solid state at -20°C in vials filled with gaseous nitrogen.

METHODS

Antx-a(s) was isolated by the method of Harada (1981) from batch cultures of A. flos-aquae strain NRC-525-17 that were grown using the method of Manmood and Carmichael (1986). Antx-a(s) in 6 µg quantities was stored as a solid in vials under nitrogen gas at -20°C prior to use. The equivalent of 35 ml of freeze-dried human plasma[a] ChE was diluted with 175 ml of pH 8 phosphate buffer and stored in 5 ml quantities at -20°C.

One hundred µl of the human plasma solution and 100 µl of either a 1 mM acetic acid solution or 0.001 µg of antx-a(s) diluted to 100 µl with 1 mM acetic acid were added to 3 ml of pH 8 phosphate buffer in a cuvette. Six samples were prepared at 1 time: 3 samples with vehicle (1 mM acetic acid) and 3 with toxin in the same volume of acetic acid. Specimens were mixed using a vortex, incubated at room temperature for 40 minutes, and assayed for ChE activity. ChE activity was determined by addition of 50 µl of dithionitrobisbenzoic acid and 20 µl of acetylthiocholine iodide followed by measurement of absorbance at 412 nm in all 6 samples simultaneously over 3 minutes with a Shimadzu 160 UV/VIS spectrophotometer.[b] Nine replicates of 6 samples each were performed. Stability of the enzyme and activity of the toxin was determined after 0, 1, 2, 3, and 6 months of storage.

RESULTS

Results of ChE assays are presented in Table 1.

DISCUSSION

Stability of the toxin has now been monitored over a period of 6 months (observations at 0, 1, 2, 3, and 6 months). Results shown in Table 1 indicate reasonable levels of enzyme stability over 6 months of storage. There appears to have been very little breakdown of the toxin; almost all the change in variability over time in the enzyme with toxin treatment group can be explained by variability in ChE enzyme activity from month to month. Acceptable stability of the toxin has now been observed for 6 months. The same degree of toxin stability has not been observed at Wright State University where antx-a(s) is stored as a solid in vials at -80°C and under which conditions there is an estimated daily

loss of 1% of toxin activity. The addition of gaseous nitrogen may slow the breakdown of toxin by removing moisture that condenses in the vials as a result of freezing/thawing and that may be resulting in toxin breakdown. At the present time, in attempts to minimize toxin loss, we recommend that antx-a(s) be stored and shipped at subzero temperatures and under gaseous nitrogen.

B. Regional Brain Cholinesterase Activity in Rats Dosed Intraperitoneally with Anatoxin-a(s) or Paraoxon

SUMMARY

Forty male Long-Evans rats weighing 300 to 380 g were dosed intraperitoneally with 1 of 3 doses of anatoxin-a(s) [antx-a(s)] that had been produced and extracted from laboratory grown Anabaena flos-aquae NCR-525-17, paraoxon, or a control solution. Each of the 5 treatments was represented in 8 different replicate groups of 5 rats in a randomized complete block design. The doses of antx-a(s) were: a) 1.5 µg/kg that was a threshold dose and produced barely detectable clinical signs; b) 3 µg/kg that produced moderate clinical signs; and c) 9 µg/kg that was consistently lethal within 1 hour. The dose of paraoxon was 800 µg/kg which produced clinical signs similar to the intermediate dose of antx-a(s).

Rats that died from antx-a(s) toxicosis were immediately bled via the caudal abdominal vena cava for whole blood cholinesterase (ChE) assays. Rats surviving 2 hours were anesthetized, bled similarly for ChE assays, and killed by exsanguination.

The brains of all rats were anatomically dissected into 8 regions: cerebellum, cortex, medulla, midbrain, hippocampus, hypothalamus,

olfactory lobes, and striatum. The anterior cervical spinal cord within the first 3 cervical vertebrae was also removed. These brain and spinal cord tissues were analyzed for ChE activity.

Whole blood ChE activity was inhibited in all rats given either antx-a(s) or paraoxon. ChE inhibition was not observed in regions of the brain or spinal cord of rats dosed with antx-a(s), but it was observed in all regions of the brain and spinal cord of rats given paraoxon. In this study, antx-a(s) did not cause detectable inhibition of ChE in the central nervous system. The inhibition of ChE in peripheral tissue (blood) but not in the central nervous system is compatible with the assertion that antx-a(s) is strictly a peripheral ChE inhibitor.

INTRODUCTION

Anatoxin-a(s) is a structurally uncharacterized, but very polar (as evidenced by solubility only in polar solvents such as water, methanol, and ethanol), low molecular weight (less than 400 daltons) neurotoxin produced by the blue-green alga Anabaena flos-aquae strain NRC-525-17 (Carmichael and Gorham, 1978; Mahmood and Carmichael, 1987). A. flos-aquae is a species of blue-green algae that has been repeatedly associated with poisoning of domestic and wild animals and is known to produce other neurotoxins and a hepatotoxin (Carmichael and Gorham, 1978; Schwimmer and Schwimmer, 1964; Carmichael et al., 1985; Carmichael, 1988).

The mechanism of toxicity of antx-a(s) has been postulated to be cholinesterase (ChE) inhibition (Mahmood and Carmichael, 1986, 1987). This is based on toxin-induced irreversible inhibition of electric eel acetylcholinesterase (E.C. 3.1.1.7) in vitro, inhibition of rat blood ChE in vivo, and clinical signs in exposed animals that were compatible with

excessive cholingeric stimulation (Mahmood and Carmichael, 1986, 1987; Cook et al., 1988). Clinically, mice and rats given antx-a(s) appear to die from respiratory failure.

The ability of ChE-inhibiting agents to cross the blood-brain barrier and inhibit brain ChE influences the resultant toxicosis (Taylor, 1985). Previously, after intraperitoneal (ip) injection, antx-a(s) was shown to inhibit plasma, red blood cell, and diaphragm ChE, but not whole brain ChE activity of mice, suggesting that this toxin is unable to cross the blood-brain barrier (Cook et al., 1988; Cook et al., in press). However, distinct regions of the brain and the anterior cervical spinal cord have not been examined to rule out the possibility that antx-a(s) causes localized inhibition of ChE in important parts of the central nervous system, such as the medulla which contains the respiratory center nuclei or the hypothalamus which has regions containing vessels that are more permeable to macromolecules (Guyton, 1976; Jacobs, 1982; Norton, 1986).

The purpose of the present study was to determine whether antx-a(s) given ip would inhibit ChE in localized areas of the rat brain. To aid in interpretation, antx-a(s) was compared with a well-known peripheral and central ChE inhibitor, the organophosphorus compound paraoxon. Whole blood ChE activity and clinical signs were monitored to quantify inhibition of peripheral ChE activity and to confirm systemic absorption of the test compounds.

MATERIALS AND METHODS

Rats

Forty male Long-Evans rats[c] weighing 300 to 380 g were housed in air-conditioned quarters on a 12/12-hour light/dark cycle and provided food[d] and water ad libitum.

Toxicant Preparation

Antx-a(s) was isolated by the method of Harada[c] from batch cultures of . flos-aquae strain NRC-525-17 that were grown by the method of Mahmood and Carmichael (1987). Thin layer chromatography indicated purity of 80 to 90%.[e] A major portion of the remaining material used in this study was low molecular weight salts from the culture media and purification process (with which toxicity has not been associated upon repeated testing). At this time it is unclear whether there are one or more forms of antx-a(s), but recently the approximate LD_{50} of a purified component was determined to be 31 µg/kg in mice dosed ip.[f] Antx-a(s) was stored under nitrogen gas at -20°C prior to use, brought into solution with 1 mM acetic acid, and diluted with physiologic saline such that the final dosing solution contained less than 0.0002% weight/volume of acetic acid. Paraoxon,[g] stored at a concentration of less than 10 mM at -20°C in dry acetone, was diluted with physiologic saline such that the final dosing solution contained less than 1% acetone. The control solution was comprised of saline containing acetic acid at the highest concentration used with antx-a(s) and was administered at a volume/body weight equal to that used with the highest dose of antx-a(s).

Experimental Design

The ip 24-hour LD_{50} of antx-a(s) was first determined using 8 rats by the up and down procedure of Bruce (1985). Thereafter, groups of rats were injected ip with antx-a(s), paraoxon, or a control solution. For these brain ChE studies, 8 rats were used per treatment group. The doses of antx-a(s) used were: a) 1.5 µg/kg that was a threshold dose and produced barely detectable clinical signs, primarily diarrhea and

decreased movement; b) 3 µg/kg that produced moderate clinical signs of salivation, lacrimation, diarrhea, decreased movement, mild tremors and fasciculations, dyspnea, and ataxia; and c) 9 µg/kg that produced a more severe spectrum of the clinical signs listed above in addition to cyanosis, clonic seizures, and consistent lethality within 1 hour of dosing. The dose of paraoxon was 800 µg/kg which produced clinical signs similar to the moderate dose of antx-a(s).

At death, rats that were lethally dosed with antx-a(s) were bled via the caudal abdominal vena cava for whole blood ChE assays. At 2 hours postdosing, surviving rats were anesthetized with carbon dioxide gas, bled similarly for whole blood ChE assays, and killed by exsanguination. The brains of rats were anatomically dissected by the procedure of Glowinski and Iversen (1966) into 8 regions: cerebellum, cortex, medulla, midbrain, hippocampus, hypothalamus, olfactory lobes, and striatum. The spinal cord within the first 3 cervical vertebrae was also removed. These regions were the smallest anatomically discernible areas of interest in the brain that could be separated by gross dissection and still provide enough tissue for ChE assays. After dissection, brain and spinal cord tissues were weighed, immediately frozen with dry ice, and stored at -20°C until assayed within 48 hours for ChE activity.

Cholinesterase Assays

ChE assays on blood were performed by a modification of the Ellman method (Ellman et al., 1981). Ten µl of heparinized whole blood was diluted to 25 ml with pH 8 phosphate buffer, and 3 ml aliquots were used for determination of ChE activity by the addition of 50 µl of 0.01 M dithiobisnitrobenzoic acid (DTNB) and 20 µl of 0.075 M acetylthiocholine

iodide (ACTI) and measurement of absorbance at 412 nm for 18 minutes on a Shimadzu 160 UV/VIS Spectrophotometer.[h] Nervous tissue ChE activity was assayed by the method of Harlin:[i] 0.05 ml of pH 8 phosphate buffer containing 1% octyl phenoxy polyethoxyethanol[j] (OPP) was used per mg of tissue for homogenization with either a Tissumizer[k] or a Biohomogenizer,[l] and 200 µl aliquots of homogenate was added to 2.5 ml of the buffer containing OPP, and ChE was assayed with DTNB and ACTI as above except with absorbance measured over 3 minutes on the spectrophotometer.

Statistical Analysis

The 24-hour LD_{50} was calculated by the method of Salsburg (1984). Comparisons among treatment groups for brain, spinal cord, and whole blood ChE activities were performed using the SAS General Linear Model with Tukey's Test (SAS Institute, 1985). A level of alpha = 0.05 was chosen to identify statistically significant differences.

RESULTS

The ip LD50 of antx-a(s) was 5.2 µg/kg. Clinically, rats given the lethal dose of antx-a(s) appeared to die from respiratory failure: the respiratory rate of rats decreased progressively over time. Inspirations became longer and greatly labored until rats became cyanotic, developed clonic seizures, and died. Expiration did not appear to be markedly affected. Results of the blood, brain, and spinal cord ChE assays are presented in Tables 2 and 3. Inhibition of whole blood ChE activity was observed in all rats given either antx-a(s) or paraoxon. ChE inhibition was not observed in any region of the brain or spinal cord of rats dosed with antx-a(s), but it was observed in all regions of the brain and spinal cord of rats given paraoxon.

DISCUSSION

When given ip, antx-a(s) does not appear to be able to inhibit ChE in the central nervous system, no inhibition was detected in any of the regions of the brain or in the anterior cervical spinal cord. ChE inhibition by antx-a(s) was not observed even in the highly cholinoceptive olfactory lobes of the brain.[m] Death of rats given antx-a(s) appeared to be due to respiratory failure, but significant ChE inhibition was not observed in the medulla oblongata which contains the respiratory center nuclei, suggesting that respiratory failure was most likely not a result of accumulation of acetylcholine in synapses of the medulla. The change in character of respiration would be consistent with a mechanism of action of the toxin that affects primarily inspiration, such as paresis or paralysis of the diaphragm. ChE inhibition was also not observed in the hypothalamus which contains the median eminence, a small area that has increased vascular permeability to macromolecules (Guyton, 1976; Jacobs, 1982; Norton, 1986).

The lack of antx-a(s) induced ChE inhibition in the central nervous system of rats supports a previously observed absence of effect of this toxin on the whole brain activity in lethally dosed mice. If the polarity of antx-a(s) *in vivo* results from strong ionization at physiological pH, the lack of ChE inhibition in the central nervous system could be a result of failure of the toxin to cross the blood-brain barrier. Strongly ionized compounds, such as quarternary amines, are normally unable to penetrate the central nervous system from the circulation (Mayer et al., 1980). Although metabolism of antx-a(s) might have reduced exposure of the brain, the toxin was absorbed from the peritoneal cavity and presented

to other sites in amounts sufficient to inhibit whole blood ChE and induce clinical signs of toxicosis including death.

The findings of the present study suggest that antx-a(s) is strictly a peripheral ChE inhibitor: whole blood ChE was inhibited by all doses of antx-a(s), while ChE inhibition was not detected in any of the tissues of the central nervous system of rats dosed ip.

FOOTNOTES

[a]Sera Chem, Fischer Co., Itasca, IL.

[b]Shimadzu Co., Columbia, MD.

[c]Charles River, Raleigh, NC.

[d]Rodent Laboratory Chow 5001, Purina Mills, Inc, Richmond, IN.

[e]Harada, K.-I., Kimura Y., Suzuki M., et al. (1988) Structural studies on a neurotoxin, anatoxin-a(s) produced by a toxic blue-green algae (I)-development of an isolation method. A paper presented at the Pharmaceutical Society of Japan Meeting, Hiroshima, Japan, April 4-6.

[f]Carmichael, W.W. (1988) Department of Biological Sciences, Wrig t State University, Dayton, OH: Unpublished data.

[g]Sigma Chemical Co., St. Louis, MO.

[h]Shimadzu Co, Columbia, MD.

[i]Harlin, K. S. and Ness D. (1986) Brain cholinesterase-normal enzyme activity levels in several large and small animal species. Amer Assn Veterinary Laboratory Diagnosticians, 29th Annual Proceedings, pp. 457-459.

[j]Triton X-100, Sigma Chemical Co, St. Louis, MO.

[k]Model SDT-1810 with a ION bit, Tekmar, Cincinnati, OH.

[l]Biospec Products, Bartlesville, OK.

[m]Shipley, M. T., and Nickell W. T. (1987) Action of soman on brain cholinergic circuits. Proceedings of the Sixth Medical Chemical Defense Bioscience Review. US Army Medical Research and Development Command. Aberdeen Proving Ground, MD, pp. 147-155.

Table 1. Results of assays run at 0, 1, 2, 3, 4, and 6 months to determine the stability of anatoxin-a(s) using human plasma ChE *in vitro*.

Treatment	Month	Mean µM/l/min	ChE SD	ChE %CV	Units inhib	% Inhib vs. control
Control	0	18.7	0.64	3.4%		
Toxin	0	8.48	0.34	3.9%	10.24	54.7%
Control	1	17.65	0.54	3.0%		
Toxin	1	7.71	0.35	4.5%	9.94	56.3%
Control	2	18.33	0.59	3.3%		
Toxin	2	8.04	0.26	3.2%	10.29	56.1%
Control	3	16.83	0.45	2.7%		
Toxin	3	7.38	0.34	4.5%	9.45	56.2%
Control	6	17.37	0.54	3.1%		
Toxin	6	7.81	0.33	3.4%	9.56	55.0%

N = 27 for all assays

Table 2. Whole blood cholinesterase activity in rats dosed ip with anatoxin-a(s), paraoxon, and a control solution.

Treatment	ChE (μmoles/l/minute) Mean ± SD	Tukey Grouping*
Control	1.1 ± 0.11	A
Antx-a(s)		
1.5 μg/kg	0.48 ± 0.33	B
3.0 μg/kg	0.15 ± 0.04	C
9.0 μg/kg	0.05 ± 0.04	C
Paraoxon (800 μg/kg)	0.13 ± 0.08	C

N = 7 or 8 for each treatment group.
*Treatment groups with different letters are significantly different ($P < 0.05$).

Table 3. Regional brain and spinal cord cholinesterase activity in mice dosed ip with antx-a(s), paraoxon, and a control solution.

Treatment	ChE (μmoles/g/minute) Mean ± SD	Tukey Grouping*
	CEREBELLUM	
Control	4.3 ± 0.24	A
Antx-a(s)		
1.5 μg/kg	4.5 ± 0.23	A
3.0 μg/kg	5.1 ± 1.82	A
9.0 μg/kg	4.1 ± 0.35	A
Paraoxon (800 μg/kg)	1.3 ± 0.25	B
	CEREBRAL CORTEX	
Control	11.5 ± 1.1	A
Antx-a(s)		
1.5 μg/kg	11.2 ± 1.3	A
3.0 μg/kg	11.4 ± 0.9	A
9.0 μg/kg	11.5 ± 1.2	A
Paraoxon (800 μg/kg)	2.3 ± 0.79	B
	HIPPOCAMPUS	
Control	8.1 ± 0.73	A
Antx-a(s)		
1.5 μg/kg	8.8 ± 1.5	A
3.0 μg/kg	8.3 ± 0.53	A
9.0 μg/kg	8.0 ± 0.46	A
Paraoxon	2.0 ± 0.41	B

Table 3. Continued

Treatment	ChE (μmoles/g/minute) Mean ± SD	Tukey Grouping*
	HYPOTHALAMUS	
Control	11.4 ± 1.6	A
Antx-a(s)		
1.5 μg/kg	11.2 ± 1.8	A
3.0 μg/kg	11.3 ± 1.6	A
9.0 μg/kg	11.8 ± 1.1	A
Paraoxon (800 μg/kg)	3.1 ± 0.54	B
	MEDULLA OBLONGATA	
Control	12.8 ± 0.59	A
Antx-a(s)		
1.5 μg/kg	12.4 ± 0.75	A
3.0 μg/kg	12.5 ± 0.91	A
9.0 μg/kg	11.8 ± 1.1	A
Paraoxon (800 μg/kg)	2.7 ± 0.56	B
	MIDBRAIN	
Control	13.7 ± 1.2	A
Antx-a(s)		
1.5 μg/kg	12.3 ± 0.75	A
3.0 μg/kg	13.7 ± 0.45	A
9.0 μg/kg	14.3 ± 1.1	A
Paraoxon (800 μg/kg)	3.1 ± 0.69	B
	OLFACTORY LOBES	
Control	5.7 ± 0.59	A
Antx-a(s)		
1.5 μg/kg	5.8 ± 0.61	A
3.0 μg/kg	5.9 ± 0.86	A
9.0 μg/kg	5.7 ± 0.45	A
Paraoxon (800 μg/kg)	1.4 ± 0.35	B

Table 3. Continued

Treatment	ChE (μmoles/g/minute) Mean ± SD	Tukey Grouping*
	SPINAL CORD	
Control	9.1 ± 0.63	A
Antx-a(s)		
1.5 μg/kg	9.1 ± 0.45	A
3.0 μg/kg	9.2 ± 0.69	A
9.0 μg/kg	8.5 ± 0.71	A
Paraoxon (800 μg/kg)	1.9 ± 0.62	B
	STRIATUM	
Control	53.4 ± 5.0	A
Antx-a(s)		
1.5 μg/kg	54.9 ± 7.1	A
3.0 μg/kg	53.8 ± 5.2	A
9.0 μg/kg	50.5 ± 13.0	A
Paraoxon (800 μg/kg)	9.9 ± 3.6	B

N = 7 or 8 for each treatment group.
*Comparisons using Tukey's test were made for the different treatments within each region of the brain (i.e., cerebellum was compared only with cerebellum, etc.). Treatment groups with different letters are significantly different ($P < 0.05$).

Figure 1. Proposed structure of anatoxin-a(s) and breakdown products (Matsunaga et al., 1989).

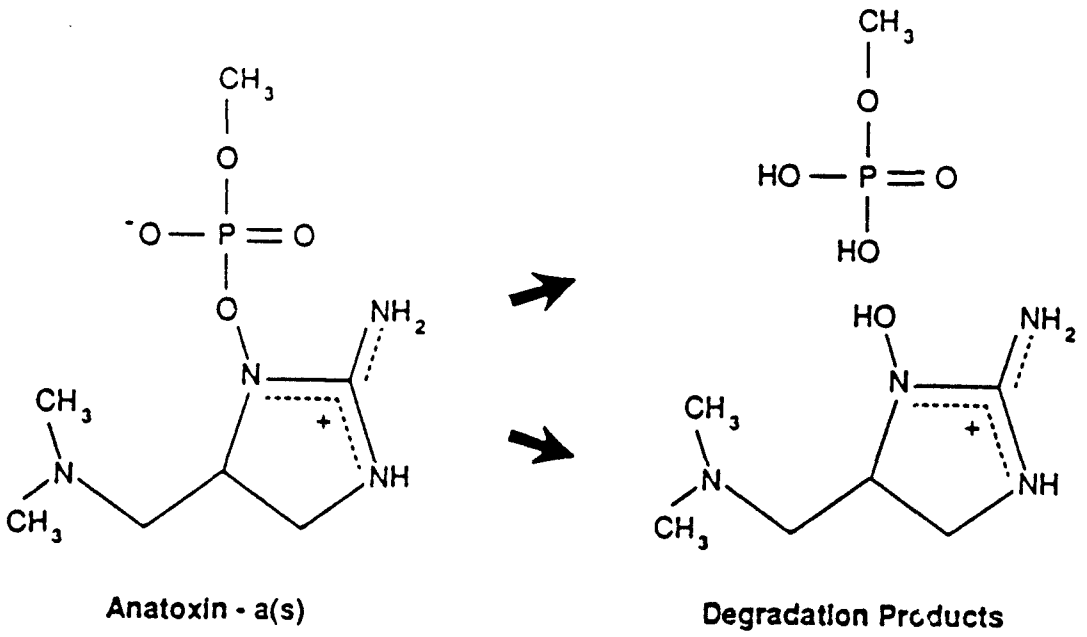

II. ELECTROMYOGRAPHIC ASSESSMENT OF THE NEUROMUSCULAR BLOCKADE PRODUCED IN VIVO BY ANATOXIN-A IN THE RAT

William Valentine, David Schaeffer

INTRODUCTION

The majority of investigations into the pharmacologic actions of (+)anatoxin-a on skeletal muscle and motor neurons have been performed in vitro, often using single cell preparations. Although experiments in vitro can yield detailed information regarding specific sites and mechanisms of action, caution must be exercised in extrapolation of these results to the intact animal. The isolation of tissues from biochemical processes and the use of high concentrations and/or prolonged periods of exposure may alter the action of the agent under investigation and precludes the influences of pharmacokinetics in vivo. Therefore, it was felt that a detailed assessment of the neuromuscular blockade produced by (+)anatoxin-a in the iv dosed rat could yield new and complementary information. This information would very likely be relevant to physiologic effects produced under circumstances of natural exposure. Specifically, the indirectly evoked compound action potentials (ECAP) of the plantar muscles of the rat were used to determine the dose response and duration of action of the neuromuscular blockade produced by (+)anatoxin-a in vivo. The effect of (+)anatoxin-a on the latency and duration of the ECAP and maximum motor nerve conduction velocity were investigated. In addition, LD_{50} values for ip administration of (+)anatoxin-a and racemic anatoxin-a in mice, and the lethal potency of (-)anatoxin-a were evaluated.

MATERIALS AND METHODS

Anatoxin-a

Hydrochloride salts of synthetic (+)anatoxin-a, (-)anatoxin-a, and racemic anatoxin-a were assessed to be > 95% pure using: a) thin layer chromatography on silica gel plates with a mobile phase consisting of 2:1:1 n-butanol-acetic acid-water and visualization by iodine vapor and ultraviolet absorption, b) chemical and electron ionization mass spectroscopy, and c) high performance liquid chromatography using a mobile phase of 9:1 0.01 M aqueous ammonium chloride-methanol and detection at 227 nm. All doses of anatoxin-a in this report refer to its hydrochloride salt.

LD_{50} Determinations

Five treatment groups each consisting of 6 male Balb/C mice weighing between 20 to 28 g were administered ip injections of 0.4 to 0.7 ml of normal saline containing (+)anatoxin-a hydrochloride or racemic anatoxin-a hydrochloride. All animals were observed for a 30-minute period following toxin administration and the number of deaths in each treatment group recorded. LD_{50}s were determined using the trimmed logit method (Sanathanan et al., 1987).

Toxicity Assessment of (-)Anatoxin-a

Male Balb/C mice (24 to 28 g) were injected ip with 1, 5, 9, 20, 40, or 73 mg/kg of (-)anatoxin-a in 0.2 to 1.0 ml of normal saline. One animal was used at each dose. The mice were observed for 30 minutes following administration of toxin at which time they were subjected to euthanasia with an ip injection of sodium pentobarbital.

Anesthesia and Electrophysiologic Measurements

Dose response and duration of action. Male Sprague-Dawley rats weighing 320 to 420 g were used in this investigation. Anesthesia was induced by

inhalation of methoxyflurane and ip injection of sodium pentobarbital at 50 mg/kg, then maintained by iv injection of sodium pentobarbital. Respiration was supported with a Harvard rodent respirator using a 16-gauge catheter as an endotracheal tube.

Assessment of neuromuscular transmission was performed as follows. The posterior tibial nerve was stimulated at the medial side of the tarsus with supramaximal electrical stimulation by pulses of 100 µsec duration applied at 0.2 Hz for single pulses and at 10 Hz for repetitive stimulation using subdermal needle electrodes. The ECAP of the lumbrical or interosseous muscles on the plantar surface of the hind foot were recorded with subdermal electrodes and a Tracor Northern EMG 3601. Nominal parameters for data acquisition were 500 data points, acquisition time 10 ms, low filter 0.5 Hz, and high filter 3,000 Hz. Temperature was maintained using radiant heat and monitored with a thermistor applied to the ventral surface of the thigh. The amplitude of the ECAP was determined from the maximum negative deflection relative to the isoelectric line. Amplitudes for repetitive stimulation were determined in the same manner and decrements calculated from the ratio of the fourth ECAP to the first ECAP.

Three treatment groups, each consisting of 4 rats, were administered iv injections of 0.1 to 0.5 ml of normal saline containing 50, 100, 200, or 800 µg of (+)anatoxin-a hydrochloride/kg body weight. A control group of 4 rats was administered 0.2 ml of normal saline.

The ECAP was measured until recovery of at least 75% of the pretoxin ECAP amplitude. The following values relating to the time profile of blockade were measured: a) onset time, the time from injection to maximum reduction of the ECAP; b) duration of action, the time from injection of anatoxin-a to 75%

recovery of the predose ECAP; and c) the maximum depression of the ECAP observed. For repetitive stimulation, the maximum decrement and the duration of a decrement > 15% were determined.

Subsequent to arcsin transformation (Winer, 1971), the statistical significance of differences between groups for percent depression and percent decrement were evaluated separately using multivariate analysis of variance followed by linear contrasts. After square root transformation to achieve homogeneous variances (Winer, 1971), the durations of action for (+)anatoxin-a hydrochloride induced depression and decrement of the ECAP were compared using one-way analysis of variance and Tukey's HSD test. Due to sample sizes and consideration of power, a significance level of $\alpha < 0.1$ was chosen for these comparisons; with one exception (Table 1) comparisons actually had $P \leq 0.05$. The ED_{50} for depression of the ECAP was estimated using the trimmed logit method (Sanathanan et al., 1987).

Nerve conduction velocity, ECAP latency, and duration measurements. Anesthesia and data acquisition parameters were the same as those described above for dose response and duration of action measurements. To measure motor nerve conduction velocity, a proximal stimulating cathode electrode was placed near the sciatic nerve and a distal stimulating cathode electrode was used on the posterior tibial nerve at the medial side of the ankle. Maximum motor nerve conduction velocity was calculated by taking the distance between the 2 stimulating sites and dividing by the difference in the latency times.

Two treatment groups, each consisting of 4 rats, were administered iv either 0.2 ml of normal saline or approximately 0.2 ml of normal saline containing 100 µg of (+)anatoxin-a hydrochloride/kg body weight. The latency, duration, and depression of the ECAP, as well as nerve conduction velocity

were determined for a period of 15 minutes following injection of saline or saline with toxin. Each data point consisted of the average of 3 measurements for each animal taken at 1-minute intervals. The 15-minute time period permitted maximal changes in these parameters to occur. Maximum motor nerve conduction velocities (m/sec) were compared using univariate repeated measures analysis. For repeated measures analysis of percent change in latency, the RTI rank transformation (Conover and Iman, 1981) was used to remove heterogeneity due to values at 2 time points for 1 treated animal being more than an order of magnitude larger than any other value in either group. Due to sample size and consideration of power, a significance level of $\alpha = 0.1$ was used for these comparisons.

RESULTS

LD_{50} Determination

Percent deaths observed for the (+)anatoxin-a hydrochloride and racemic anatoxin-a hydrochloride treatment groups plotted against dose are shown in Figure 1. The LD_{50}s (95% confidence limits) for (+)anatoxin-a hydrochloride and racemic anatoxin-a hydrochloride were 386 µg/kg (365, 408 µg/kg) and 913 µg/kg (846, 985 µg/kg), respectively. No deaths or clinical signs were observed in mice dosed with (-)anatoxin-a hydrochloride at up to 73 mg/kg.

Dose Response and Duration of Effect

A typical response of the ECAP following administration of (+)anatoxin-a at 100 µg/kg is shown in Figure 2. The amplitude of the ECAP decreased rapidly and the negative component of the action potential increased in duration in response to (+)anatoxin-a. There was a gradual return toward a normal amplitude and shape of the action potential. The mean responses for depression of the ECAP following single stimulations from doses of

(+)anatoxin-a hydrochloride at 0, 50, 100, and 200 µg/kg are shown in Figure 3. The individual responses of the ECAP in 4 rats administered 800 µg/kg (+)anatoxin-a hydrochloride are presented in Figure 4. The time corresponding to the final measurement represents the survival time in this group of animals. The survival times, defined as time between dosing and cessation of heart beat despite continuous ventilation, were 135, 150, 150, and 225 minutes.

The maximum depression, onset time for maximum depression, and duration of effect for each dose of (+)anatoxin-a hydrochloride are presented in Table 1. Significant differences for maximum depression were observed at each dose of (+)anatoxin-a hydrochloride. The ED_{50} for depression of the ECAP was 47 µg/kg (95% confidence limits of 39 and 57 µg/kg). A significant difference for duration of effect existed among the 50 µg/kg, 100 µg/kg, and control groups but not between the 100 µg/kg and 200 µg/kg treatment groups. Animals administered 800 µg/kg (+)anatoxin-a did not recover 75% of the predose ECAP amplitude.

The decrease in amplitude of the ECAP following repetitive stimulation in a rat dosed with (+)anatoxin-a at 100 µg/kg is shown in Figure 5. The mean decrements of the fourth ECAP as a function of time following repetitive stimulation for groups of 4 animals dosed with (+)anatoxin-a hydrochloride at 0, 50, 100, or 200 µg/kg are depicted in Figure 6. The maximum decrements and durations of a decrement of > 15% at each dose are listed in Table 2.

Latency and Duration of the ECAP and Nerve Conduction Velocity

The ranges of the mean percent changes in latency of the ECAP were 0.1 to 3.1 for the control group and 1.7 to 11.8 for the (+)anatoxin-a (100 µg/kg) treatment group. No significant changes in latency of the ECAP were observed.

The mean percent changes for amplitude and duration of the ECAP with respect to time are shown in Figure 7. There was no change observed in either parameter following administration of normal saline. After (+)anatoxin-a administration, the mean (SD) values for maximum depression in the amplitude of the ECAP and time to maximum depression were 85 (7) percent and 8.5 (1.4) minutes. The mean (SD) maximum percent increase in the duration of the negative component of the action potential was 87 (39).

Mean nerve conduction velocity values with respect to time for the 2 treatment groups are presented in Figure 8. Mean predose values of nerve conduction velocities (SD) for the control and (+)anatoxin-a groups were 43 (0.2) and 40 (3.5) m/s, respectively. No significant differences in nerve conduction velocities were observed between the treatment and control groups either before or after treatment.

DISCUSSION

Evaluations of agonist potency using contracture of frog rectus abdominis in vitro have previously indicated that (+)anatoxin-a was 2.5 and 150 times more potent than racemic anatoxin-a and (-)anatoxin-a, respectively (Swanson et al., 1985; Spivak et al., 1983). If the lethal action of anatoxin-a in mammals is mediated via neuromuscular blockade in skeletal muscles, similar ratios of the LD_{50}s for the various forms of anatoxin-a should be expected. Our LD_{50} values indicate that, in mice, (+)anatoxin-a was 2.4 (95% confidence limits of 2.1 and 2.7) and at least 180 times as potent as racemic and (-)anatoxin-a, respectively. The approximately 2-fold difference between (+)anatoxin-a and racemic anatoxin-a and the inability to produce death with (-)anatoxin-a suggest that (-)anatoxin-a has minimal effect, either as an agonist or antagonist, at the lethal site(s) of action.

Electromyography has been shown to correlate with tension measurements of muscle contraction for assessment of neuromuscular blockade (Calvey, 1984) and presents technical advantages over tension measurements. For example, electromyography does not necessitate perfect alignment or constant tension for accurate measurements. Additionally, electromyography can provide insight into the electrical events occurring in muscle not available from force measurements. The precision obtained with this technique for anatoxin-a has proven sufficient to establish dose response relationships that can be used for future comparisons of responses following various therapeutic agents or protocols.

A percentage of postsynaptic acetylcholine receptors must be blocked before there is a decrease in function of a muscle, and this percentage is referred to as the "margin of safety for neuromuscular transmission" (Paton and Waud, 1967). The margin of safety will vary with the muscle and species involved but is typically greater than 70% (Paton and Waud, 1967; Waud and Waud, 1972). The diaphragm has been shown to have a greater margin of safety than other skeletal muscles both *in vivo* and *in vitro* (Paton and Waud, 1967; Waud and Waud, 1972; Taylor et al., 1964, Lu, 1970). The decreased potency for paralysis of the diaphragm has been termed the "respiratory sparing effect." This increased resistance of the diaphragm to neuromuscular blockade dictates that a greater concentration of neuromuscular blocking agent must be present at this site to experience a given degree of paralysis when compared to other skeletal muscles. Ratios of the ED_{50} for paralysis of a peripheral muscle, to the LD_{50} of neuromuscular blocking agents have been used as indices of their respiratory sparing effect. These ratios depend on the agent, species, and muscles involved but are typically less than 3 for neuromuscular

blocking drugs that are used clinically (Taylor et al., 1964; Lu, 1970). Comparing the ED_{50} of 47 µg/kg obtained for neuromuscular blockade of the plantar muscles of the rat to the LD_{50} of 386 µg/kg in mice yields a ratio of 8 for the respiratory sparing effect of (+)anatoxin-a. The higher respiratory sparing effect may be a property of anatoxin-a or a result of comparing values from two species. Neuromuscular blocking agents, especially depolarizing agents, demonstrate considerable species dependency regarding potency. Indeed, with regard to both the LD_{90} and the ability of anatoxin-a to produce neuromuscular blockade in vitro, there is a 2- to 3-fold difference between mallard ducks and ring-necked pheasants (Carmichael et al., 1978). Therefore, LD_{50} determination of (+)anatoxin-a in the rat would be desirable to assess more accurately the respiratory sparing effect in this species.

A clear dose dependency for (+)anatoxin-a induced maximum depression of the ECAP is demonstrated in Figure 1 and Table 1. The onset time for maximum depression appeared to be shorter with larger doses as evidenced by the values of 8.5 minutes (Figure 7) and between 1 to 5 minutes (Table 1) observed for 100 µg/kg and 800 µg/kg, respectively. A more critical comparison of onset times was not possible due to the 4-minute interval between measurements in the 800 µg/kg trial.

There is little published information on dose response and pharmacodynamic aspects of the effects of neuromuscular blocking agents in the rat, making comparisons with anatoxin-a difficult. It has been shown for pancuronium, one of the most potent neuromuscular blocking agents used medically, that doses required to produce a 90% neuromuscular blockade in peripheral muscle are: 30 µg/kg in the cat; 17 µg/kg in the dog; 36 µg/kg in man; and 73 µg/kg in the pig (Maclagan, 1976). The iv dose of (+)anatoxin-a producing a similar degree

of blockade in the rat is between 100 to 200 µg/kg. Tubocurarine possesses one of the longest durations of action for commonly used neuromuscular blocking agents. The intervals from injection of doses of tubocurarine producing a 90% neuromuscular blockade to 50% recovery in several species were: 20 minutes in the cat; 20 to 40 minutes in the dog; and 35 minutes in man (Maclagan, 1976). Intravenous doses of (+)anatoxin-a producing a similar blockade required approximately 80 to 90 minutes for 75% recovery in the rat. The return of neuromuscular function following iv doses of anatoxin-a at 200 µg/kg or less in the rat is in sharp contrast to the response observed following po administration in a 6-week-old calf in which spontaneous respiration did not occur, although the animal was supported for 30 hours (Carmichael et al., 1975; Carmichael et al., 1977).

If one mechanism accounted for both the depression of the ECAP from single stimulation and the decrement of the ECAP following repetitive stimulation, a correlation between the degree of depression and decrement would be expected. Such a correlation was not observed for anatoxin-a. Depression of the ECAP followed a well-defined dose dependency, whereas the decrement demonstrated an all or none response. Also, the amplitude of the ECAP after a single stimulus was reduced by 50% at doses of anatoxin-a insufficient to produce a decrement after repetitive stimulation.

Amplitude of the ECAP after a single stimulus and decrement of the ECAP following repetitive stimulation are modified electrophysiologic counterparts of peak tetanic tension and tetanic fade, respectively. The sensitivity of peak tetanic tension relative to tetanic fade differs for d-tubocurarine, pancuronium, and hexamethonium (Galvinovic, 1979). These results in conjunction with measurements of miniature endplate potentials and endplate

potentials (Gibbs and Marshall, 1984; Galindo, 1971), posttetanic repetitive activity (Standaert, 1964; Riker et al., 1957; Baker et al., 1986), and quantification of evoked release of acetylcholine (Vizi et al., 1987) support the existence of presynaptic sites of action for nicotinic antagonists. Decrease of peak tetanic tension is considered to result from occupancy of postjunctional acetylcholine receptors by an antagonist (Paton and Waud, 1967; Bowman, 1980). Tetanic fade is believed to occur from either a presynaptic action on the nerve, which decreases the amount of transmitter released (Gibbs and Marshall, 1984; Galindo, 1971; Standaert, 1964; Vizi et al., 1987; Bowman, 1980), or an additional frequency-dependent postsynaptic event. Proposed mechanisms for a presynaptic action that decreases the release of transmitter include: 1) membrane stabilization, 2) interference with metabolic turnover or mobilization of acetylcholine, and 3) prevention of positive feedback on the motor nerve terminal by acetylcholine. Molecules acting as ion channel conductance modulators through direct interaction with open ion channels present a possible postsynaptic mechanism for a frequency dependent failure of neuromuscular transmission (Gibbs and Marshall, 1984; Bowman, 1980; Colquhoun et al., 1979; Dreyer, 1982). Because the interaction is dependent on the channels being in the open state, this type of action will be modulated by processes affecting the population of open channels such as repetitive stimulation. Such an interaction with open ion channels has not been observed for anatoxin-a (Aronston and Witkop, 1981; Spivak et al., 1980). Therefore, the results obtained here support the presence of a presynaptic site of action in addition to the nicotinic agonist activity of anatoxin-a on postjunctional receptors. This conclusion was corroborated by the observation that (+)anatoxin-a produced a concentration dependent decrease in the quantal

content of endplate potnetials of frog sartorius muscle evoked from nerve stimulation at 5, 10, and 20 Hz *in vitro* (Biggs and Dryden, 1977). The mechanism producing the decrement is important when considering a natural toxicosis due to the fact that units in normal muscle can fire at rates of 20 to 50 Hz (Zaimis, 1976).

Of the 4 animals administered 800 µg/kg, none had 75% return of the amplitude and all animals died within 4 hours of toxin administration despite continuous mechanical support of respiration. All 4 animals dosed at 800 µg/kg seemed to show a trend of partial return of the ECAP until deterioration occurred just prior to death. Although in 3 animals, return of the ECAP was never greater than 5%, it is notable that one animal temporarily experienced a return of approximately 60%, an amount typically sufficient for voluntary respiration. Observations of mice injected ip with (+)anatoxin-a at doses of 350 to 450 µg/kg not provided respiratory support (during the LD_{50} determination) demonstrated an acute onset of clinical signs with death occurring within 15 minutes of toxin administration. Mice surviving the first 15 minutes recovered. The results obtained here suggest that sufficiently high doses of (+)anatoxin-a can be lethal through at least 2 apparently different mechanisms. The first and more sensitive could result from a rapidly developed neuromuscular blockade, i.e., respiratory paralysis, and a second, unrelated to respiration, developing over several hours. Therefore, with sufficient exposure to anatoxin-a, therapeutic measures in addition to respiratory support and detoxification are likely to be required.

Anatoxin-a decreases the rate of rise, amplitude, and overshoot and prolongs the decay time of the ECAP. The decrease in amplitude of the ECAP, at least in part, results from failure of individual muscle fibers to generate

an action potential. The increased duration of the ECAP may result from a direct action on individual fibers before complete neuromuscular blockade and/or a desynchronization in latency of the single cell action potentials producing a temporal expansion of the ECAP.

Differential slowing of conduction velocities in motor neurons of a nerve could expand the range of latencies observed. Although not unequivocal, this appears unlikely considering the absence of either a decrease in the maximal motor nerve conduction velocity or an increase in the latency of muscle fibers innervated by the fastest conducting neurons. Similarly, if the variation in time interval between action potentials of fibers within the same motor unit (termed "jitter") increased due to variations in synaptic delay as observed for d-tubocurarine (Ekstedt and Stalberg, 1969), a desynchronization of the individual action potentials would result. An increase in jitter is suggested by the larger variation in values of latency and maximal nerve conduction velocity observed for the (+)anatoxin-a treated rats compared to controls. Because of the composite nature of the ECAP, either of the above processes could contribute to the observed increase in duration.

A third explanation could involve processes on the cellular level which might alter the shape of the individual action potentials. This would represent an effect of anatoxin-a on the muscle cell other than complete blockade of neuromuscular transmission. Evidence that such changes at least contribute to the effects of anatoxin-a on the ECAP can be derived from results obtained using single-cell preparations in vitro. Qualitatively the changes observed for single-cell preparations produced by carbachol in vitro (Nastuk, 1971) and (+)anatoxin-a in vitro (Spivak et al., 1980) were identical to those reported here for the ECAP after anatoxin-a administration in vivo.

Therefore, mechanisms producing a change in the individual action potentials of muscle cells may independently account for the anatoxin-a induced alterations of the ECAP.

In summary, electromyography can be used to quantify the degree of neuromuscular blockade produced by anatoxin-a *in vivo* with adequate precision to enable evaluation of therapeutic agents and protocols. Results obtained from our repetitive stimulation investigations support earlier reports from studies *in vitro* which suggested a physiologically significant presynaptic site of action for anatoxin-a. Exposures to anatoxin-a producing a blockade of up to 95% of neuromuscular transmission were reversible with mechanical support of respiration. However, sufficiently high exposures to anatoxin-a appear to be lethal through at least 2 apparently different, but dose-dependent, mechanisms so that at higher doses therapeutic measures in addition to respiratory support are likely to be required.

Table 1. Maximum depression, onset time for maximum depression, and duration of action for depression of the ECAP from (+)anatoxin-a.[a]

(+)Anatoxin-a (μg/kg)	Maximum depression (%)	Onset time (min)	Duration of effect (min)
0	3 ± 4 (A)[b]	--	--
50	53 ± 15 (B)	10	31 ± 11 (A)
100	82 ± 7 (C)	10	80 ± 24 (B)[c]
200	95 ± 2 (D)	10	93 ± 48 (B)
800	100 ± 1 (E)	< 5	--

[a]Values are means ± SD.
[b]Values with different letters are significantly different ($P_{actual} < 0.05$).
[c]$P_{actual} = 0.065$.

Table 2. Maximum decrement and duration of > 15% decrement of the fourth ECAP from (+)anatoxin-a following repetitive stimulation.[a]

(+)Anatoxin-a (μg/kg)	Maximum decrement of the ECAP (%)	Duration of > 15% decrement (min)
0	6 ± 5 (A)[b]	--
50	13 ± 22 (A)	4 ± 7 (A)
100	46 ± 18 (B)	24 ± 14 (B)
200	59 ± 8 (B)	69 ± 27 (C)

[a]Values are mean ± SD.
[b]Values with different letters are significantly different ($P_{actual} < 0.05$).

Figure 1. Percent deaths observed following ip administration of either (+)anatoxin-a (●; given at 350, 365, 385, 400, or 450 µg/kg BW) or racemic anatoxin-a (Δ; given at 800, 850, 950, 1,000, or 1,050 µg/kg BW). Each dose was given to a group of 6 male Balb C mice. The fraction of dosed animals that died (percent dead) is plotted against dose (log scale).

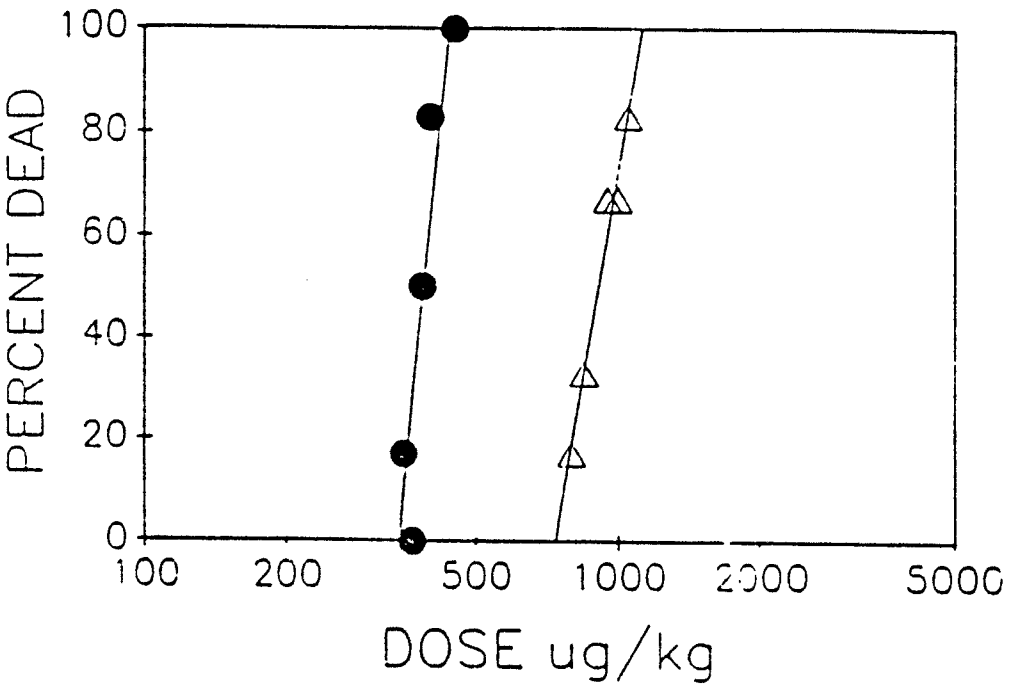

Figure 2. Evoked compound action potentials in a rat predose (a), and at 1 minute (b), 10 minutes (c), 60 minutes (d), and 120 minutes (e) after IV administration of (+)anatoxin-a hydrochloride at 100 µg/kg.

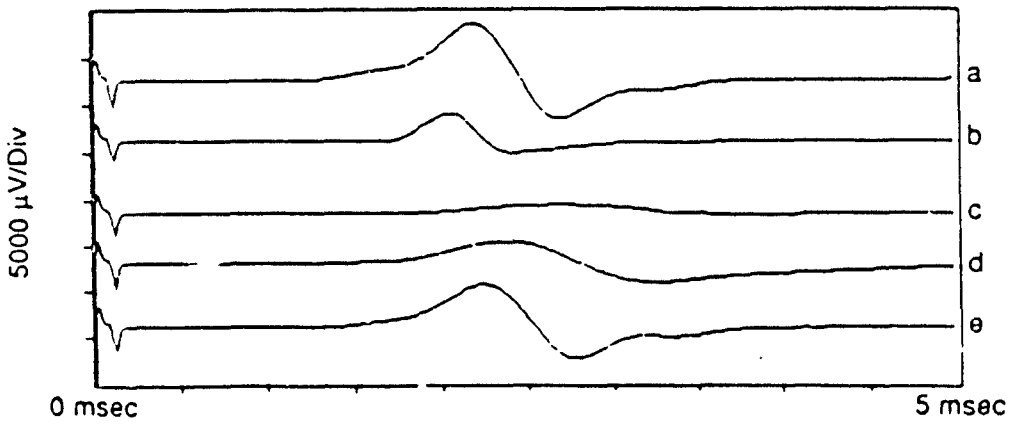

Figure 3. Mean responses for the depression in amplitude of the evoked compound muscle action potential as a function of time following IV administration of (+)anatoxin-a hydrochloride (N = 4).

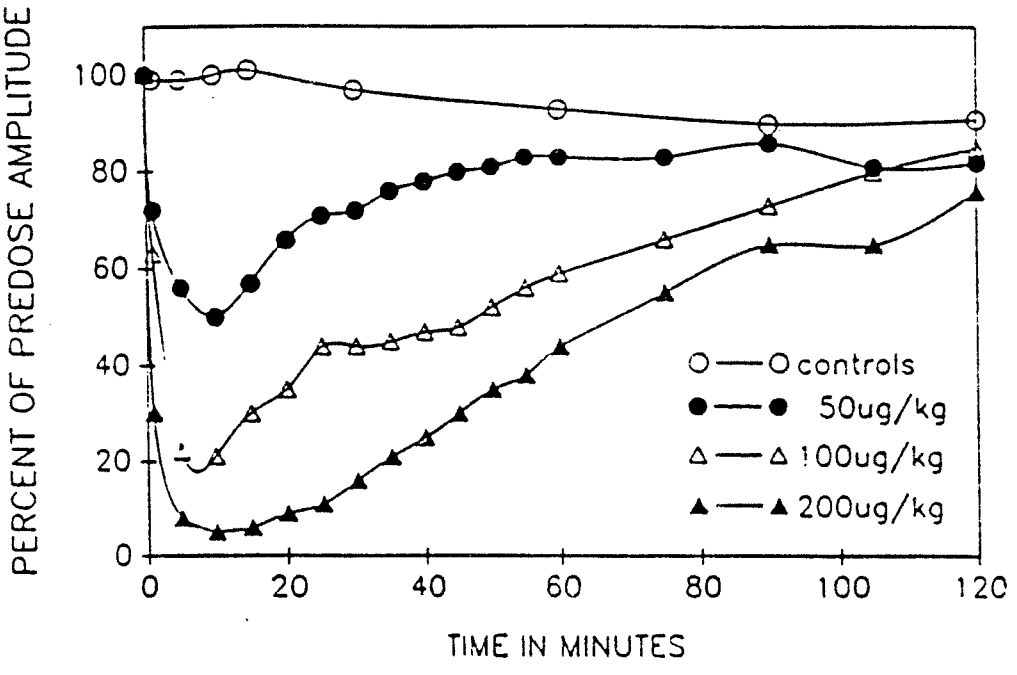

Figure 4. Percent depression of the evoked compound muscle action potentials in 4 animals as a function of time following iv administration of (+)anatoxin-a hydrochloride at 800 µg/kg body weight. Survival times are indicated by the time of the final measurement (before death).

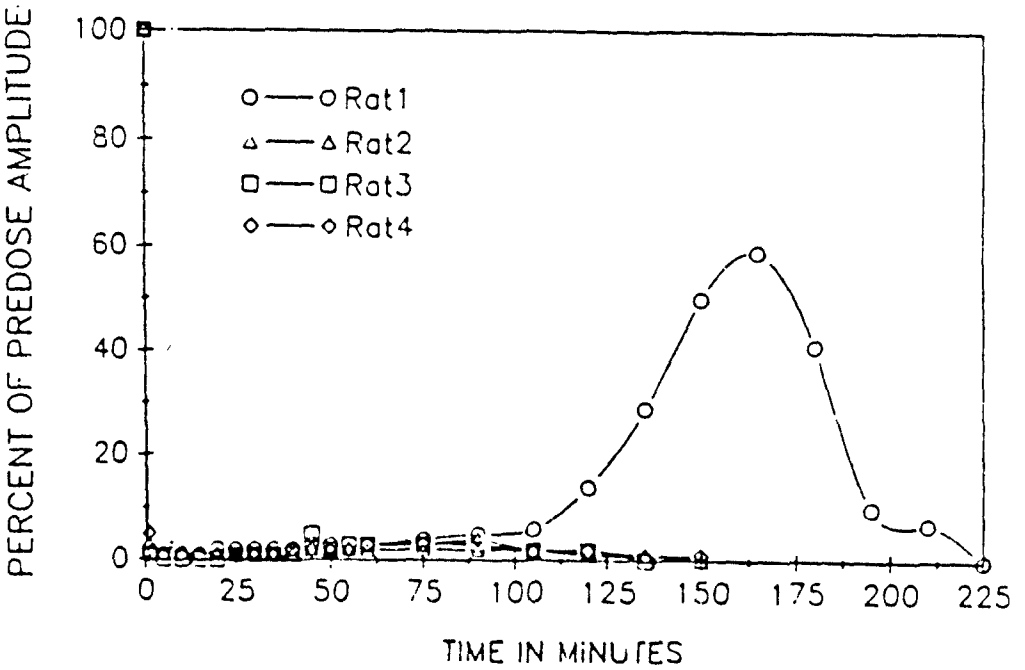

Figure 5. Evoked compound muscle action potentials in a rat resulting from 4 repetitive stimulations applied at 10 Hz (A) before and (B) 10 minutes after iv administration of (+)anatoxin-a hydrochloride at 100 ug/kg.

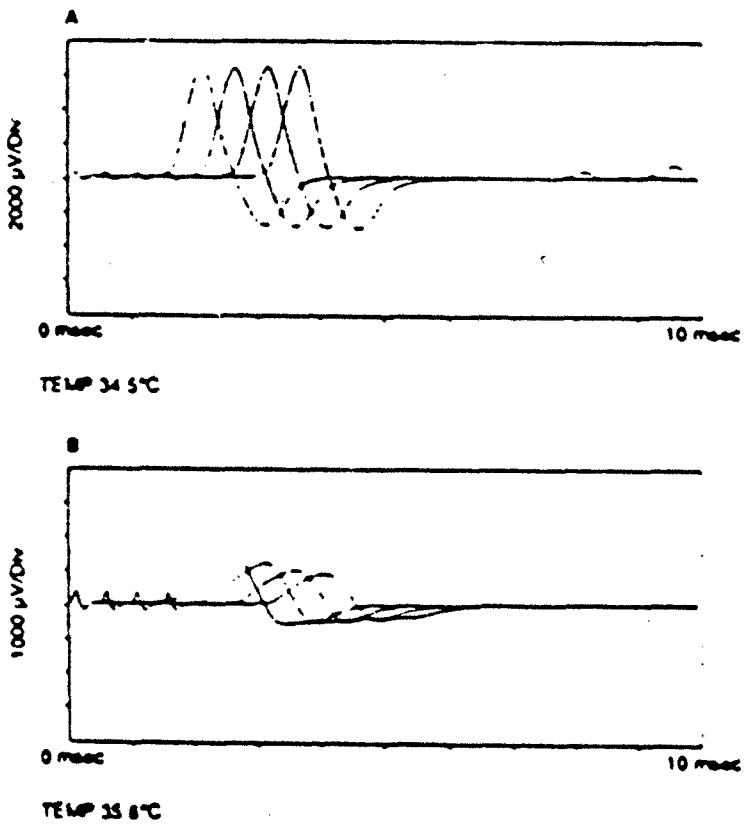

Figure 6. Mean responses for the decrement of the fourth evoked compound muscle action potential relative to the first action potential in a train of 4 repetitive stimulations at 10 Hz as a function of time following IV administration of (+)-tubocurarine hydrochloride (N = 4).

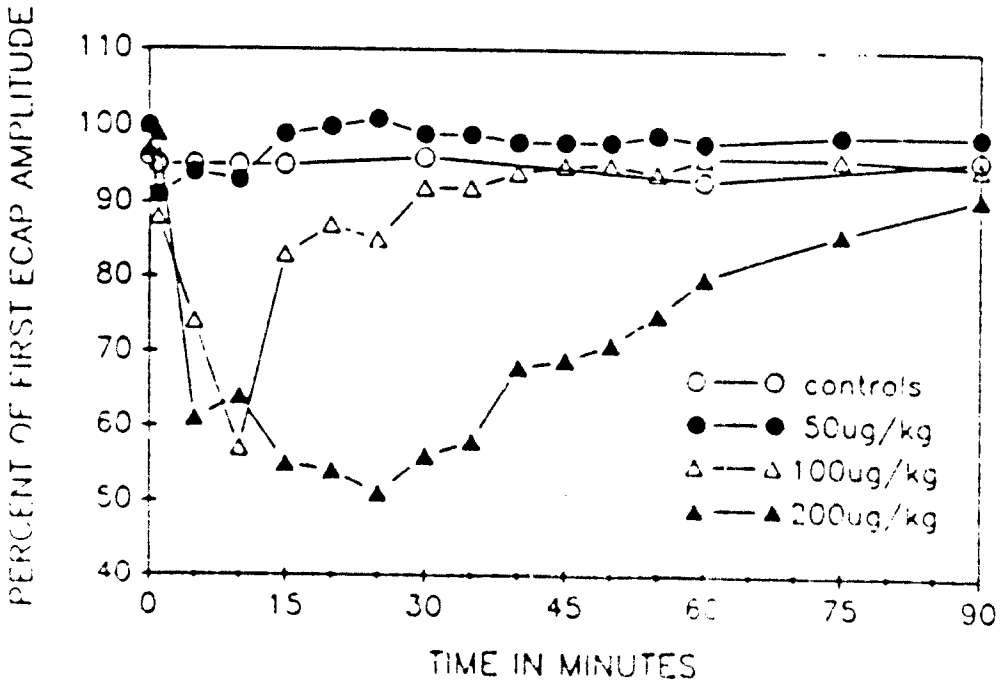

Figure 7. Mean percent changes (and their SD: which are shown when larger than the symbol size) in amplitude and duration of the evoked compound action potential following IV administration of normal saline or (+)anatoxin-a at 100 µg/kg (N = 4).

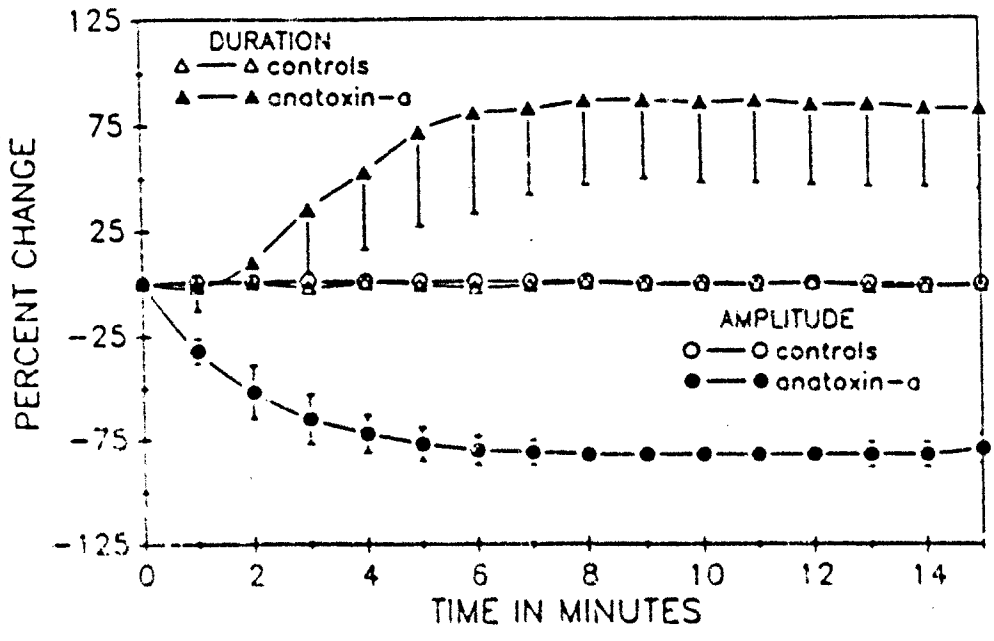

Figure 8. Mean motor nerve conduction velocities (and their SD: which are shown when larger than symbol size) in rats administered iv normal saline or (+)anatoxin-a at 100 µg/kg.

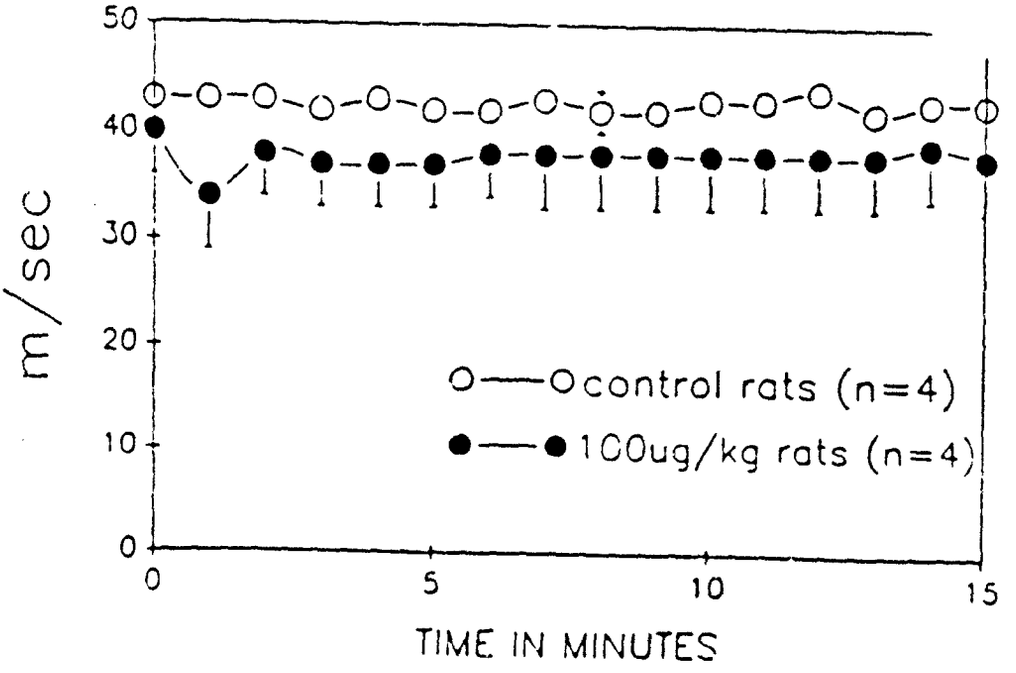

III. REFERENCES

Aronston, R. S., and Witkop, W. (1981) Anatoxin-a interactions with cholinergic synaptic molecules. Proc. Natl. Acad. Sci. 78:4639.

Baker, T., Aguero, A., Stanec, A., and Lowndes, H. E. (1986) Prejunctional effects of vecuronium in the cat. Anesthesiology 65:480.

Beers; W. H., and Reich, E. (1970) Structure and activity of acetylcholine. Nature 228:917.

Biggs, D. F., and Dryden, W. F. (1977) Action of anatoxin I at the neuromuscular junction. Proc. West. Pharmacol. Soc. 20:461.

Bowman, W. C. (1980) Prejunctional and postjunctional cholinoceptors at the neuromuscular unction. Anesth. Analg. 59:935.

Bruce, R. D. (1985) An up-and-down procedure for acute toxicity testing. Fundam. Appl. Toxicol. 5:151.

Calvey, T. N. (1984) Assessment of neuromuscular blockade by electromyography: A review. J. R. Soc. Med. 77:56.

Carmichael, W. W. (1988) Toxins of freshwater algae. In: A T. Tu (ed.), Handbook of Natural Toxins: Marine Toxins and Venoms, Vol. 3. Marcel Dekker, New York, p. 121.

Carmichael, W. W., Biggs, D. F., and Gorham, P. R. (1975) Toxicology and pharmacological action of Anabaena flos-aquae toxin. Science 187:542.

Carmichael, W. W., Gorham, P. R., and Biggs, D. F. (1977) Two laboratory case studies on the oral toxicity to calves of the freshwater cyanophyte (blue-green alga) Anabaena flos-aquae NRC-44-1. Can. Vet. J. 18:71.

Carmichael, W W., and Biggs, D. F. (1978) Muscle sensitivity differences in two avian species to anatoxin-a produced by the freshwater cyanophyte Anabaena flos-aquae NRC-44-1. Can. J. Zool. 56:510.

Carmichael, W. W., and Gorham, P. R. (1978) Anatoxins from clones of Anabaena flos-aquae isolated from lakes of western Canada. Mitt. Internat. Verein. Limnol. 21:285.

Carmichael, W. W., Biggs, D. F., and Peterson, M. A. (1979) Pharmacology of anatoxin-a, produced by the freshwater cyanophyte Anabaena flos-aquae NCR-44-1. Toxicon 17:229.

Carmichael, W. W., Jones, C. L., Mahmood, N. A., and Theiss, W. C. (1985) Algal toxins and water based diseases. CRC Crit. Rev. Envir. Control 15:275.

Colquhoun, D., Dryer, F., and Sheridan, R. E. (1979) The actions of tubocurarine at the frog neuromuscular junction. J. Physiol. 293:247.

Conover, W. I., and Iman, R. L. (1981) Rank transformation as a bridge between parametric and nonparametric statistics. Am. Stat. 35:124.

Cook, W. O., Beasley, V. R., Dahlem, A. M., Dellinger, J. A., Harlin, K. S., and Carmichael, W. W. (1988) Comparison of effects of anatoxin-a(s) and paraoxon, physostigmine and pyridostigmine on mouse brain cholinesterase activity. Toxicon 26:750.

Cook, W. O., Dahlem, A. M., Hooser, S. B., Haschek-Hock, W. M., Harlin, K. S., Carmichael, W. W., and Beasley, V. R. Reversal of cholinesterase inhibition in plasma red blood cells, and diaphragm; clinical signs, and postmortem findings in mice after intraperitoneal injection of anatoxin-a(s), paraoxon, or pyridostigmine. Submitted for publication.

Devlin, J. P., Edwards, O. E., Gorham, P. R., Hunter, N. R., Pike, R. K., and Stavric, B. (1977) Anatoxin-a a toxic alkaloid from Anabaena flos-aquae NCR-44h. Can. J. Chem. 55 1367.

Dreyer, F. (1982) Acetylcholine receptor. Br. J. Anaesth. 54:115.

Ekstedt, J., and Stalberg, E. (1969) The effect of nonparalytic doses of d-tubocurarine on individual motor end-plates in man, studied with a new electrophysiological method. Electroencepnalogr. Clin. Neurophysiol. 27:536.

Ellman, G. E., Courtney, K. D., Andres, V., and Featherstone, R. M. (1961) A new and rapid colorimetric determination of acetylcholinesterase activity. Biochem. Pharm. 7:88.

Galindo, A. (1971) Prejunctional effect of curare: Its relative importance. J. Neurophysiol. 34:289.

Galvinovic, M. I. (1979) Presynaptic action of curare. J. Physiol. 290:499.

Gibbs, A. J., and Marshall, I. G. (1984) Pre- and postjunctional effects of tubocurarine and other nicotinic antagonists during repetitive stimulation in the rat. J. Physiol. 351:275.

Glowinski, J., and Iversen, L. L. (1966) Regional studies of catecholamines in the rat brain--I: The disposition of [^{3}H]norepinephrine, [^{3}H]dopamine, and [^{3}H]dopa in various regions of the brain. J. Neurochem. 13:655.

Guyton, A. C. (1976) The blood-cerebrospinal fluid and blood brain barriers. In: Textbooks of Medical Physiology, 5th ed. W. B. Saunders, Philadelphia, p. 413.

Harada, K.-I., Kimura, Y., Suzuki, M., Dahlem, A. M., Beasley, V. R., and Carmichael, W. W. (1988) Structural studies on a neurotoxin, anatoxin-a(s) produced by a toxic blue-green algae (I)-development of an isolation method. Pharmaceutical Society of Japan, Hiroshima, Japan, April 4-6.

Jacobs, A. M. (1982) Vascular permeability and neurotoxicity. In: C. L. Mitchell (ed.), Nervous System Toxicology. Raven Press, New York, p. 285.

Koskinen, A. M. P., and Rapoport, H. (1985) Synthetic and conformational studies on anatoxin-a: A potent acetylcholine agonist. J. Med. Chem. 28:1301.

Lu, T. (1970) Affinity of curare-like compounds and their potency in blocking neuromuscular transmission. J. Pharmacol. Exp. Ther. 174:560.

Maclagan, J. (1976) Competitive neuromuscular blocking drugs. In: E. Zaimis (ed.), Neuromuscular Junction. Springer-Verlag, New York, p. 421.

Mahmood, N. A., and Carmichael, W. W. (1986) The pharmacology of anatoxin-a(s), a neurotoxin produced by the freshwater cyanobacterium Anabaena flos-aquae NRC-525-17. Toxicon 24:424.

Mahmood, N. A., and Carmichael, W. W. (1987) Anatoxin-a(s), an anticholinesterase from the cyanobacterium Anabaena flos-aquae NRC-525-17. Toxicon 25:1221.

Matsunaga, S., Moore, R. E., Niemczura, W. P., and Carmichael, W. W. (1989) Anatoxin-a(s), a potent anticholinesterase from Anabaena flos-aquae. J. Am. Chem. Soc. 111:8021.

Mayer, S. E., Melmon, K. L., and Gilman, A. G. (1980) Central nervous system and cerebrospinal fluid. In: A G. Gilman, L. S. Goodman, T. W. Rall, F. Murad (eds.), The Pharmacologic Basis of Therapeutics, 6th ed. Macmillan Publishing Co., New York, p. 10.

Nastuk, W. L. (1971) Mechanisms of neuromuscular blockade. Ann. N.Y. Acad. Sci. 183:171.

Norton, S. (1986) Toxic responses of the nervous system. In: C. D. Klaassen, M. O. Amdur, and J. Doull (eds.), Casarett and Doull's Toxicology, 3rd ed. Macmillan, New York, p. 359.

Paton, W. D. M., and Waud, D. R. (1967) The margin of safety of neuromuscular transmission. J. Physiol. 191:59.

Riker, W. F. Jr., Roberts, J., Standaert, F. G., and Fujimori, H. (1957) The motor nerve terminal as a primary focus of drug-induced facilitation of neuromuscular transmission. J. Pharmacol. Exp. Ther. 121:286.

Salsburg, D. S. (1984) Statistics for Toxicologists. Marcel Dekker, New York, p. 21.

Sanathanan, L. P., Gade, E. T., and Shipkowitz, N. L. (1987) Trimmed logit method for estimating the ED_{50} in quantal bioassay. Biometrics 43:825.

SAS Institute. SAS User's Guide: Statistics, 5th ed. SAS Institute Inc., Cary, NC, p. 433.

Schwimmer, M., and Schwimmer, D. (1964) Medical aspects of physiology. In: D. F. Jackson (ed.), Algae, Man and Environment. Plenum Press, New York, p. 368.

Spivak, C. E., Witkop, B., and Albuquerque, E. X. (1980) Anatoxin-a: A novel potent agonist at the nicotinic receptor. Mol. Pharmacol. 18:384.

Spivak, C. E., and Albuquerque, E. X. (1982) Dynamic properties of nicotinic acetylcholine receptor ion' channel complex: Activation and blockade. In: I. Hannin and A. M. Goldberg (eds.), Progress in Cholinergic Biology: Model Cholinergic Synapses. Raven Press, New York, pp. 323.

Spivak, C. E., Waters, J., Witkip, B., and Albuquerque, E. X. (1983) Potencies and channel properties induced by semirigid agonists at frog nicotinic acetylcholine receptors. Mol. Pharmacol. 23:337.

Standaert, F. G. (1964) The action of d-tubocurarine on the motor nerve terminal. J. Pharmacol. Exper. Ther. 143:131.

Swanson, K. L., Allen, C. N., Dronston, R. S., Rapoport, H., and Albuquerque, E. X. (1985) Molecular mechanisms of the potent and stereospecific nicotinic receptor agonist (+)anatoxin-a. Mol. Pharmacol. 29:250.

Taylor, D. B., Prior, R. D., and Bevan, J. A. (1964) The relative sensitivities of diaphragm and other muscles of the guinea pig to neuromuscular blocking agents. J. Pharmacol. Exper. Ther. 143:187.

Taylor, P. (1985) Anticholinesterase agents. In: A. G. Gilman, L. S. Goodman, T. W. Rall, F. Murad (eds.), The Pharmacologic Basis of Therapeutics, 7th ed. Macmillan Publishing Co., New York, p. 110.

Vizi, E. S., Somogyi, G. T., Nagashima, H., Duncalf, D., Chaudhy, I. A., Kobayoshi, O., Goldiner, P. L., and Foldes, F. F. (1987) Tubocurarine and pancuronium inhibit release of acetylcholine from the mouse hemidiaphragm preparation. Br. J. Anaesth 59:226.

Waud, B. E., and Waud, D. R. (1972) The margin of safety of neuromuscular transmission in the muscle of the diaphragm. Anesthesiology 37:417.

Winer, B. J. (1971) Statistical Principles in Experimental Design. McGraw-Hill, New York.

Zaimis, E. (1976) Depolarizing neuromuscular blocking drugs. In: E. Zaimis (ed.), Neuromuscular Junction. Springer-Verlag, New York, pp. 365.

VRB:llm/97
06/05/90